TÉCNICO LISBOA

Acoustic study of sandwich panels for use in aeronautic applications: Computational Model

João Pedro Martins Ramos

Thesis to obtain the Master of Science Degree in

Aerospace Engineering

Supervisors: Prof. Aurélio Lima Araújo

Prof. Jorge Américo Oliveira Pinto Belinha

Prof. Filipa Andreia de Matos Moleiro

Examination Committee

Chairperson: Prof. Filipe Szolnoky Ramos Pinto Cunha

Supervisor: Prof. Aurélio Lima Araújo

Member of Committee: Prof. Fernando José Parracho Lau

November 2016

I Acknowledgements

This thesis is the result of the work performed during the last 7 months of study at Instituto Superior Técnico. During this period the knowledge obtained in acoustic studies and finite element programs has been undeniably one of the best experience in my short intellectual career.

Firstly, I would like to thank all the support and dedication provided by my supervisors, Professor Aurelio Araujo, Professor Jorge Belinha and Professor Filipa Moleiro for all their knowledge, experience and time provided In order to develop this thesis.

Secondly, the Portuguese Air Force for proposing this amazing project and opportunity to validate our results with experimental values.

To conclude, all my friends and family, for their constant support during all my academic career. Especially to my parents and sister for being role models with their hard work and ethics, that pushed me to try to achieve academic success in my field of study.

II Abstract

This work investigates the effect of sandwich panels in sound absorption, where composite materials (carbon fiber and glass fiber) and foams (Airex) are analyzed in different layups.

The main objective of this study is to identify which panel design is better in sound absorption, for low frequency values. These panels are studied in order to optimize a UAV structure (Portuguese Air Force) and support an experimental thesis performed to solve the problem proposed. This topic is of particular importance, given the growing interest in sandwich panels for the construction of aircraft structures, especially on UAVs. This work was performed using FEM simulations, in the commercial program Ansys.

The acoustic behavior of sandwich panels is predicted from the Transmission loss frequency plots obtained from three different setups developed in this work: acoustic cavity (ideal), suspended panel surrounded by fluid (simulating experimental conditions) and reverberation-anechoic chamber system (simulating experimental conditions). These setups were tested and optimized, for reference panels, throughout this work.

After the setups and panel design are optimized, multiple panels with varying: thickness, materials and damping were tested and the respective transmission loss frequency plots obtained. By analyzing the Transmission Loss plots it was concluded that panels with a skin of carbon fiber (outside) and glass fiber (inside) with a core of Airex C70.75 foam with 7mm creates the best configuration for application on the UAVs structure, due to its high transmission loss for low frequency values and the first structural mode occurs outside the frequency range of interest.

Keywords: Sandwich panels, Transmission Loss frequency plot, harmonic response, Carbon fiber panels, Glass fiber panels

III Resumo

Este trabalho baseia-se na investigação da absorção de som em painéis sandwich, constituídos por materiais compósitos (fibra de carbono e fibra de vidro) e espuma estrutural (Airex C70.75).

O objetivo principal deste estudo consiste em identificar os painéis, que possuem menor transmissibilidade para baixas frequências. Estes painéis são estudados de forma a otimizar a estrutura de UAVs (Força Aérea Portuguesa) e facilitar a análise dos resultados experimentais. Este tipo de trabalhos é extremamente importante devido ao aumento do interesse verificado em materiais compósitos para aplicações aeronáuticas, especialmente em UAVs. Este trabalho foi realizado usando modelos FEM (Finite Element model), com o programa comercial Ansys.

O comportamento acústico de painéis sandwich é analisado através de curvas de transmissibilidade acústica obtidos a partir de três diferentes modelos: Cavidades acústicas (ideal), painel suspenso em fluido infinito (simulação de condições experimentais) e sistema de duas câmaras: de reverberação e anecóica (simulação de condições experimentais). Estes modelos foram testados e otimizados através de estudos paramétricos realizados para placas de referência.

Utilizando os modelos otimizados, múltiplos painéis foram analisados com diferentes: espessuras, materiais e amortecimento obtendo assim as curvas de transmissibilidade acústica para cada painel. A partir da análise destes gráficos foi possível concluir que um painel constituído por peles de fibra de carbono (exterior) e fibra de vidro (interior) e um núcleo de espuma Airex C70.75 apresenta melhor comportamento devido à sua elevada transmissibilidade acústica para baixas frequências e o primeiro modo estrutural (ressonância) que ocorre fora da frequência operacional

Palavras-chaves: Placas sandwich, transmissibilidade acústica, Resposta harmónica, Placas de fibra de carbono, Placas de fibra de vidro

Contents

IV List of Tables

V List of Figures

VI Acronyms

1C – single cavity model

2C – two cavity model

Abs – Absorbing

AM – Acoustic mode

BEM - Boundary Elements Method

B.E.L - Back Enclosed Loudspeaker

B.L. – Bare Loudspeaker

CD- Constant Damping

CDC – Constant Damping coefficient

FEM – Finite Elements method

FSI – Fluid-Solid interaction

PML – Perfectly matched layers

SM – Structural mode

SPL – Sound Pressure Level

STL – Sound Transmission Loss

Ref - Reflective

TL – Transmission Loss

UAV – Unmanned Aerial Vehicle

VII Nomenclature

Greek Symbols

α- absorption coefficient

α' - Constant for Mass Matrix

β – Constant for Stiffness matrix

ξ – Constant Damping Coefficient

μ - Mass per unit area of the sandwich

ν – Poisson ratio

ρ – Density

$\overline{\overline{\sigma}}$ – solid stress tensor

Roman Symbols

[M] – Mass Matrix

[K] – Stiffness Matrix

[C] – Damping Matrix

B – Loss factor of core

E – Young Modulus

f – Frequency

G – Shear modulus

I – Intensity

P – Pressure

P_0 – Reference Pressure

P_{ext} – Exterior Pressure

P_{int} – Interior Pressure

q - mathematical simplification $p = \dot{q}$

SPL – Sound Pressure Level

STL – Sound Transmission Loss

t_{fiber} – thickness of fibers (layer)

t_{foam} – thickness of foam

TL – Transmission Loss

Chapter 1 Historical Background

1.1. Learning Outcomes:

The learning outcomes of this chapter are:

- Composites in history
- Definition of composites and sandwich panels
- Introduction to UAVs
- Theoretical models
- Numerical models

1.2. Composites in history

Since the beginning of aircraft design, the most important concern has been weight. For this reason different materials have been used throughout history, beginning from simple materials like wood to advanced composite materials.

Considering these weigh concerns, aircraft design has been forced to adapt due to the necessity of materials to sustain: high flight loads, moisture problems and corrosion. With these three constraints, materials have changed: from wood to steel, to titanium and now composite materials are the main focus for current developers and researches in modern technology [1].

The concept of composite material is as old as nature itself, examples of this are wood (cellulose fibers), bones, adobe and straw bricks. Nevertheless the modern concept of composite has only started being developed in the end of the 19th century, when Thomas Edison produced carbon fiber filaments for the use in lamps [2].

The use of composite materials in aircraft design started after the invention of polyester resin, glass fiber and graphite filaments. This development started in the "Royal Aerospace Establishment" and ended with high resistance graphite fibers in Japan. The first aircraft that used modern composite material was the Grumman F-14, which used a boron/epoxy coating in the stabilizers. In present designs, aircraft structures such as the two most used commercial airplanes, the Airbus A350 [3] and the Boeing B787 [4], are comprised of 52% and 50% of the weight in composite materials, respectively.

1.3. Definition of composites and sandwich panels

A composite is the shortened version of what is called a composition material. It is defined by several materials that are combined together in order to form an overall structure with different properties from its components.

Composite materials are extremely good to manufacture critical components like airframes, wing structures, wing skins, fins, etc [5] due to the property ranges available. These properties can be adapted to a specific work load and conditions plus due to the great strength to weight ratio are particularly good for aeronautic applications.

Sandwich panels are multilayered structures that have two face sheets (skins) which are relatively thin, with high strength and stiffness, which enclose a relatively thick low density core in order to maintain the extremely high stiffness to mass ratio necessary in aeronautic applications. With the variability of skins and core materials, relative thicknesses and topology of cores can offer an unlimited scenarios for applications.

These materials, as mentioned before, are in theory perfect for aeronautic applications, but they have generally a major drawback in terms of acoustic performance and sound absorption. This bad acoustic behavior commonly occurs due to the lightweight nature of composite materials [6], making numerical and experimental acoustic results particularly important in sandwich panels design.

1.4. Unmanned aerial vehicles (UAV)

In 2007 a survey was performed where it was shown that UAVs: are in service in more than 50 countries, registered more than 500.000 flight hours and it is expected to grow at a logarithmic rate. This expectation occurred due to the focus of maximizing payload capacity and endurance the market for composite materials in UAVs is poised to grow 300% and will account for $55 billion (USD) by 2018[7].

In UAV design the weight consideration is especially important: from the 200 UAV designed [7] all of them include some composite parts. Glass and quartz fibers are used in sensors and nose cones while carbon fiber is used in the airframe structure. The wide range of UAVs sizes and configuration can be seen from the examples mentioned below.

- *Large fixed-wing* – aircraft with wingspans greater than 9.1m and powered by a turbine or turbofan jet engine. Examples include Northrop Grumman's RQ-4 *Global Hawk*; General Atomics' RQ-1 *Predator.*
- *Medium fixed-wing* – aircraft with wingspans ranging from 4.5m to 9.1m. Examples include AAI Corp.'s; *Shadow 200* and *Shadow 400*
- *Small/micro fixed-wing* – aircraft with wingspans less than 0.3m to 4.5m. Examples include RQ-11B *Raven* and *Wasp*.
- *Vertical takeoff and landing (VTOL)* – These unmanned systems include traditional helicopter, ducted-fan and tilt-rotor designs. Examples: Northrop Grumman's RQ-8 *Fire Scout*, A-160 *Hummingbird*, Bell Helicopter Textron's *Eagle Eye*.

1.5. Theoretical models

In this subchapter, we are going to study some early theoretical models developed in order to predict the sound absorption in sandwich panels. The authors being mentioned below developed models around isotropic cores and validated their model with experimental data:

Previously to introduce any theoretical model, it is important to introduce some important concepts in acoustics like sound pressure level and sound transmission loss.

Sound pressure level (SPL) is the logarithmic measure of the ratio between a measured pressure (P) and a reference sound pressure (P_0=20μPa) as seen in equation 1.

$$SPL = 10\log_{10}\left(\frac{P}{P_0}\right) = 10\log_{10}\left(\frac{P}{20\mu\text{Pa}}\right) \qquad (1)$$

Sound transmission Loss (STL) or Transmission Loss (TL) describes the decrease in acoustic power that occurs through a surface and is defined by the ratio between the acoustic power of the incident wave and the transmitted wave as shown in equation 2.

$$STL = TL = 10\log_{10}\left|\frac{W_i}{W_t}\right| \qquad (2)$$

Kurtze and Watters [8] investigated the propagation speed of both flexural and shear waves, the authors assumed that face sheets respond as thin elementary panels in bending, and an incompressible core where shear effects are added. The sum of bending and shear components is equal to the total impedance on the sandwich panel. This model is extremely important in applications, where it is necessary to prove that coincidence frequency can be moved to outside the range of interest. This can be performed by using different cores with variable shear wave speed.

Ford [9] investigated the effect of the natural frequencies, on the transmission loss of the sandwich panels. This model is based in a simply supported panel, where the core is modeled as a compressible three dimensional elastic medium with the core behavior being described by the following equations:

$$w_c(x,y,z)\sin(\omega t) = \left[\frac{(A_1+A_2)}{2} + \frac{(A_1-A_2)z}{2}\right]\sin(k_1x)\sin(k_2y)\sin(\omega t) \qquad (3)$$

$$u_c(x,y,z)\sin(\omega t) = \left[\frac{(B_1+B_2)}{2} + \frac{(B_1-B_2)z}{2} + D_1\cos\left(\frac{\pi z}{d}\right)\right]\cos(k_1x)\sin(k_2y)\sin(\omega t) \qquad (4)$$

$$v_c(x,y,z)\sin(\omega t) = \left[\frac{(C_1+C_2)}{2} + \frac{(C_1-C_2)z}{2} + D_2\cos\left(\frac{\pi z}{d}\right)\right]\sin(k_1x)\cos(k_2x)\sin(\omega t) \qquad (5)$$

Where:

1. u_c, v_c, w_c are displacements in the core along x,y and z
2. $k_1 = m\pi/L_1$, $k_2 = n\pi/L_2$ with n, m $\in \mathbb{Z}$ and L_1, L_2 are the in plane dimensions
3. d is core thickness
4. A_1, A_2, B_1, B_2, C_1, C_2, D_1 and D_2 are generalized coordinates

The generalized coordinates are obtained from the Rayleigh-Ritz minimum energy principle (8 equations for 8 unknowns). In further studies this eight equation system can be divided in anti-symmetric and symmetric motions uncoupling the system.

Ford to test his model, he investigated three different cores with increasing stiffness acoustic behavior. These experiments showed that opposite behaviors occurred in terms of the coincidence frequency: the symmetric modes increases and the anti-symmetric modes decreases, this could create dips in the transmission loss of the panels for much lower frequencies.

Smolenski and Krosky [10] developed a model that improved on the Ford model. These authors added to the model the influence of volumetric and shear terms in energy formulation. This study is based in the influence of cores on the natural frequencies and experimentally verified that the Poisson ratio and core thickness influences significantly the natural frequencies of the symmetrical modes.

Dym and Lang [11] were the first authors to consolidate a theoretical model that predicted the STL in unidirectional sandwich panels that assumed: thin panels only stretch and bend, transverse shear deformation and rotatory inertia are negligible in the skin but applied in the cores, and damping is not considered. The author derived a new model defined by a set of symmetrical and unsymmetrical displacements equations (6 and 7) that lead to a model that predicted transmission loss applying the Hamilton's principle consisting in two decoupled system of partial differential equations

$$[D_{symm}]\begin{Bmatrix}\bar{u}\\ \bar{w}\\ g\end{Bmatrix} = -\begin{Bmatrix}0\\ p_1 + p_2\\ 0\end{Bmatrix} \qquad (6)$$

$$[D_{ant}]\begin{Bmatrix}\tilde{u}\\ \tilde{w}\end{Bmatrix} = -\begin{Bmatrix}0\\ p_1 + p_2\\ 0\end{Bmatrix} \qquad (7)$$

Where 1. D_{symm} and D_{ant} are matrices of differential operators

2. $\bar{u}$,$\bar{w}$, $\tilde{u}$ and $\tilde{v}$ are the symmetric and anti-symmetrical displacements for x and y respectively
3. P_1 pressure load on the top skin (Sum of Incident pressure P_i and Reflected pressure P_r)
4. P_2 is the transmitted pressure

In order to introduce the transmission loss calculation a matrix $\bar{Z}$(symmetric), $\tilde{Z}$(Antisymmetric) and a modified Acoustic impedance Z_a.

$$\dot{\bar{w}}\bar{Z} = -(p_1 + p_2) \quad \dot{\bar{w}}\tilde{Z} = (p_1 - p_2) \quad Z_a = \frac{\rho_A c_a}{\cos\theta} \qquad (8.a, b, c)$$

With: $\rho_A, c_a \; and \; \theta$ are the air density, speed and angle of incidence of acoustic waves.

$$STL = 10\log_{10}\left|\frac{p_i^2}{p_t^2}\right| = 20\log_{10}\left|\frac{\left(1+\frac{\tilde{Z}}{2Z_a}\right)\left(1+\frac{\bar{Z}}{2Z_a}\right)}{\frac{\bar{Z}}{2Z_a}-\frac{\tilde{Z}}{2Z_a}}\right| \qquad (9)$$

It is important to note if the symmetric and anti-symmetric are coincident the transmission loss is reduced to zero which is verified by experimental results [10].

Narayanan and Shanbhag [12] model added damping in infinite sandwich panels separating two semi-infinite air spaces. The unidirectional equation 10 of motion of a three layer sandwich derived from the meads formulation [29]

$$\frac{\partial^6 w}{\partial x^6} - g'(1+Y)\frac{\partial^4 w}{\partial x^4} + \frac{\mu}{D_t}\left[\frac{\partial^4 w}{\partial x^2 \partial t^2} - g'\left(\frac{\partial^2 w}{\partial t^2}\right)\right] = \frac{1}{D_t}\left(\frac{\partial^2 p}{\partial x^2} - g'p\right) \qquad (10)$$

Where: g' = 2G (1-v^2) (1+iβ)/ (Etd) is the shear parameter of the core

Y=3(1+d/t) ^{2} is the geometric parameter

μ is the mass per unit area of the sandwich

G is the shear modulus of the core

β is the loss factor of the core

d is the thickness of the core

t is the thickness of the face sheets

v Poisson ratio

E is the young modulus of the skin

p resulting pressure loading on the panel

Assuming that the core bending stress is negligible compared with the face panel direct stresses, sandwich panel exhibits only anti-symmetric motion (there is no dilatational effect), the shear strains in the face panels in planes perpendicular are negligible as well. With this model it is possible to obtain radiated pressure on the skin surfaces using the transverse displacement when a harmonic acoustic wave is applied on the top surface. From the pressure radiated study, it was shown that the shear properties of the foam highly influence the transmission loss.

1.6. Numerical Models

Theoretical models are good to predict the acoustic behavior of panels with simple configurations but lack precision when sandwich panels start to become more complex, especially in the influence on core. This coupled with the development in computational power, has unbalanced the scales from using theoretical models to numerical models in the STL study of sandwich panels

Finite and boundary element models

The finite element method (FEM) [13] model discretizes both structural and acoustic. This makes the model appropriated in applications where the model is subjected to low frequencies, due to the unacceptable computational cost required for higher frequencies, since the size of the fluid elements is proportional to the

wavelength size. The discretization of the acoustic domain creates a major disadvantage in the FEM model so boundary element method (BEM) was introduced, which avoids the discretization of the fluid domain [14].

Assaf and Guerich [15] proposed a model where an "element-boundary" element is added, separating the structural model from the acoustic model. The structural model is discretized using the strain and kinetic energies using a three nodes triangular finite element. This model is applied in viscoelastic damped sandwich panels subjected to an acoustic plane wave or a diffuse field excitation. In order to validate this model a comparison between the transmission loss prediction and experimental results available in the literature [16] are conducted for low frequency.

Zhou and Crocker [17] introduced the two boundary element formulations with the coupled mode FEM/BEM to predict the sound transmission. The two boundary element formulation is defined by a light fluid approximation for the eigenmode series (structural domain) and an air loading that is treated as an added mass. The sandwich model is divided in skin and core, the skin is defined by panel elements (2 rotational and 3 translation degrees of freedom per node) and the core is defined by solid elements with three translational degrees of freedom. The results of this model was performed in a commercial model for aluminum and graphite fibers skins with a honeycomb filled foam and validated by experimental results for low frequencies [18].

Kim and Han [19] introduced HAFEM a hybrid analytical/finite element method to investigate the STL of composite sandwich panel. This model is the first that used a finite element approximation in the thickness direction, this creates a necessity for constant thickness layers and properties. This method can be accurate with using a single element for each layer, assuming that the displacement is approximated by the modal displacement. This model interpolates the equations of motion in the thickness dimension, by applying the virtual work principle. The HAFEM model is validated for a wide frequency range for an aluminum-foam-aluminum sandwich panel in the experimental domain, except for low frequencies due to the finite size effect of the specimen.

Statistical Energy analysis

This analyses was developed due to the increase in computational power necessary to perform FEM simulation for high frequencies. Lyon [20] introduced the statistical energy analysis. This type of analyses is used for high frequency regions being the results based on an energy method. The fundamental equation is obtained from the power balance of three different systems: source room, receiving room and the panel this calculation method is schematically represented in figure 1.

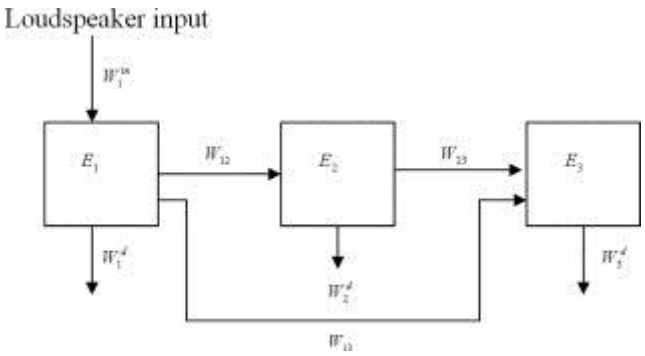

Figure 1 Statistical Energy analysis power balance for 3 subsystems

Where: W_1^{in} represents the input power

W_l^d represents the power dissipated

W_{ij} represents the power exchange between systems

E_i is total energy in the subsystem

This analyses has been improved in further studies by authors like Guyader and Lesuerur [21], Zhou and Crocker[22], Wang [23].

Chapter 2 Introduction

2.1. Learning Outcomes

The learning outcomes of this chapter are:

- Finite Element Program and the acoustic extension.
- Reference configurations (Panel dimension, Materials and Fiber orientation).

2.2. About this work

The aim of this work is to predict the acoustic behavior of sandwich panels in order to protect sensitive materials located inside a UAV structure from: sound and vibrations. This study was introduced by the Portuguese Air Force with the following objectives: optimize the plate design through FEM simulations and provide results that can be used in experimentally model.

The FEM simulations are going to be performed using a commercial finite element program (ANSYS) with an acoustic extension. This program was selected due to the straightforwardness of the modelling and theoretical material accessible.

Taking into consideration the objectives of this work, simulations are going to be modeled and parametric studies performed. The purpose of this study is to optimize the simulation setups and the panel design. Subsequently multiple sandwich panels, with different materials, thicknesses, layups and damping, are introduced and compared so that the best design for our problem is identified.

In this chapter, we begin our work by introducing the finite element program and the tasks involved in the modeling of the setups. Furthermore, panel dimensions, fiber orientation and available materials are going to be defined and introduced. These parameters are important to create standards and references, which will stay constant throughout this thesis.

2.3. Finite Element Program

The finite element program being used in this work is going to be ANSYS workbench version 15.0.7 with the extension ExtAcoustics150.43. This extension was incorporated in our standard Ansys workbench because it adds all the tasks required to perform the acoustic studies.

The tasks added are going to be explained in the succeeding sections:

- **Acoustic Body**

This task mainly transforms solid bodies, using solid elements (SOLID186), into a corresponding fluid body, defined by fluid elements (Fluid220). The Acoustic/Fluid bodies are defined by the following parameters in figure 2, where air properties are indicated and Fluid-Structure interaction is selected.

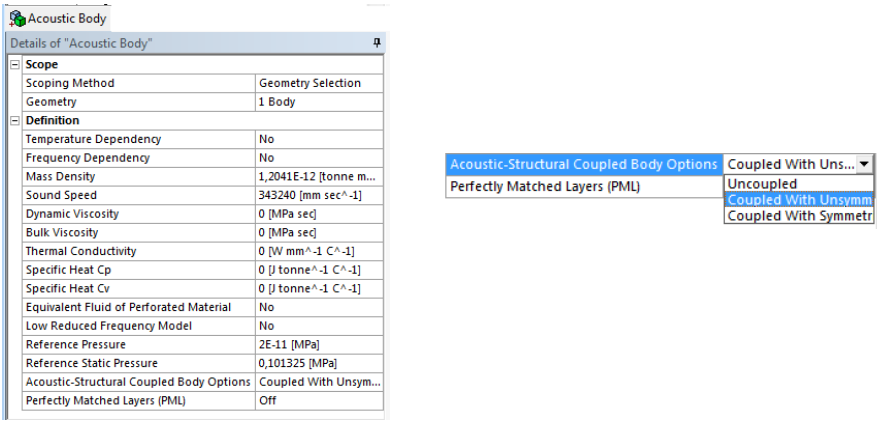

Figure 2 Acoustic Body function parameters and Acoustic Structural coupling options

The acoustic Structural Coupling can be uncoupled, coupled with unsymmetrical algorithm and coupled with symmetric algorithm. The uncoupled algorithm does not generate an interface between solid and fluid bodies, this means that pressure in the fluid creates no displacement in the structure and, conversely, displacements creates no pressure [24].

Symmetric and unsymmetrical algorithms need to create an interface between the fluid and the structure (FSI). Knowing this, both algorithms need to verify the following two conditions in the interface: the structure load is equal to the pressure load (equation 11.a) and the displacement of the structure is equal to the displacement of the fluid (equation 11.b)

$$\overline{\overline{\sigma}}(\overrightarrow{u_s})\vec{n} + p\vec{n} = 0 \qquad \vec{n} \cdot \overrightarrow{u_s} - \vec{n} \cdot \overrightarrow{u_f} = 0 \qquad (11.a, b)$$

The unsymmetrical algorithm [25] is obtained from the Mass and Stiffness matrices with the addition of a fluid pressure load (f^{pr}) as seen in the structural equation 12

$$[M_s]\ddot{\vec{u}} + [C_s]\dot{\vec{u}} + [K_s]\vec{u} = \{f_s\} + \{f^{pr}\} \qquad (12)$$

Although the structural equation is described, it is necessary to work it in order to transform our equation into a complete finite element discretized equations as shown in equation 13.

$$\begin{bmatrix} [M_s] & 0 \\ \overline{\rho_0}[R]^T & [M_F] \end{bmatrix} \begin{Bmatrix} \{\ddot{u_e}\} \\ \{\ddot{p_e}\} \end{Bmatrix} + \begin{bmatrix} [C_s] & 0 \\ 0 & [C_F] \end{bmatrix} \begin{Bmatrix} \{\dot{u_e}\} \\ \{\dot{p_e}\} \end{Bmatrix} + \begin{bmatrix} [K_s] & -[R] \\ 0 & [K_F] \end{bmatrix} \begin{Bmatrix} \{u_e\} \\ \{p_e\} \end{Bmatrix} = \begin{Bmatrix} f_s \\ f_f \end{Bmatrix} \quad (13)$$

Where:

- M_S, M_F, C_S, C_F, K_s and K_F are the mass, damping and stiffness matrices for solid and fluid elements, respectively.
- u_e and p_e represents element displacements and pressure.
- $[R] = \iint \{N'\}\{N\}^T \cdot \{n\} ds$ with N representing shape functions in order to discretize the displacement

Note: This equation assumes that the body size is not altered by the forces applied.

The symmetric algorithm [25] is a simpler version of the unsymmetrical algorithm that allows us to save: computational power and time. This algorithm is used when we are working with harmonic pressure loads in the frequency domain. The following equation can be introduced.

$$p = \dot{q} = j\omega q \quad (14)$$

By coupling equation 13 with equation 14, the coupled matrix equation is given by:

$$\left(-\omega^2 \begin{bmatrix} [M_s] & 0 \\ 0 & -\dfrac{[M_F]}{\overline{\rho_0}} \end{bmatrix} + j\omega \begin{bmatrix} [C_s] & -[R] \\ -[R]^T & -\dfrac{[C_F]}{\overline{\rho_0}} \end{bmatrix} + \begin{bmatrix} [K_s] & 0 \\ 0 & -\dfrac{[K_F]}{\overline{\rho_0}} \end{bmatrix} \right) \begin{Bmatrix} \{u_e\} \\ \{q_e\} \end{Bmatrix} = \begin{Bmatrix} f_s \\ \dfrac{jf_F}{\omega\overline{\rho_0}} \hat{f} \end{Bmatrix} \quad (15)$$

- Acoustic Excitations

Experimentally the most common excitations used are either a uniform pressure field distribution or common loudspeakers. In order to recreate this excitation numerically, surface velocity and loudspeaker approximations are going to be used.

The Surface velocity is used to achieve a uniform pressure field distribution across the top skin of our panel as verified in figure 3. We obtain a uniform pressure field by imposing a normal velocity on the faces of the fluid [24].

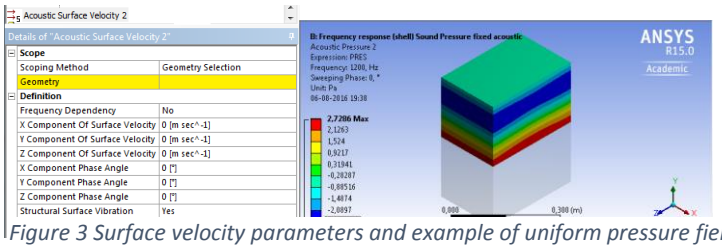

Figure 3 Surface velocity parameters and example of uniform pressure field

The acoustic wave source recreates loudspeakers in the computational domain. This basically approximates back enclosed loudspeakers and bare loudspeakers from monopoles and dipoles, respectively. Also the advantages and limitations of loudspeakers are going to be explained in further detailed in chapter 5 [24].

- Boundary conditions

The available boundary conditions include acoustic boundary conditions such as the acoustic radiation boundary and acoustic absorption surface.

The Acoustic Radiation boundary condition recreates a non-reflective surface. This condition is vital to model anechoic chambers, ducts and open “infinite” fluid domains.

The acoustic absorption surface is similar to the acoustic radiation boundary condition. Nonetheless, instead of merely being able to create a non-reflective surface, it can create partial reflective surfaces, which is a more realistic surface. This boundary condition is defined by the absorption coefficient α (alpha), which is the ratio between absorbed waves and incident waves, as seen in equation 16 [24].

$$\alpha = \frac{I_{absorved}}{I_{incident}} \quad (16)$$

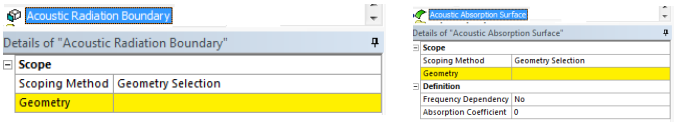

Figure 4 Acoustic Radiation Boundary and Acoustic Absorption Surface parameters

- Results

In this study, it is particularly important to scrutinize the pressure distribution and the panel total deformation, to identify acoustic modes and structural modes, in both harmonic response and modal studies. The identification of these modes is critical due to the unfavorable effect they have in the Transmission Loss through the panel. The acoustic pressure [24] and Total deformation [26] are shown in figure 5, for a specific frequency value in Hertz.

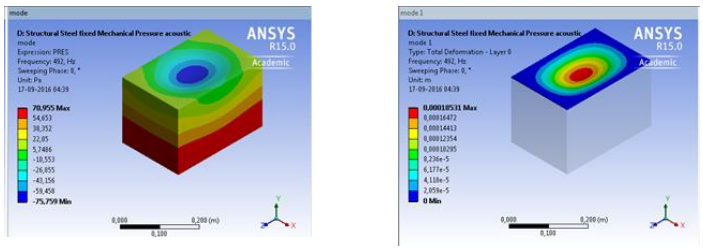

Figure 5 Example of pressure distribution and Total deformation

Taking into account that both acoustic pressure and total deformation only show us the results for a specific frequency, the acoustic sound pressure level (SPL) frequency plot is introduced and illustrated in figure 6

$$SPL = 20\log_{10}\left(\frac{P}{P_0}\right) \quad (17)$$

where P is the root mean square sound pressure and P_0 is the reference pressure (20µPa).

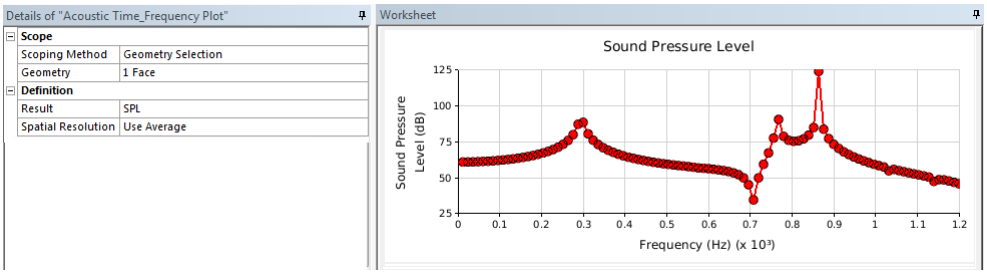

Figure 6 Example of an acoustic_time_frequency plot and its parameters

This type of plot is going to be essential to obtain the transmission loss versus frequency, SPL versus frequency and Pressure versus frequency plots that appear throughout this work. These are critical in predicting the acoustic behavior and identifying critical points of our panels.

2.4. Panel Dimensions

In this subchapter, we begin by defining the parameters that will remain constant throughout the work, starting with the most relevant: the panel dimensions.

Taking into consideration that the UAV is still in a preliminary stage of development, the dimensions of the panel are not explicitly provided, however the value of several parameters were established in order to obtain results as close to the final design as possible: an easy to model and to build geometry, a good length to width ratio, overall size and materials required.

The chosen geometry was a rectangular panel with 300mm x 200mm (Figure 7) because it ensures a simple geometry, overall small size, minor amount of materials needed and the 3/2 aspect ratio works well since double modes are avoided.

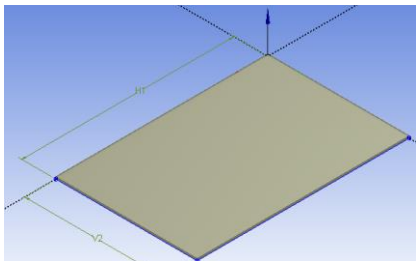

Figure 7 Panel geometry and dimensions

2.5. Available Materials

The available materials provided by the Portuguese Air Force are going to be carbon fiber, glass fiber and an aeronautic foam Airex C70.75 [10], being the last one described in detail in chapter 6.

Both Carbon Fiber and Glass fiber are orthotropic materials, so in order to define these fibers the following ten properties are required: mass density (ρ), Young moduli (E_1 , E_2 , E_3), Poisson coefficients (ν_{12} , ν_{13} , ν_{23}) and shear moduli (G_{12} , G_{13} , G_{23}). These properties are obtained using an inverse identification technique from the measured natural frequencies obtained in the experimental thesis and validated in chapter 3.

Taking into account that both carbon fiber and glass fiber are orthotropic materials, it is important to add an isotropic material like structural steel (standard material in Ansys) in order to simplify initial simulations without introducing material orientation problems, like auxiliary axis.

The following tables show both structural steel, carbon fiber and glass fiber properties:

	Carbon Fiber	Glass Fiber
ρ	1.5 g/cm^3	2.5 g/cm^3
E_1	78594 MPa	44603 MPa
E_2	11441 MPa	12626 MPa
E_3	11441 MPa	12626 MPa
ν_{12}	0.2079	0.34917
ν_{13}	0.2079	0.34917
ν_{23}	0.2079	0.34917
G_{12}	3502.1 MPa	5532.3 MPa
G_{23}	2927.6 MPa	4823.2 MPa
G_{13}	4083.1 MPa	5210.6 MPa

Table 2 Carbon Fiber and Glass Fiber properties

	Structural Steel
ρ	7.85 g/cm^3
E	200000 MPa
ν	0.3

Table 1 Structural Steel properties

2.6. Fiber Orientation

To finalize this chapter, fiber orientations are going to be defined. Knowing that in the experimental thesis the hand layup technique [27] is going to be used to build the panels, only 0º and 90º are going to be used in order to avoid a non-uniform fiber distribution and orientation, as well as an irregular thickness across the layup.

Chapter 3 Natural Frequencies and Modes Shapes

3.1. Learning Outcomes

The learning outcomes of this chapter are:

- Natural Frequencies and Structural modes of single material panels.
- Natural Frequencies and Acoustic modes of an acoustic cavity.
- Assessment of Solid Shell elements for single material panels.

3.2. Introduction

Before beginning any type of harmonic response analysis, multiple modal studies must be performed. These modal studies are critical for our analyses because of the importance of identifying acoustic and structural modes in the SPL versus frequency plots.

Initially in this chapter, the structural natural frequencies and mode shapes are calculated and identified for single material panels, with both clamped and free boundary conditions. Also for the carbon and glass fiber panels, these natural frequencies are going to be used to validate the properties introduced in chapter 2 by comparing the numerical natural frequencies with the experimental ones.

Subsequently after all structural natural frequencies and mode shapes are identified, the study of the acoustic domain begins. A modal study is performed for an acoustic cavity, in order to obtain acoustic modes and the respective natural frequencies. After all the acoustic modes and structural modes are recognized, we have all the information necessary to identify critical points in Pressure/SPL/TL versus frequency plots.

Lastly, a comparison between shell and solid elements is going to be performed. This study is made taking into account the computational time required when using solid elements, versus the precision in the analysis obtained for each type of element.

3.3. Procedures

In order to create simulations in ANSYS, three different sections need to be defined: Engineering data, geometry and model. Engineering data is where materials are added and its properties (density, isotropic/orthotropic elasticity and damping coefficients) are. After the engineering data is verified, it is necessary to draw the panels in terms of length, width and thickness in the geometry, section as seen in figure 8, for both solid and shell elements.

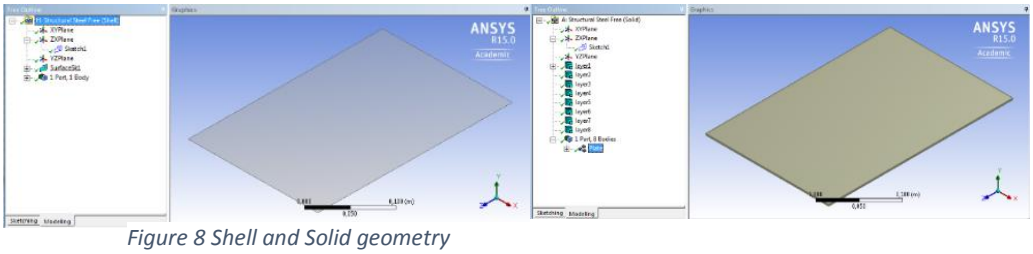

Figure 8 Shell and Solid geometry

For the shell elements, only a 300mm x 200mm surface is required, being the layup and thicknesses defined in the modeling section. However, for solid elements it is necessary to create one solid per panel layer and define the respective thickness.

In the modeling part, materials, orientations, excitations, boundary conditions and mesh are defined. Both shell and solid models are seen in figure 9.

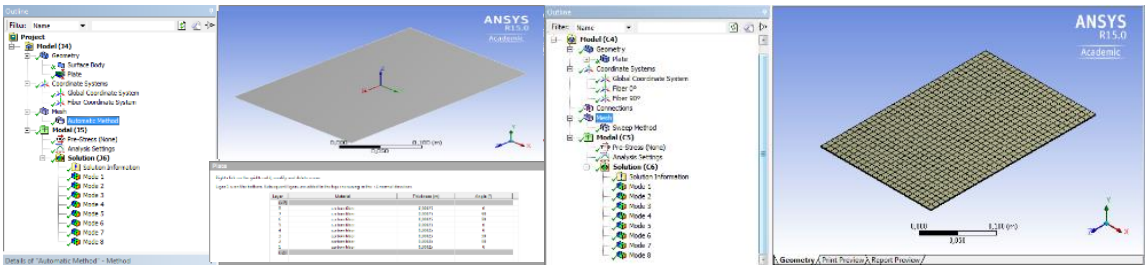

Figure 9 Shell and Solid panel model

For shell elements, the first step in the modelling section is to fully define the panel being studied. From the geometry section, we know that the number of layers, respective thicknesses, materials and fiber orientations need to be defined. Also, an auxiliary axis needs to be added in order to align the fiber direction with the main direction of our axis. This is important when working with orthotropic materials.

In terms of mesh options, an all quad method is selected and mid-side nodes are activated with a body sizing option.

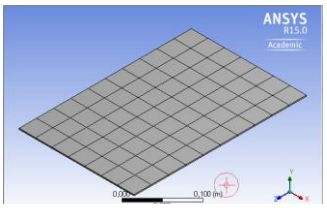

Figure 10 Example of Shell mesh

After the panel and mesh are completely defined, the boundary conditions are applied to the 4 edges of the surface (free or clamped).

For solid elements a similar process is applied, with the following differences: the thicknesses are defined in the geometry section and each layer is treated as a different body, where fiber orientation and material are applied separately.

Regarding the mesh, a quadrilateral dominant mesh, with mid-size nodes is applied, as seen in figure 11.

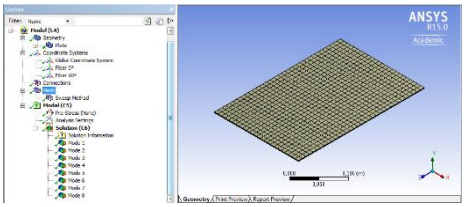

Figure 11 Solid model and mesh

3.4. Convergence of highest mode

In order to work with finite elements, it is always necessary to perform a convergence study, to define the finite element dimensions that can be applied, minimizing numerical errors. This study is performed by using elements with dimensions of 100 mm and then switching to smaller elements, until the 8th natural frequency (highest experimental mode detected) converges, as seen in figure 12 for both shell(SHELL181) and solid

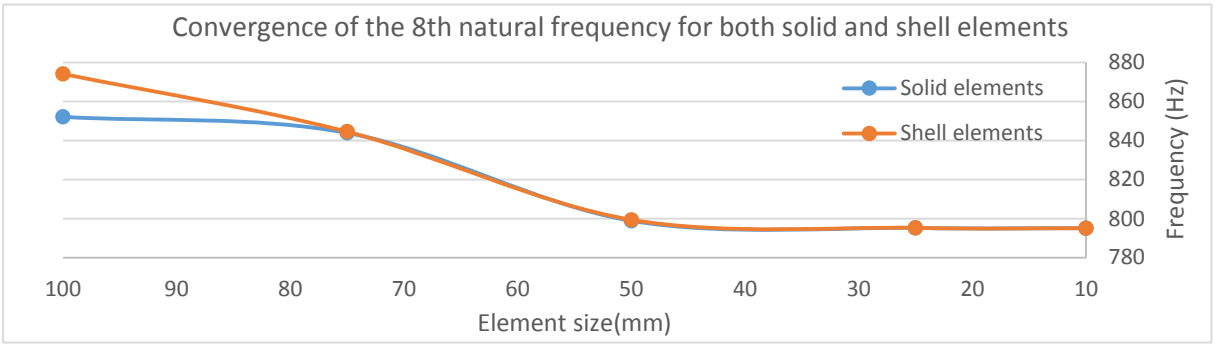

Figure 12 Convergence of the 8th natural frequency for both shell and solid elements

elements(SOLID186).

Solid and shell elements converge for finite elements equal or smaller than 50 mm, with a relative error of 0.54% and 0.47%, respectively. Taking these errors into account, solid and shell elements smaller than 50 mm are going to be used in future studies.

However, in this chapter we also want to identify the acoustic modes for an acoustic cavity of 300mm x 200mm x 200mm, so fluid elements need to be introduced. Similarly to the study performed for structural elements, the convergence of the 8th mode is considered for fluid elements (FLUID220), starting with elements of size 100 mm, as seen in figure 13.

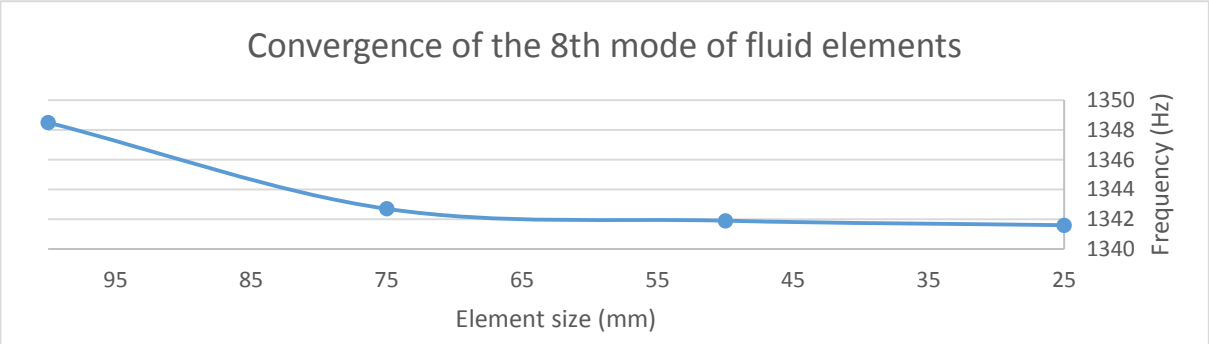

Figure 13 Convergence of the 8th natural frequency for fluid elements

Similarly to solid and shell elements, fluid elements start to converge after 75mm, with a relative error of 0.81%. So for an acoustic cavity study 75mm or smaller elements are going to be used.

These elements sizes are selected taking into account: the numerical errors, computational power and time required.

3.5. Structural Natural Frequencies for Free and Clamped panels

In this section, the single material panels are being analyzed and information regarding the mesh used for both solid and shell discretizations is shown in table 3. Additionally, the natural frequencies for both clamped and free boundary conditions are presented in tables 4, 5 and 6 and compared to the experimental ones, if available.

Single material Panels (Reference Panels)

	Structural Steel Panel	Carbon Fiber Panel	Glass Fiber Panel
Dimensions			
Length	300mm	300mm	300mm
Width	200mm	200mm	200mm
Thickness	3mm	2mm	4mm
Mesh Information			
Solid Mesh Type	Quadrilateral	Quadrilateral	Quadrilateral
Solid Mesh element	SOLID186	SOLID186	SOLID186
Solid Mesh size	50mm	50mm	50mm
Shell Mesh Type	QUAD	QUAD	QUAD
Shell Mesh element	SHELL181	SHELL181	SHELL181
Shell Mesh size	50mm	50mm	50mm
Layup			
Stacking	$[0/90/90/0]_s$	$[0/90/90/0]_s$	$[0/90/90/0]_s$
Layer thickness	0.375mm	0.25mm	0.5mm

Table 3 Single material panel dimensions, mesh, stacking and thickness

Structural Steel Panel

Mode	Free (solid)	Free (shell)	Difference (%)	Clamped (solid)	Clamped (shell)	Difference (%)
1	161.98Hz	162,06Hz	0,049389	491.8Hz	492,46Hz	0,134201
2	173.43Hz	173,45Hz	0,011532	758.83Hz	762,93Hz	0,540305
3	373.42Hz	373,55Hz	0,034813	1201.8Hz	1208,2Hz	0,532535
4	404.05Hz	404,28Hz	0,056924	1209Hz	1222,2Hz	1,091811
5	466.39Hz	466,66Hz	0,055747	1449.2Hz	1468,8Hz	1,35247
6	541.43Hz	541,8Hz	0,068338	1829.4Hz	1864Hz	1,89133
7	691.68Hz	692,64Hz	0,138793	1870.5Hz	1923,3Hz	2,822775
8	795.08Hz	795,26Hz	0,022639	2270.9Hz	2307,4Hz	1,607292

Table 4 Structural Steel natural frequencies and shell/solid comparison

Table 4 shows the natural frequencies for structural steel panels. The maximum error obtained in this panel is 2.8% for the 7th mode in clamped conditions

Carbon Fiber panel

Mode	Free (solid)	Free (shell)	Difference	Exp. values	Difference	Clamped (shell)	Clamped (solid)	Difference
1	53,449Hz	53,499Hz	0,093%	53Hz	0,840%	293,92Hz	294,32Hz	0,136%
2	130,74Hz	130,76Hz	0,015%	125Hz	4,390%	458,4Hz	460,15Hz	0,381%
3	169,81Hz	169,85Hz	0,023%	164Hz	3,421%	723,28Hz	726,86Hz	0,494%
4	255,72Hz	255,86Hz	0,054%	265Hz	3,621%	770,26Hz	776,15Hz	0,764%
5	276,86Hz	276,95Hz	0,032%	285Hz	2,940%	823,26Hz	831,79Hz	1,036%
6	360,52Hz	360,88Hz	0,099%	345Hz	4,304%	1053,1Hz	1075,8Hz	2,155%
7	361,63Hz	361,64Hz	0,008%	365Hz	0,931%	1210,9Hz	1228,4Hz	1,445%
8	394,17Hz	394,64Hz	0,119%	378Hz	4,102%	1383,9Hz	1405,4Hz	1,553%

Table 5 Carbon Fiber panel natural frequencies and shell/solid comparison

Table 5 shows us the natural frequencies for a fully carbon fiber panels and the corresponding experimental values. The maximum error obtained in this panel is of 2.15% for the 6th mode in clamped conditions. It can also be observed a relatively good agreement between the numerical and the experimental natural frequencies, with deviations lower than 5%. Manufacturing issues and irregular geometry of the carbon fiber panel are responsible for these deviations, as the material properties used in this studied were identified using an inverse technique.

Glass Fiber panel

Mode	Free (solid)	Free (shell)	Difference	Exp.Values	Difference	Clamped (solid)	Clamped (shell)	Difference
1	102,69Hz	102,72Hz	0,029%	98Hz	4,567%	388,48Hz	388,53Hz	0,012%
2	160,93Hz	160,96Hz	0,018%	163Hz	1,286%	607,44Hz	608,43Hz	0,162%
3	263,44Hz	263,48Hz	0,015%	257Hz	2,444%	945,6Hz	948,69Hz	0,326%
4	328,85Hz	329,03Hz	0,054%	295Hz	10,293%	998,89Hz	1003,7Hz	0,481%
5	382,92Hz	383,11Hz	0,049%	352Hz	8,074%	1110,5 Hz	1116,6 Hz	0,549%
6	449,89Hz	450,34Hz	0,100%	454Hz	0,913%	1432 Hz	1447,5Hz	1,082%
7	541,07Hz	541,6Hz	0,097%	526Hz	2,785%	1543,3 Hz	1560,3Hz	1,101%
8	557,18Hz	557,41Hz	0,041%	540Hz	3,083%	1787,8 Hz	1811,6Hz	1,331%

Table 6 Glass Fiber panel natural frequencies and shell/solid comparison

Table 6 shows us the natural frequencies for a fully glass fiber panels and the corresponding experimental values. The maximum error obtained in this panel is of 1.33% for the 8th mode in clamped conditions. It can also be observed a relatively good agreement between the numerical and the experimental natural frequencies, with deviations lower than 10.5%. Similar to the carbon fiber panel manufacturing issues and irregular geometry of the glass fiber panel are responsible for these deviations, as the material properties used in this studied were identified using an inverse technique.

3.6. Structural Steel Panel Clamped modes and Acoustic Natural Frequencies and Acoustic modes

Knowing that in future chapters SPL vs frequency plots are going to be analyzed, it is necessary to identify structural modes and acoustic modes that appear in these plots. These modes appear as an increase in SPL for specific frequency values. In order to identify these modes, both total deformation in the panel and pressure distribution in the acoustic cavity are necessary. The modes shapes of structural steel panel (Reference Panel) are shown in figure 15:

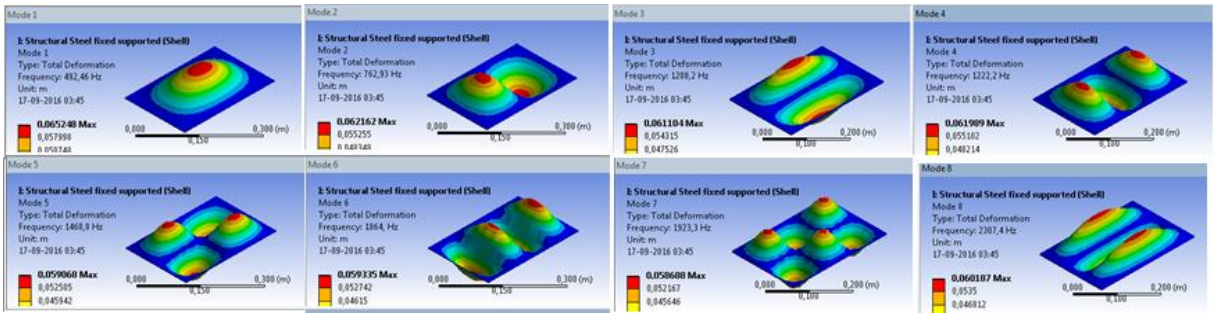

Figure 15 Structural mode shapes for a clamped Structural Steel Panel

After the structural modes are obtained we proceed to study the acoustic cavity. This cavity dimensions and mesh parameters are discretized in table 7.

From the model study, the cavity the modes frequencies and shapes are shown in table 8 and figure 17 respectively:

Dimensions	
Length	300mm
Width	200mm
Height	200mm
Fluid Mesh Type	Quadrilateral
Fluid Mesh element	FLUID220
Fluid Mesh size	75mm

Table 7 Acoustic Cavity dimensions and Mesh

Mode	Acoustic Cavity
1	572,07Hz
2	858,11Hz
3	858,11Hz
4	1031,3Hz
5	1031,3Hz
6	1144,2Hz
7	1213,5Hz
8	1341,6Hz

Table 8 Acoustic cavity natural frequencies

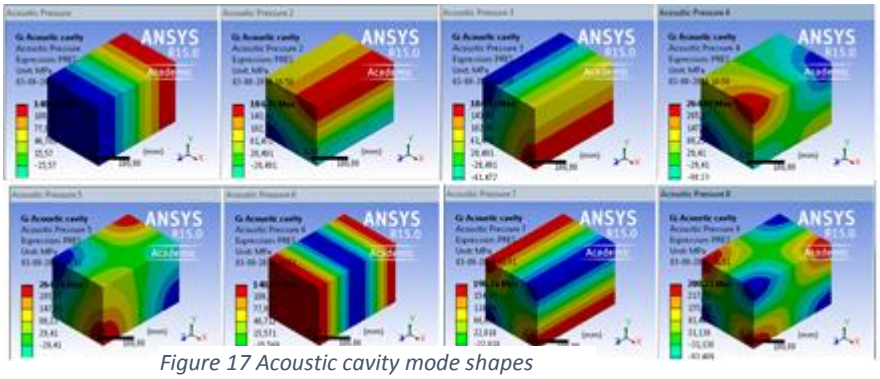

Figure 17 Acoustic cavity mode shapes

3.7. Solid Shell comparison

To finalize this chapter the differences between the shell element and the solid element are going to be discussed. Knowing that from seeing tables 4, 5 and 6 the maximum relative error is 2.8%, which is negligible in the terms of this work. We can conclude that shell elements can be used in one material panels in order to predict its acoustic behavior, which is going to save in both simulation time and computational power.

To finalize this chapter, the differences between the results obtained using the shell elements and the solid elements are going to be discussed. From analyzing tables 4, 5 and 6, one can conclude that the maximum deviation is 2.8%, which is negligible in the terms of this work. We conclude that shell elements can be used with advantage in single material panels in order to predict the acoustic behavior, since they are much less demanding in terms of computational resources than the solid elements.

Chapter 4 Acoustic Cavity with mechanical excitation

4.1. Learning Outcomes

The learning outcomes of this chapter are:

- Acoustic cavity model.
- Panel + acoustic cavity natural frequencies and mode shapes.
- Effect of concentrated forces.
- Effect of response measurement locations.
- Effect of different boundary conditions.
- Effect of different cavity dimensions.

4.2. Introduction

In this chapter the study of harmonic response is conducted, starting with a simple ideal acoustic cavity with a mechanical pressure excitation on top of the panel. The objective of performing this ideal setup is to obtain the SPL versus frequency plot in a specific frequency range [0, 1200Hz]. The plots obtained are going to show us the acoustic behavior of panels and critical points in this frequency range. Knowing the frequency values for critical points, it is possible to identify if these points correspond to either an acoustic or a structural resonance. Moreover, in order to improve this setup and check the effect of numerous parameters, multiple simulations have been performed and compared.

4.3. Model

This model is composed by a panel (red), discretized with Shell181 (25mm) elements and an acoustic cavity below (grey), defined with Fluid220 (25mm). The panel is made of structural steel with 4mm thickness and is clamped on all sides. The acoustic cavity delimited by fully reflective rigid walls in order to recreate a reverberation chamber.

Subsequently, after the panel and acoustic cavity are fully defined: the SPL versus frequency plot can be obtained and an example of this type of plot can be seen in figure 18. This plot shows the acoustic behavior of the panel in response to a uniform mechanical pressure of 1Pa applied on top of the panel.

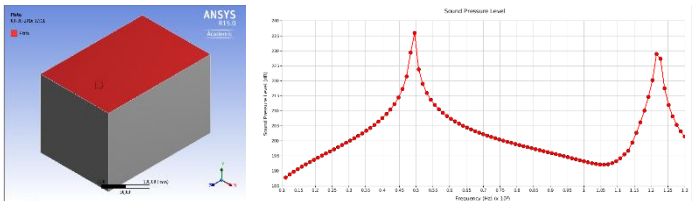

Figure 18 Acoustic cavity with mechanical excitation model and example of SPL vs frequency

Also in figure 18, we can see that the frequency range in the plot above starts at 0Hz and ends at 1200Hz. This frequency range was chosen taken into account that the main source of acoustic pressure will come from the UAV motor, which in normal operational conditions works between 300-600Hz.

4.4. Procedure

As explained in the model, this setup consists of a panel coupled with an acoustic cavity system. Since the engineering data and plate geometry are described in chapter 2, only the acoustic cavity needs to be defined here. Taking into account the dimensions of the panel, the acoustic cavity consists of a parallelepiped with the following dimensions 300mm x 200mm x 200mm.

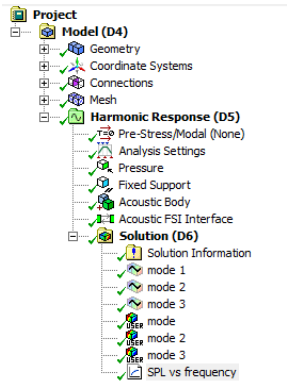

Figure 19 Single cavity model

In Figure 19 all the tasks applied in the modeling can be seen: the 1Pa pressure applied on top of the panel, the clamped boundary conditions and the Acoustic FSI interface that creates a connection between the panel and the fluid.

Also in figure 19 we can see the Results section where: a SPL versus Frequency plot is obtained from the pressure measured in the center of the bottom face and the total panel deformation and Acoustic pressure for critical frequencies.

4.5. Natural frequencies for single cavity model

In this section, the modal study results of the panel coupled with an acoustic cavity (system frequency) is performed and its acoustic modes and structural modes are identified.

In table 9 we can see the natural frequencies for three different modal study: system (panel + cavity), panel and acoustic cavity. Taking into account the three modal studies results we can conclude that:

Mode	System Frequency	Panel Frequency	Acoustic Cavity Frequency
1	492.01Hz	492,46Hz	572,07Hz
2	571.72Hz	762,93Hz	858,11Hz
3	762.3Hz	1208,2Hz	858,11Hz
4	857.93Hz	1222,2Hz	1031,3Hz
5	858.68Hz	1468,8Hz	1031,3Hz
6	1031.2Hz	1864Hz	1144,2Hz
7	1031.9Hz	1923,3Hz	1213,5Hz
8	1143.7Hz	2307,4Hz	1341,6Hz

Table 9 Natural Frequency System Panel coupled with an acoustic cavity, Panel and acoustic cavity

- Structural modes occurs when system frequencies are similar to panel frequencies and the acoustic pressure distribution follows the pressure created by the displacement of the panel.
- Acoustic modes occurs when the acoustic cavity frequency is similar to system frequencies and the acoustic pressure distribution resembles acoustic modes obtained in chapter 1 for the acoustic cavity without the panel.

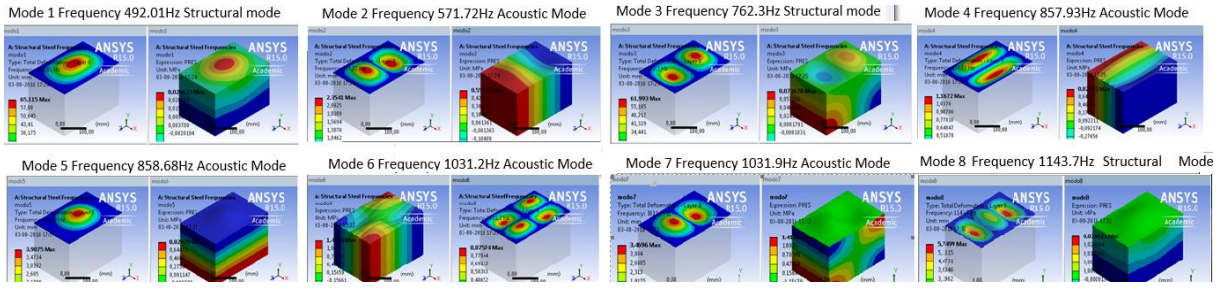

Figure 20 Structural modes and Acoustic modes

Analyzing figure 20, it can be seen that system mode 1(492.01Hz), 3(762.3Hz) and 8(1143.7Hz) are structural modes and correspond to the panel frequencies mode 1 (492.46Hz), mode 3 (762.3Hz) and mode 4 (1222.2Hz) respectively, also it can be seen that the pressure field is a consequence of the panel displacement.

Subsequently, modes 2(571.72Hz), 4(857.93Hz), 5(858.68Hz), 6(1031.2Hz) and 7(1031.9Hz) are acoustic modes and correspond to the acoustic cavity mode 1 (572.07Hz), mode 2(858.11Hz), mode 3(858.11Hz), mode 4(1031.3Hz) and mode 5(1031.3Hz), respectively. Furthermore the pressure fields seen in figure 20 can be compared with the ones obtained in the acoustic cavity in figure 17.

4.6. SPL frequency plots

Once the single cavity modal study was performed and the critical modes are identified, we can now start our harmonic study.

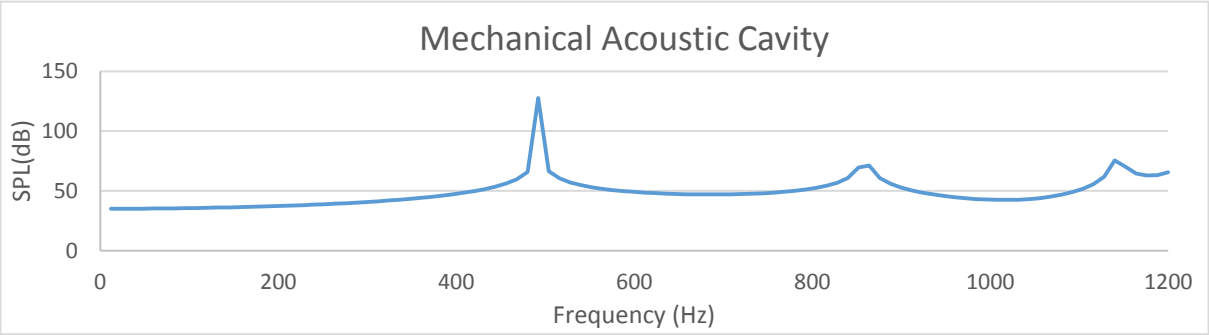

Figure 21 Structural modes and Acoustic modes of Panel + Acoustic cavity model

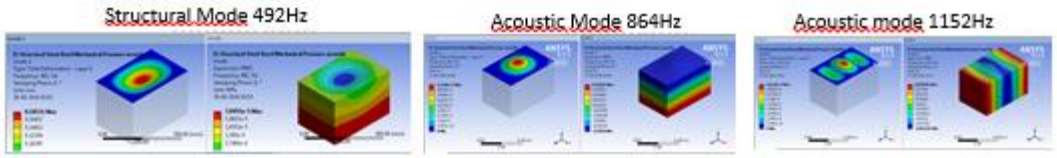

Figure 22 Structural and acoustic modes detected in the SPL vs frequency

In figure 21, the SPL frequency plot exhibits the acoustic behavior of a structural steel panel. By analyzing the plot it can be seen, that there are 3 different critical points, where the SPL increases drastically located at 492Hz, 864Hz and 1152Hz.

- The 492Hz mode is a structural mode that corresponds to the first structural mode 492.46Hz from the single cavity modal study.
- The 864Hz mode is an acoustic mode, this mode corresponds to the 5th mode of the panel acoustic system and the third acoustic mode 858.68Hz.
- The 1152Hz mode is an acoustic mode that doesn't appear in the fluid plus panel system model, but this acoustic mode corresponds to the 6th mode 1144.2Hz obtained in the acoustic cavity model study performed in chapter 3

Logically, only some modes appear in the SPL frequency plot. This can be explained by structural modes that create a zero change in the acoustic cavity volume(structural mode 2 and 3) and acoustic modes that generate an average amplitude of zero in the center point of the bottom face (acoustic modes 2, 3 and 4).

4.7. Effect of concentrated forces

In this subchapter the uniform pressure of 1Pa is going to be replaced by a concentrated force, applied at different locations. This is performed to understand the effect of the excitation in the acoustic behavior of a structural steel panel. Also, in order to compare both of these types of excitation, the magnitude of the force is defined by equation 18:

$$F = PA = 1 \times 0{,}06 = 0{,}06N \quad (18)$$

Knowing that the corresponding magnitude is 0.06N, the only variation remaining is the position where the concentrated force is applied. In figure 23 two different points are seen: one placed in the center of the top panel and another one placed at a point away from the center.

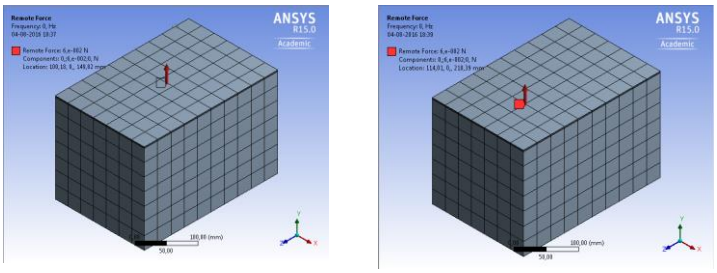

Figure 23 Location of concentrated forces

The following plot shows the acoustic behavior of the structural steel panel for the three different excitations:

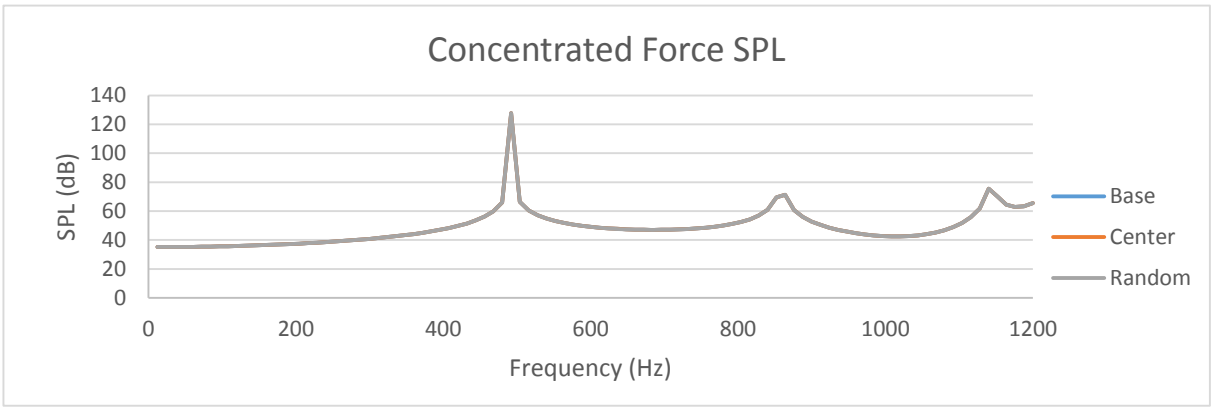

Figure 24 Comparison between concentrated forces and uniform pressure field

Analyzing the plot above, it is possible to conclude that applying a concentrated force at different locations, only small changes in the SPL frequency plot are obtained. These small changes occur in the 0.03dB range which can be neglected since the normal working range is around 40-60dB for the 0Hz to 1200Hz range.

4.8. Effect of response measurement location

After the concentrated force study, the next step is to test different response measurement locations. This study is performed with the intention of seeing if different measurement locations can register more modes than the one used in the reference setup. To perform this test, three different simulations are going to be studied: point 1 is going to be the center point of the bottom plane, point 2 is going to be placed away from the center and to finalize this study the bottom face is also tested with the results being shown in figure 25:

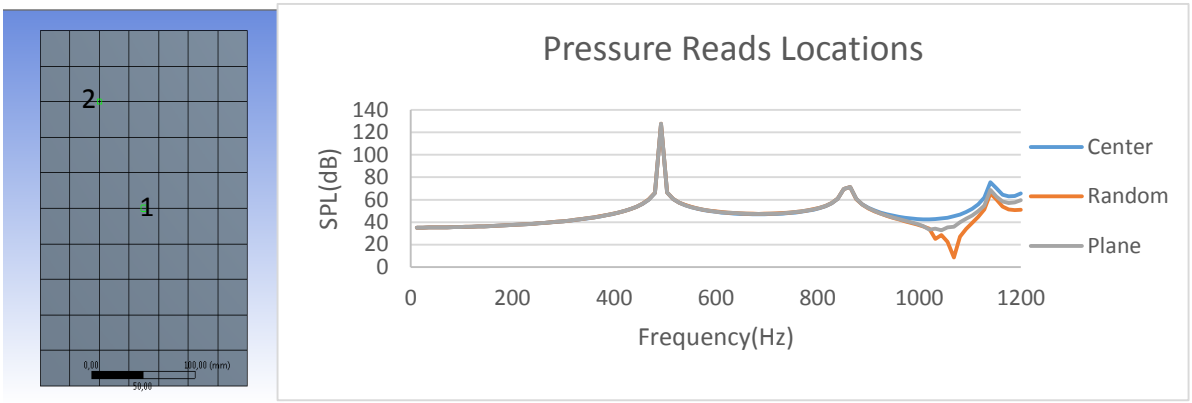

Figure 25 Pressure reads location and SPL comparison between different measurement point locations

Knowing the SPL frequency plot for the three variants mentioned above, it can be seen that significant differences occur in the 984-1200 Hz frequency range. The highest difference in SPL occurs at the frequency of 1068Hz.

In figure 26 the pressure distribution (1068Hz) is shown and it can be seen that a decrease in SPL occurs as we get closer to the acoustic walls normal to the z axis. This explains the decrease in SPL seen in the random point.

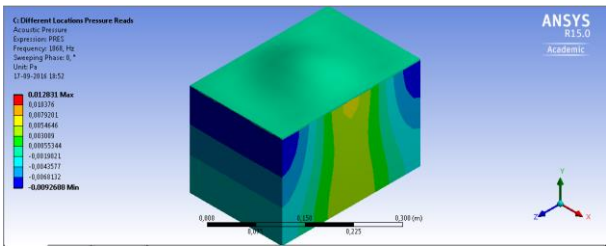

Figure 26 Pressure distribution for 1068Hz

The bottom face study reveals a similar acoustic behavior to the one seen in the center point, only with a slight decrease in the SPL (≈3dB). This effect can be explained due to the fact that the pressure drops closer to the acoustic cavity walls and since this SPL is obtained from the average SPL of all points in the bottom face, these points closer to the walls are going to present lower pressures than the ones measured at the center point.

With this study it can be concluded that the choice of the pressure measurement location is extremely important in order to detect points where a reduction in the SPL occurs. Taking into account this study, it is important to mention that we can have a decrease in SPL without changing the panel design. This can be important when working with pressure sensitive materials. However, in this work the objective is to create an optimized setup to compare different panels, knowing this we can choose a random location. For simplicity point 1 is going to be used in future studies.

4.9. Effect of different boundary conditions

Most acoustic studies in ideal conditions are performed in either acoustic cavities or ducts. With this in mind and knowing that the only difference between those two models are their boundary conditions it is important to see the effect of these conditions in the acoustic behavior of the panels.

To study this effect, three different models are going to be introduced: acoustic cavity (reverberation chamber), duct (bottom face is non-reflective) and open (anechoic chamber) as shown in figure 27.

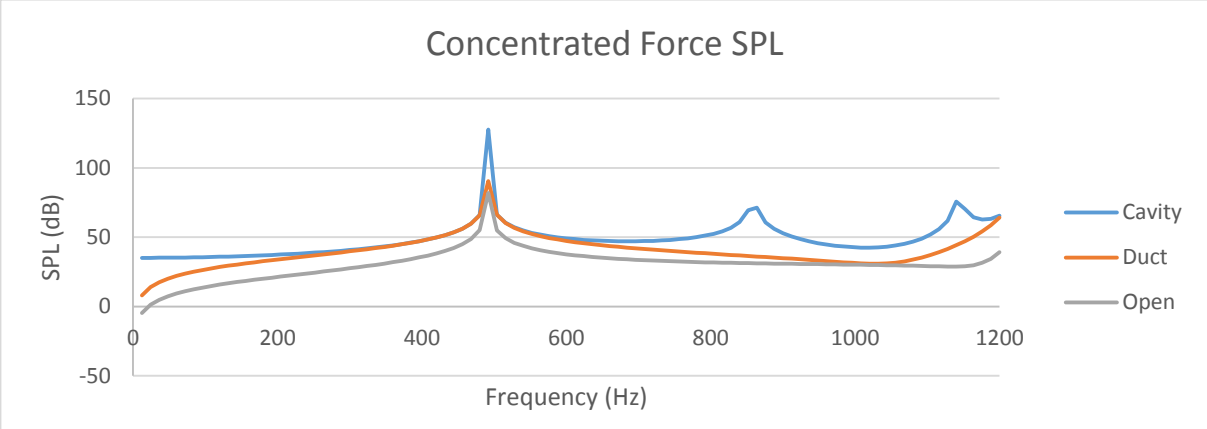

Figure 27 SPL comparison for different boundary condition

From the SPL frequency plot, we can see that the structural mode (492Hz) suffers a reduction in SPL for both the duct and the open conditions, this can be explained by the waves absorbed on the acoustic cavity walls. The effect of the bottom wall being non-reflective can be obtained from comparing the acoustic cavity with the duct where a decrease of 37.1dB (127.63dB to 90.53dB) is calculated. Using a similar procedure to compare the duct and open conditions, the effect of non-reflective side walls is a decrease in SPL of 8.57dB (90.53dB to 81.96).

After seeing the effect of boundary conditions in structural modes, the analyses of acoustic modes begin. From the plot we can see that both acoustic modes are absorbed when one non-reflective surface is applied in the setup. Figure 28, shows the pressure distribution for both frequency values (876Hz and 1148Hz) and we can clearly see a drastic change in the pressure distribution.

,

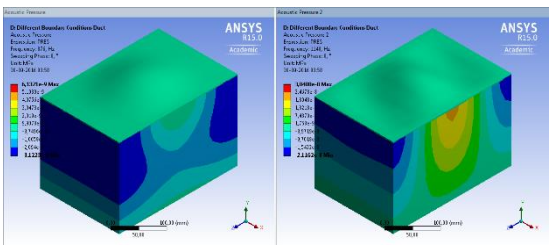

Figure 28 Pressure distribution at 876Hz and 1148Hz

4.10. Effect of the height of the acoustic cavity

The effect of the cavity height in the acoustic behavior will be studied now, for a structural steel panel. In order to perform this study three different cavity heights (100mm, 200mm and 300mm) are going to be tested.

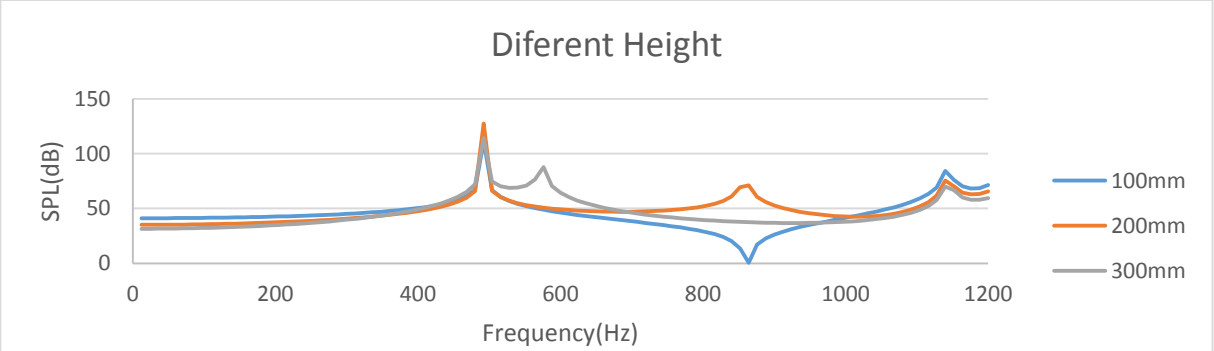

Figure 29 SPL comparison for different acoustic cavity height

The plot above shows the SPL vs frequency results for three acoustic cavities with variable height. The first acoustic mode detected seen in figure 29.

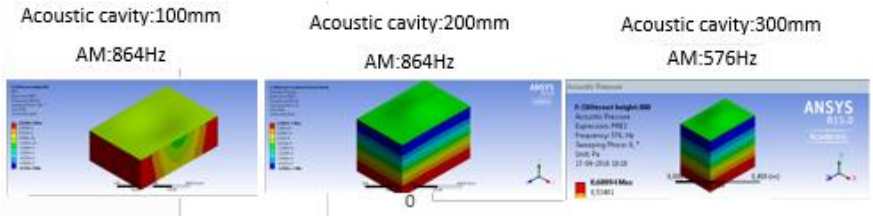

Figure 30 First detected acoustic mode for each acoustic cavity

From figure 30, we can see that the acoustic modes 864Hz (200mm) and 576Hz (300mm) are similar in terms of pressure distribution and acoustic behavior, with the only difference occurring in the frequency value. However for mode 864Hz (100mm) a difference in mode and acoustic behavior occurs as seen in the respective pressure distribution.

The second acoustic mode has a frequency of 1140Hz and is shown in figure 31. This mode has a particular behavior both the frequency value and the mode do not depend on the cavity height. This conclusion can be validated by the pressure distribution shown below, where it is clear that this mode is independent from the height of the cavity.

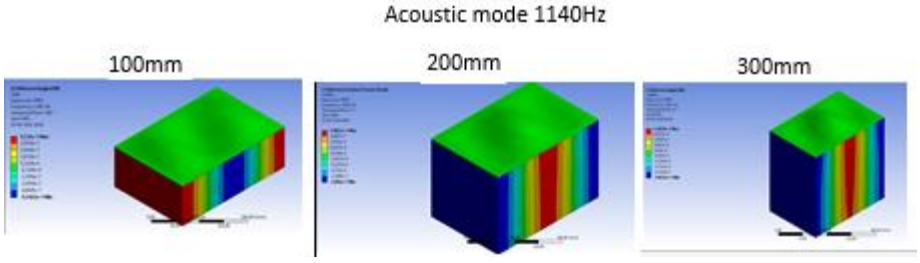

Figure 31 Second detected acoustic mode 1140Hz

Chapter 5 Two Acoustic Cavities with Sound Pressure Excitation

5.1. Learning Outcomes

The learning outcomes of this chapter are:

- Two acoustic cavities model.
- Natural frequencies and mode shapes
- Comparison between the one cavity model and two cavity model.
- Effect of different sound pressure excitation.
- Effect of reflection on the panel.
- Effect of damping on the panel.

5.2. Introduction

In this chapter, we introduce the two acoustic cavities model. This model is presented in order to understand the effect of sound pressure excitation on the acoustic behavior of our panels.

To show the results of this model, an example is shown for the acoustic behavior of a structural steel panel (defined with solid elements) where the critical modes are identified. After the results are analyzed, a comparison in terms of SPL between the single cavity and two cavity models is performed, in order to see if the acoustic behavior changes between these models.

5.3. Model

This model is composed by two acoustic cavities with the panel separating them as seen in figure 32. The bottom cavity is fully constrained with reflective walls, and the top cavity is a duct with the top face fully absorbing. This boundary condition is used in order to be able to apply a uniform pressure gradient as seen in figure 32.

To obtain a uniform pressure field in the z0x plane, a constant velocity is applied normal to the top face with a velocity of 1.2099mm/s. This velocity is applied in order to obtain a 1Pa pressure on top of the panel, as seen in figure 32, where there is a constant pressure across the frequency range, except on the frequency 492Hz that corresponds to the first structural mode where there is a pressure of 0.38Pa.

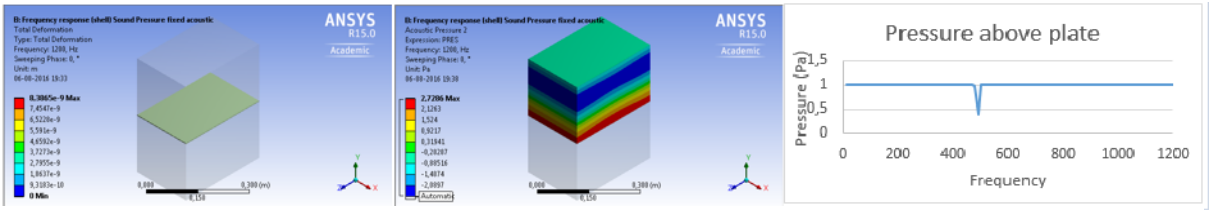

Figure 32 Two cavity model, uniform pressure field applied and pressure above the panel

5.4. Procedure

Using the geometry defined in subchapter 4.4 for the singly cavity model an addition is made to recreate the second acoustic cavity (300mmx200mmx200mm).

The model can be seen in figure 33 and similar conditions are applied in both acoustic cavities, except on the top cavity where a radiant boundary condition is needed to be made in order to obtain the uniform pressure field.

Also, it is important to note that the panel is defined with solid elements (Solid186 with 25mm) in order to avoid problems in applying the FSI conditions.

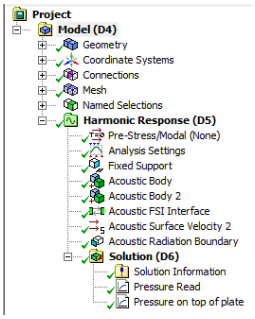

Figure 33 Two cavity modelling

5.5. Natural Frequencies, Modes and Harmonic response

In order to analyze the results of this model, a similar procedure from the single cavity model (1C) is going to be used. First the modal study is performed with the values for the two cavity model (2C) shown in table 10. Then the harmonic study to obtain the panel (structural steel) acoustic behavior.

Mode	Frequency2C	Frequency1C
1	491.6Hz	492.01Hz
2	571.37Hz	571.72Hz
3	572.07Hz	762.3Hz
4	761.71Hz	857.93Hz
5	857.73Hz	858.68Hz
6	858.12Hz	1031.2Hz
7	858.12Hz	1031.9Hz
8	859.23Hz	1143.7Hz

Table 10 Sound Pressure and Mechanical acoustic natural frequencies

Knowing that both acoustic cavities have the same dimensions, it is expected that the acoustic modes are going to be doubled, for example mode 2 (571.72Hz) of the one cavity model occurs in the two cavity models as seen in modes 2 and 3 (571.37Hz and 572.07Hz). The two cavities modes are represented in figure 34 and by seeing the pressure distribution the double modes can be detected.

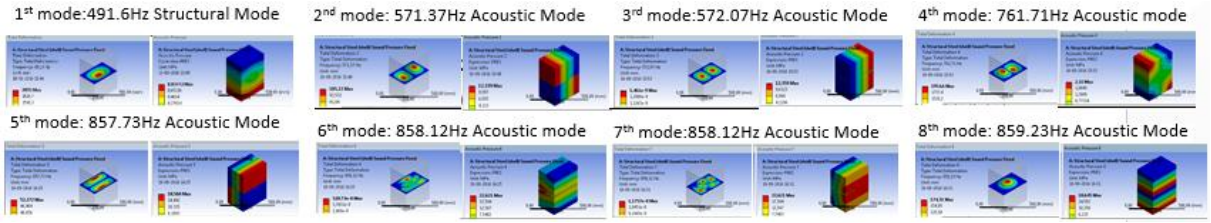

Figure 34 Acoustic and Structural modes for the two cavities setup

The harmonic study for the two acoustic cavity model is now conducted. In order to compare the modes, the same measurement location is applied, obtaining the following SPL frequency plot (figure 35) with the critical points identified in figure 36.

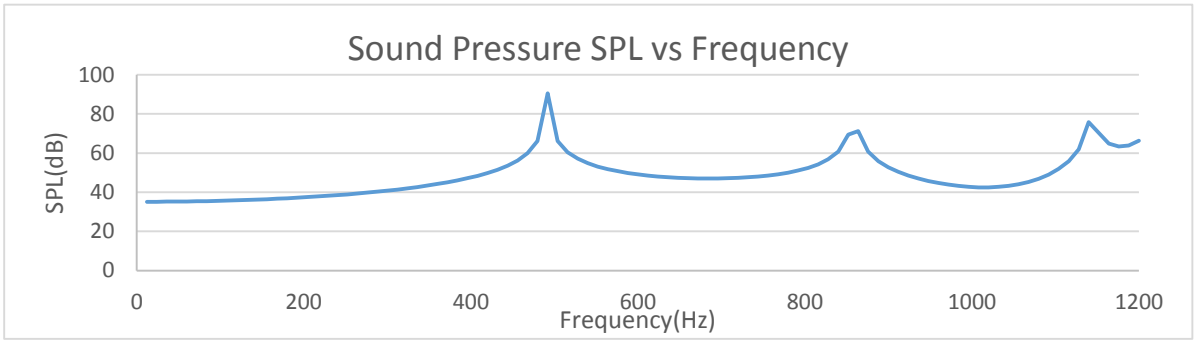

Figure 35 SPL vs frequency plot for the two acoustic cavity system

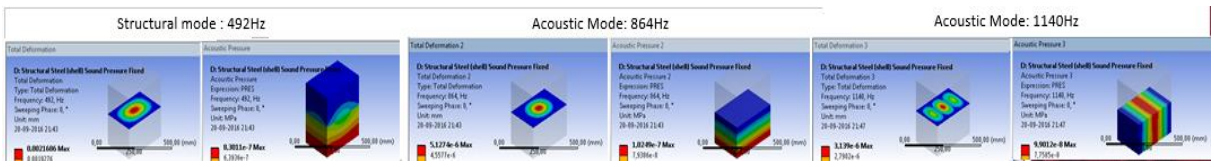

Figure 36 Acoustic and structural modes detected in the SPL vs frequency plot

5.6. Comparison between single cavity model and two cavity models

In figure 37 both SPL frequency plots are shown, for the single cavity model (1C) and two cavity model (2C).

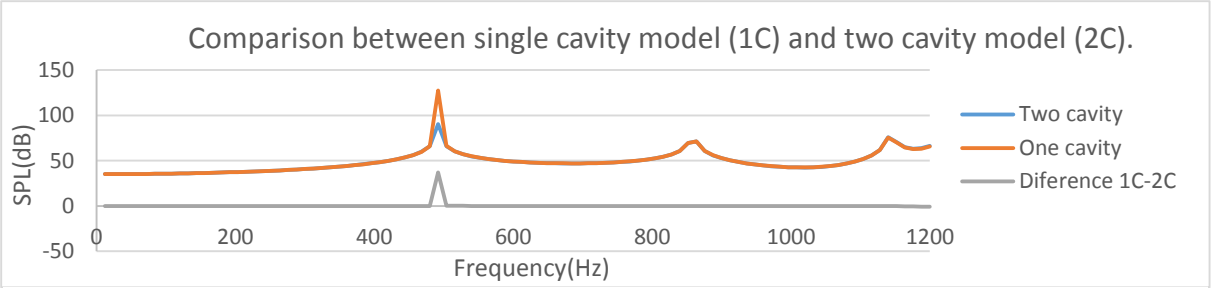

Figure 37 SPL comparison between Sound Pressure and mechanical and difference between them

Comparing the two models SPL plots, there is almost no difference between the two curves. The only difference occurs in the structural mode (492Hz) where there is a 37.13dB decrease in the sound pressure level; this can be explained by the effect of the structural mode on the top cavity as it decreases the pressure applied on top of the panel to 0.38Pa instead of the 1Pa wanted.

However, in both models the structural mode is easy to identify, the acoustic behavior is similar and the acoustic modes don't change as seen in figure 22 and 36. Also taking into account that the objective of this work is to compare different panels, we can conclude that the single acoustic cavity model can be used without significant changes in the overall result.

5.7. Different types of excitation

Having in mind the experimental application of this work, and the difficulty to recreate uniform pressure fields, some loudspeaker models are going to be tested.

The loudspeaker models available are Bare Loudspeaker (B.L.) and Back Enclosed Loudspeaker (B.E.L.). Although in order to give some coherency to the results, the pressure magnitude of these loudspeakers are going to be adapted in order to obtain a 1Pa pressure on top of the panel as seen in figure 38.

After performing some simulations, it was seen that when a loudspeaker is applied in a closed cavity the pressure on top of the panel varies as displayed in figure 38. In order to obtain a more uniform pressure field, anechoic chamber conditions were applied to obtain the pressure distribution seen in figure 38.

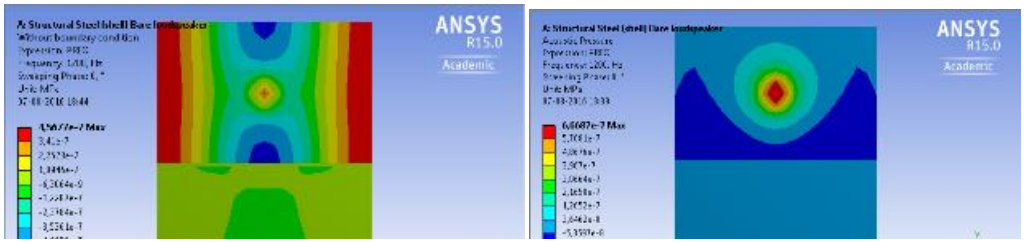

Figure 38 Pressure distribution from a back enclosed loudspeaker in a reverberation chamber and in an anechoic chamber

Back enclosed loudspeaker (B.E.L)

In order to apply a back enclosed loudspeaker excitation, the following variables need to be defined: its location in x, y and z, environment data (air properties) and the radius of the loudspeaker, as seen in the figure 39.

A back enclosed loudspeaker resembles a loudspeaker that has the rear portion contained, this means that this type of loudspeaker does not account for the interference that occurs between the front and rear faces of the driver cone. The acoustic behavior is similar to a monopole (figure 39), the only difference being a factor of 4 or 12dB in the sound pressure created, assuming that both have the same pressure amplitude and radius. The Ansys modeling of the back enclosed loudspeaker does not take into account: vibration and sound radiation provided by the faces themselves and enclosed effect behind the loudspeaker. [24].

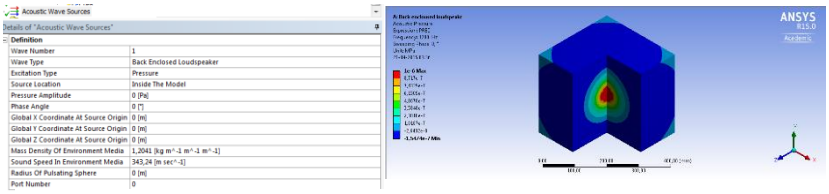

Figure 39 Back encloused loudspeaker pressure field and defining parameters

Bare loudspeaker (B.L.)

In order to apply a bare loudspeaker excitation similar parameters need to be introduced, with the addition of the dipole information as seen in figure 40. This type of loudspeaker is going to create a positive wave in the front face, a negative wave in the rear face and in the middle of these faces an interference occurs, as seen in the acoustic pressure distribution on figure 40[24]. This pressure distribution is similar to a dipole.

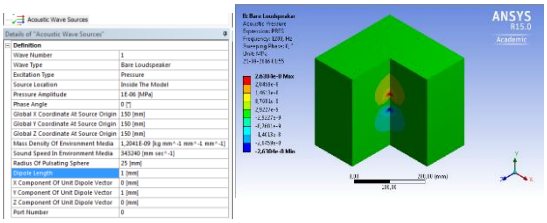

Figure 40 Bare Loudspeaker pressure field and defining parameters

Comparison between 5 different loudspeakers

To test different types of excitation, the following loudspeakers were introduced with varying: types, locations, radiuses and dipole variations, as seen in table 11.

Back Enclosed Loudspeaker Variables (B.E.L.)			
	1	2	3
Pressure	12.5Pa	4.35Pa	8.7Pa
X	100mm	100mm	100mm
Y	100mm	100mm	200mm
Z	150mm	150mm	150mm
Radius	10mm	20mm	10mm

Bare Loudspeaker Variables (B.L.)		
	1	2
Pressure	500Pa	25Pa
X	100mm	100mm
Y	200mm	100mm
Z	150mm	150mm
Radius	10mm	10mm
Dipole Length	1mm	10mm

Table 11 Back enclosed and Bare loudspeaker parameters

From table 11, the values of loudspeaker pressures are tested in order to verify if the pressure on top of the panel resembles a uniform pressure of 1Pa across the frequency range.

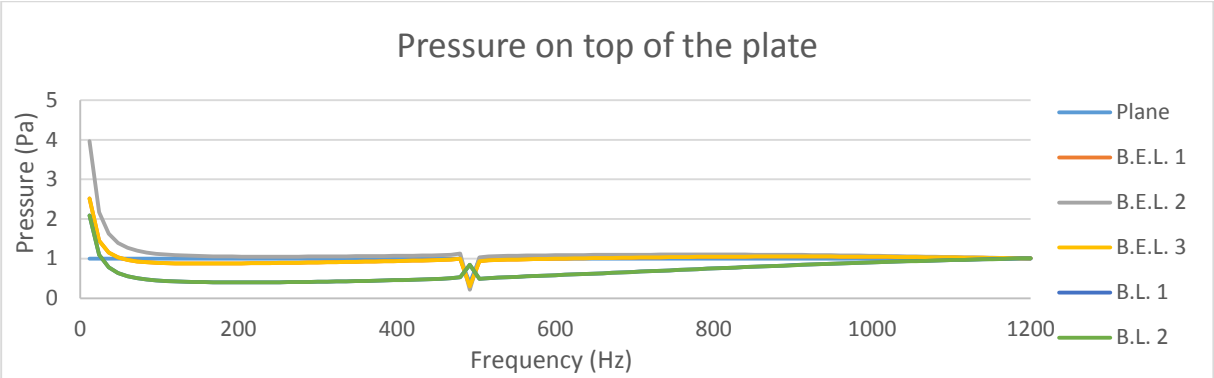

Figure 41 Pressure on top of the panel for different sound pressure excitations

Comparing the 6 different types of excitation seen in figure 41, it can be concluded that for low frequency values the pressure tends to its static value as expected, but converges to 1Pa around 150Hz for the back enclosed loudspeakers. The bare loudspeaker pressure values differ across the frequency range and converge for higher frequencies, while needing a pressure significantly higher (500Pa, 25Pa) than the back enclosed loudspeakers (12.5Pa, 4.35 Pa, 8.7Pa).

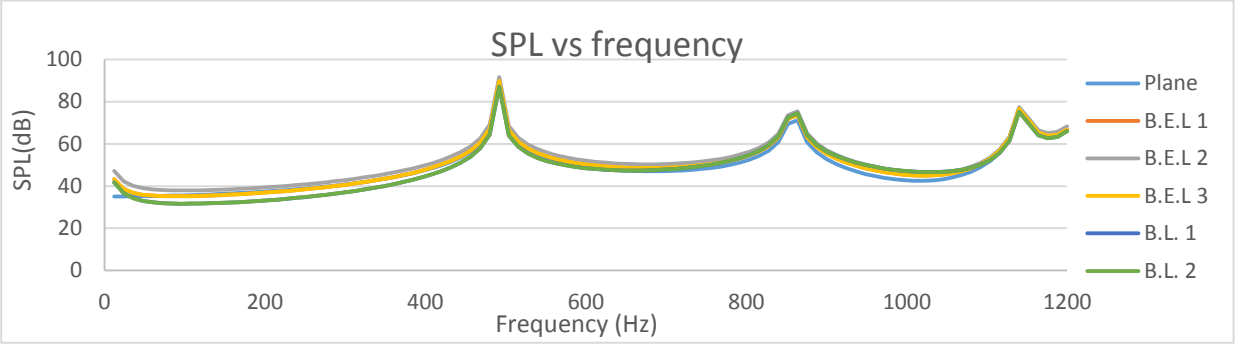

Figure 42 SPL vs Frequency for different sound pressure excitations

In order to study the acoustic behavior of the structural steel panel for different loudspeakers, 6 harmonic response simulations where conducted with the results shown in figure 42. By analyzing the pressure after the panel, it can be seen that all excitations maintain the panel behavior: structural modes and acoustic modes frequency values don't change, the SPL values suffer minor changes. This minor changes occur due to the variation on top of the panel seen in figure 41.

From the plots in figure 42, it is possible to conclude that both types of loudspeakers can be used, with back enclosed loudspeaker being better because of the minor differences in the SPL results expect for extremely low frequencies. This is going to be important when working with experimental setups.

5.8. Effect of reflection on the panel surfaces.

In this subchapter, the effect of the absorption coefficient on the panel surfaces is going to be studied. The absorption coefficient (α) is going to be used in both faces of the panel, where the outside face is the one facing the loudspeaker and the inside face the one in contact with the bottom acoustic cavity. Having the following possibilities:

- 1st: Inside face: reflective surface (α=0) | Outside face: reflective surface (α=0)
- 2nd: Inside face: absorbing surface (α=1) | Outside face: reflective surface (α=0)
- 3rd: Inside face: reflective surface (α=0) | Outside face: Absorbing surface (α=1)
- 4th:Inside face: Absorbing surface (α=1) | Outside face: absorbing surface (α=1)

These four different possibilities are plotted below for a structural steel panel:

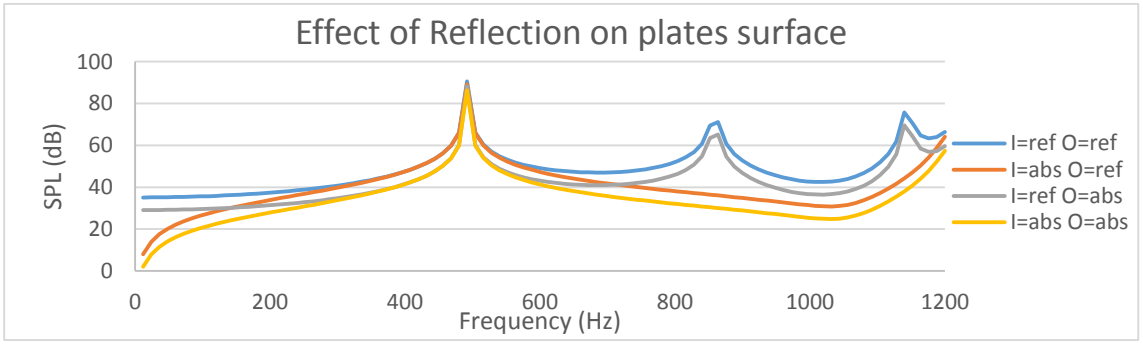

Figure 43 SPL comparison for different surface finishing

By analyzing the plot above, there are considerable differences among different absorption coefficients. Taking the first combination as a reference, and comparing it with the second one it can be seen a decrease in the SPL of ≈-6dB. This is the effect of the absorbed waves on top of the panel. Comparing now the first with the third combination, it can be seen that the acoustic modes are absorbed and the behavior is similar to the duct behavior, where for lower frequencies the SPL drops significantly, which is extremely important for the panel design. Also the ability to absorb acoustic modes can be important depending on the acoustic dimensions of the UAV structure.

5.9. Effect of damping

Damping is a natural property of the structure, but in the computational domain theoretical model approximations needs to be applied. Damping is due to internal energy dissipation which reduces and prevents vibrations, and is also extremely important to reduce structural born noise emissions [24].

This effect is studied by using two different types of damping models: constant damping coefficient and Rayleigh damping coefficient.

5.9.1. Constant damping coefficient

The viscous damping ratio ξ is the easiest type of damping model that can be applied in a structure. It is the ratio between the actual damping and the critical damping, as seen below. [24]

$$\xi = \frac{Actual\ Damping}{Critical\ Damping} \qquad (19)$$

Different damping coefficients for structural steel ξ=0, ξ=0.01, ξ=0.1 and ξ=0.3 are used to obtain the SPL frequency results shown in figure 44.

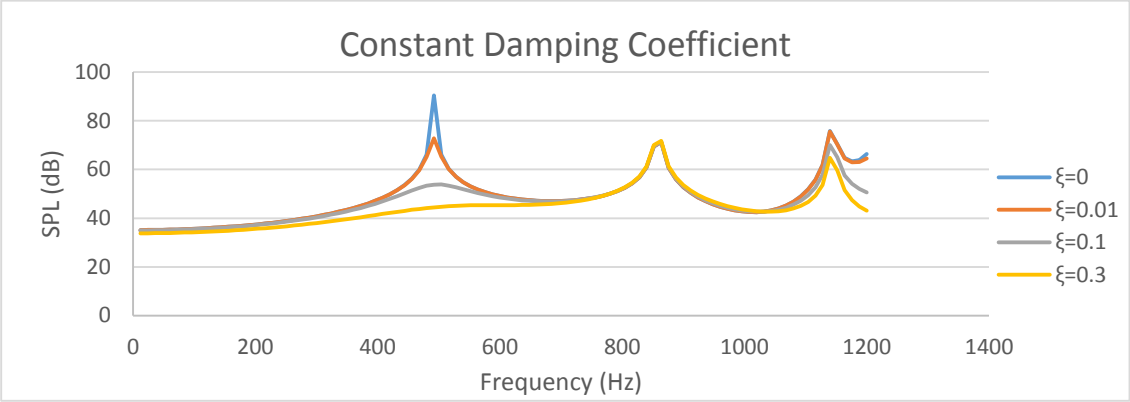

Figure 44 SPL for different Constant damping coefficient

Analyzing figure 44, it can be seen that the structural mode 492Hz suffers a major decrease in the SPL, it goes from 90.50dB to 44.44dB with the addition of ξ=0.3 to panel material. However for frequency values outside the 1st structural mode it can be seen that the damping does not create a significant difference. Also, it is important to mention that the 864Hz acoustic mode presents no difference, while the acoustic mode at 1140Hz suffers a small decrease with the increase of damping.

5.9.2. Rayleigh damping coefficient

The Rayleigh damping coefficient is a linear/proportional combination between the mass and stiffness matrices [24]. Thus, a damping matrix C is defined by the following equation with two constants α and β.

$$C = \alpha M + \beta K \qquad (20)$$

Where α and β can be defined by the following equations, assuming: a constant damping ratio ξ, a constant frequency range$[\omega_1, \omega_2]$ and that α and β are nearly constant over the specific frequency range.

$$\alpha' = 2\xi \frac{\omega_1 \omega_2}{\omega_1 + \omega_2} \qquad \beta = \frac{2\xi}{\omega_1 + \omega_2} \qquad (21)$$

With ω_1 and ω_2 being the initial and final frequency value.

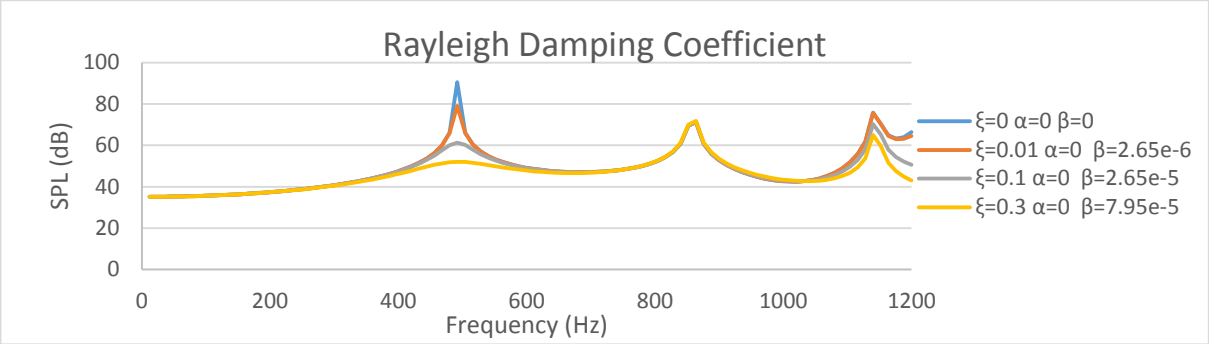

Figure 45 Rayleigh damping coefficients SPL vs Frequency plot

Analyzing figure 45, it can be seen that the Rayleigh damping coefficient creates similar results to the ones shown for the constant damping coefficient. These two models are compared in figure 46, and the differences between these models occur near the structural mode and can be explained by figure 47, where a decrease in the total damping occurs between the frequency ranges, this explains the increased of SPL in the Rayleigh damping model.

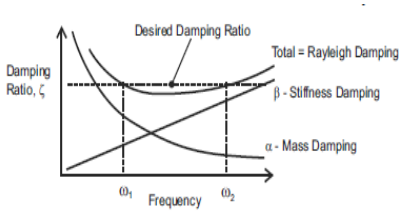

Figure 47 comparison between desired damping ratio and Rayleigh damping

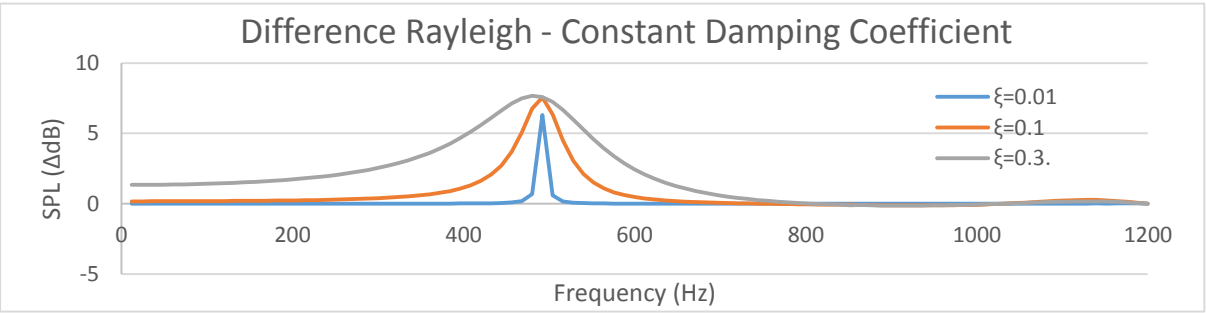

Figure 46 Difference between the Rayleigh and constant damping coefficient

Chapter 6 Sandwich Panels

6.1. Learning Outcomes

The learning outcomes of this chapter are:

- Solid-Shell comparison for sandwich panels.
- Effect of foam stiffness.
- Effect of foam Poisson coefficient
- Effect of foam Density
- Foam dominant in damping.

6.2. Introduction

In this chapter foams are going to be introduced. To start the study with two material panels (skin + core), a new shell-solid comparison is necessary [29], in order to recheck if the shell simplification can give proper results for sandwich panels with foam core. This is going to be performed by introducing different foams with varying Young modulus ranging from 10MPa to 100GPa.

After the proper elements have been selected, a study of the effects of the foam properties in the first structural mode is going to be performed, namely: the Young modulus, Poisson coefficient and mass density. Also, it is important to note that these studies are performed around the reference plate: structural steel skin and 7mm thick foam with the following properties: Young modulus of E=100MPa, Poisson ratio ν=0.3, density of ρ=7850kg/m^3. These foam properties are defined taking into account the skin (Structural Steel) properties in order to reduce the number of variables in our problem. All these effects are tested using the single cavity model (dimensions, mesh type and mesh density are not altered).

To finalize this chapter, a study is going to be performed to assess if the damping in the foam is dominant with respect to the damping of the skins. This means that the damping of the skin can be neglected.

6.3. Foams

For the comparison between solid-shell elements, 10 different foams are going to be introduced in the computational model, these foams are going to have constant density (same density as the skin used), and Poisson ratio, as seen in table 12.

	Foam 1	Foam 2	Foam 3	Foam 4	Foam 5	Foam 6	Foam 7	Foam 8	Foam 9	Foam 10
E	10 MPa	50 MPa	100 MPa	250 MPa	500 MPa	1 GPa	10 GPa	25 GPa	50 GPa	100 GPa
ν	0.3									
ρ	7850kg/m^3									
Layup	[0,90,90,0,0,0,90,90,0]									
t_{fiber}	0.375mm									
t_{foam}	5mm									

Table 12 Foam properties for Solid shell comparison

6.4. Solid-shell natural frequencies

	Mode	Solid(Hz)	Shell(Hz)	Error (%)		Mode	Solid(Hz)	Shell(Hz)	Error (%)
Foam 1	1	77,949	62,331	20,036	Foam 6	1	336,62	335,86	0,225
	2	93,722	74,811	20,177		2	399,56	398,92	0,160
	3	141,93	94,173	33,648		3	664,59	661,09	0,526
	4	165,02	108,02	34,541		4	790,83	786,51	0,546
	5	173,7	113,08	34,899		5	827,3	822,02	0,638
	6	193,22	119,31	38,251		6	904,07	897,01	0,780
Foam 2	1	140,71	132,51	5,8275	Foam 7	1	414,78	414,64	0,03375
	2	171,16	159,55	6,7831		2	464,39	464,41	0,00430
	3	233,91	206,19	11,850		3	928,59	928,27	0,03446
	4	278,88	238,32	14,543		4	1052	1052,3	0,02851
	5	282,48	247,49	12,386		5	1179,4	1179,8	0,03391
	6	308,53	262,22	15,009		6	1349,3	1349,6	0,02223
Foam 3	1	182,68	177,17	3,0162	Foam 8	1	434,3	434,21	0,02072
	2	221,76	213,79	3,5939		2	478,45	478,48	0,00627
	3	304,65	284,38	6,6535		3	987,1	986,97	0,01317
	4	362,02	331,53	8,4221		4	1099,6	1100	0,03637
	5	368,67	341,23	7,4429		5	1248,5	1249,1	0,04805
	6	399,2	363,34	8,9829		6	1439,4	1440,1	0,04863
Foam 4	1	247,29	244,56	1,1039	Foam 9	1	452,9	452,84	0,01324
	2	299,14	295,37	1,2602		2	494,78	494,82	0,00808
	3	431,83	420,11	2,7140		3	1035,2	1035,1	0,00966
	4	518,35	499,94	3,5516		4	1142,9	1143,3	0,03499
	5	520,35	503,65	3,2093		5	1304,9	1305,6	0,05364
	6	566,28	543,81	3,9680		6	1508,8	1509,6	0,05302
Foam 5	1	295,47	294,02	0,4907	Foam 10	1	482,02	481,98	0,00829
	2	355,11	353,4	0,4815		2	523,6	523,63	0,00573
	3	547,2	540,43	1,2372		3	1105	1104,9	0,00905
	4	656,01	646,58	1,4374		4	1212,5	1213	0,04123
	5	668,27	657,49	1,6131		5	1389,2	1390	0,05758
	6	726,61	712,96	1,8785		6	1608,9	1609,7	0,04972

Table 13 Solid Shell natural frequencies comparison

The results shown on table 13 come from modal studies similar to the ones performed in chapter 4, where now the foam is introduced in the geometry and the model. This modal study is performed for all 10 different foams using both shell and solid elements in order to obtain the first six natural frequency.

Taking the natural frequency values and comparing both solid and shell elements by the relative error in equation 22.

$$Error_i(\%) = \frac{\left|f_{i_{shell}} - f_{i_{solid}}\right|}{f_{i_{solid}}} \times 100 \qquad (22)$$

Being $f_{i_{shell}}$ the natural frequency obtained from shell elements for mode i and $f_{i_{solid}}$the natural frequency obtained from solid elements.

Carbon fiber and glass fiber skins were also tested and in Figure 48 the error is plotted for the 6th mode for the three different skin types: structural steel, carbon fiber and glass fiber.

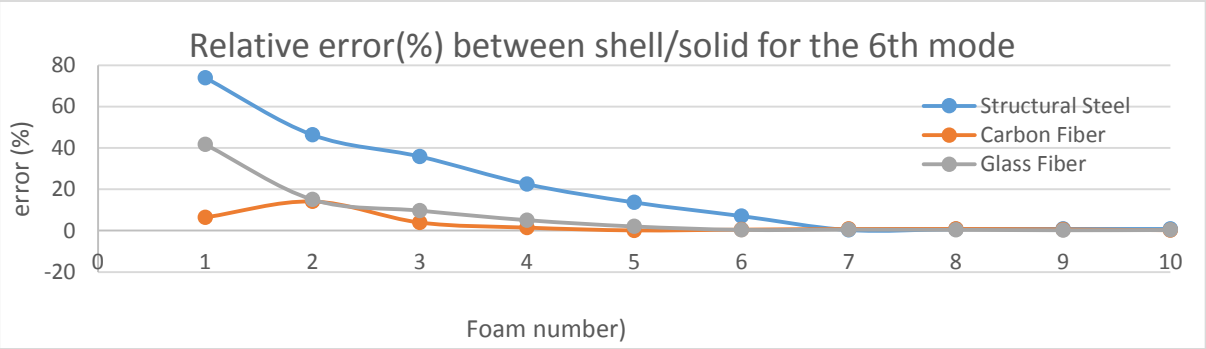

Figure 48 Relative error of the 6th between solid and shell elements

From figure 48, it can be seen that for low Young modulus of the foam core major errors occur. However the shell and solid elements don't converge to the same foam Young modulus: Structural Steel panel converges after foam 7(10GPa) and both Carbon Fiber and Glass fiber panel converges after foam 6(1GPa). Taking this into account it can be seen that shell elements only work well when materials have similar Young modulus.

In conclusion, the use of solid elements is necessary when working with sandwich panels. With this comparison and taking into account that foams used in aeronautic appliances range between 50MPa and 150MPa [30], it will be necessary to use the solid elements for the sandwich panels used in this work.

6.5. Solid-shell SPL vs frequency

Taking into account the modal study in the previous subchapter, it is expected that shell elements are going to create a completely different behavior from the solid elements when the foam has small Young modulus. However, with the increase of the foam Young modulus it is expected that this differences in behavior across the frequency doamin will tend diminish. In order to verify this phenomenon, 3 different foams with: 10MPa, 1GPa and 100GPa were tested using the single cavity model (FLUID220 25mm) for a structural steel skin. The following SPL vs frequency plots show us the difference in behavior between the two elements, where Solid elements (SOLID186 25mm) and shell elements (SHELL181 25mm) were used.

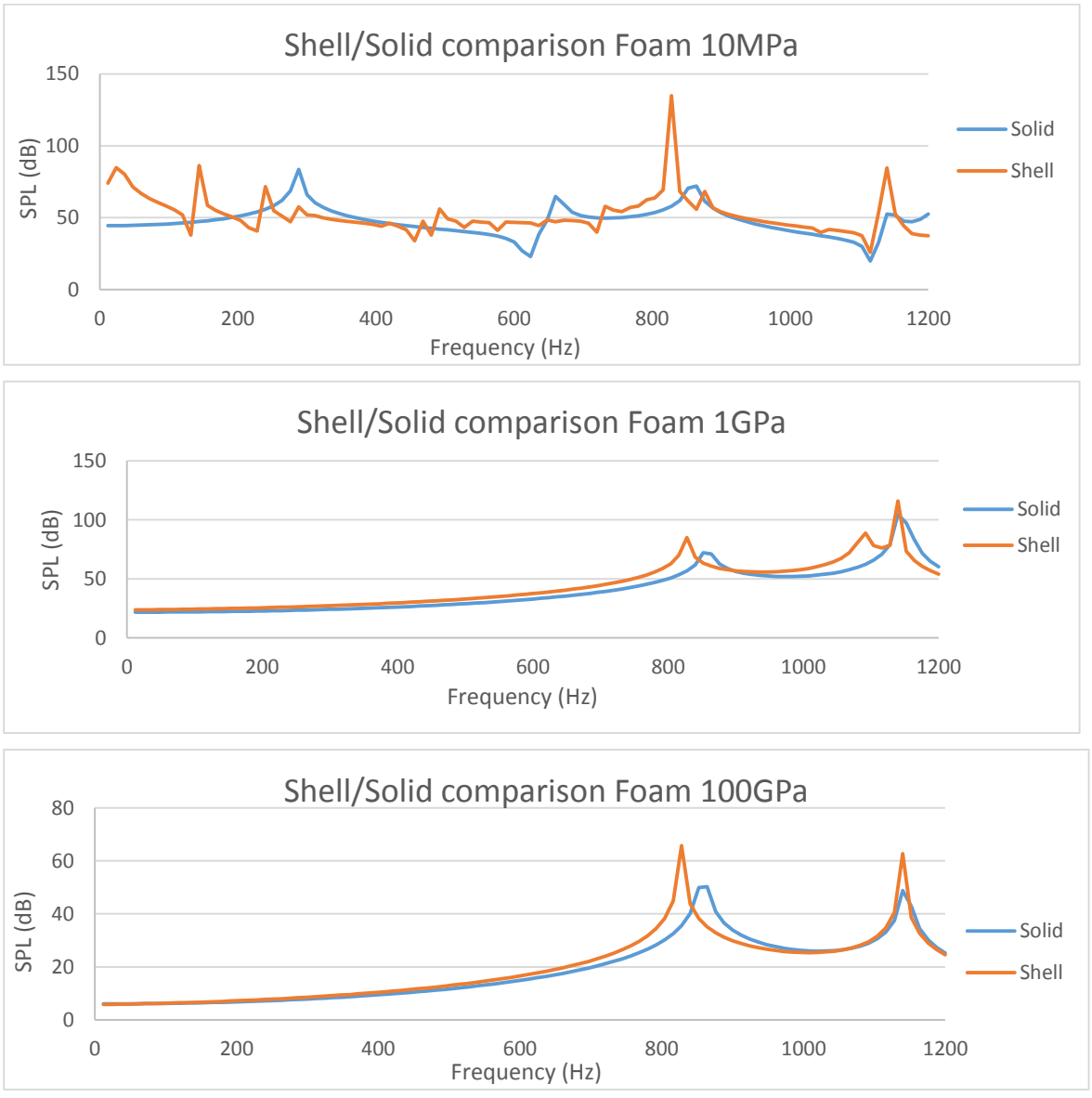

Figure *49 SPL comparison between solid and shell elements for different foams*

With this three plots, the shell-solid study ends. It is possible to conclude that shell elements cannot be used on panels, where the skin and the core have different magnitude young modulus, however they give good results when skin and core have similar properties.

6.6. Effect of the young modulus of the foam

Before any type of parametric studies are performed, a quick study into foams used in aeronautic applications is made [29] in order to see the young modulus range. With these range in mind, three foams were tested with varying young modulus: 50MPa, 100MPa and 150MPa with the results shown in figure 50. Also, these simulations are going to be performed using SOLID186 (25mm) elements and FLUID220 (25mm) elements

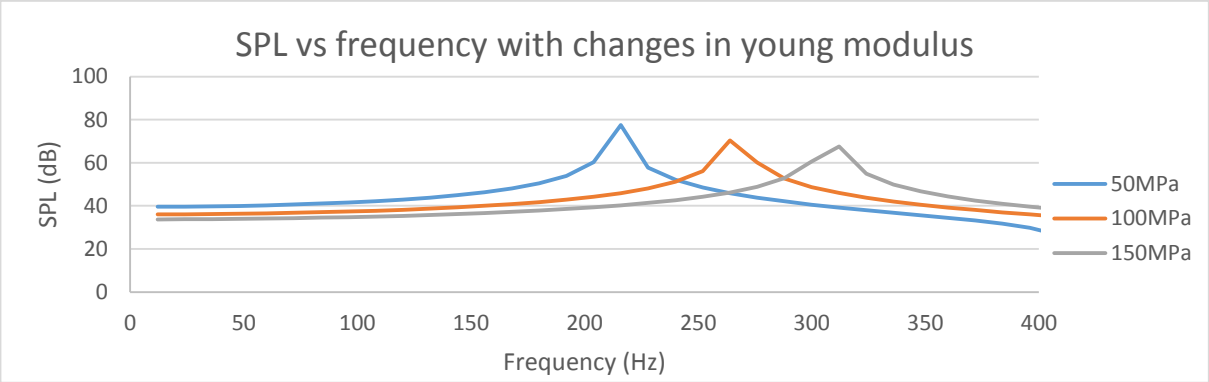

Figure 50 SPL comparison for foam with different Young modulus

By Analyzing figure 50, it is possible to see two different phenomenon:

- The 1st structural mode moves to higher frequencies with the increase of the foam Young modulus (216Hz to 312Hz). This is particularly important when we pretend to move the structural mode to outside the UAV operation frequency range.
- There's a decrease in the SPL registered in the structural mode, it decreases from 77.46dB to 67.53dB with the increase in Young modulus

6.7. Effect of Poisson coefficient of the foam

Taking into account the ranges available for the Poisson ratio in Ansys (0 to 0.5). This version of ansys does not take into account the existence of auxetic materials. Auxetics are materials that when stretched become thicker in the perpendicular direction to the stretch. The values selected for this study are v=0.1, v=0.3 and v=0.45 as seen figure 51.

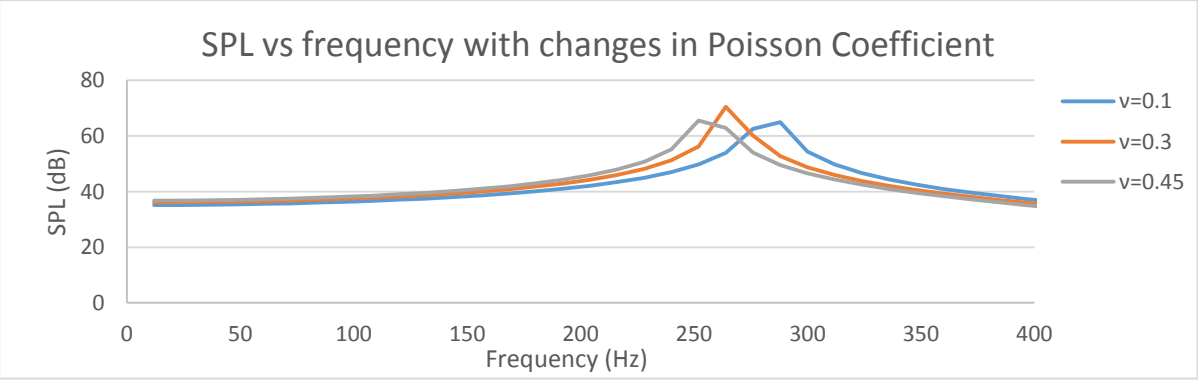

Figure 51 SPL comparison for foams with different Poisson Ratio

By analyzing figure 51, two different phenomenon can be seen for the different Poisson ratios:

- The 1st structural mode moves to higher frequencies with the decrease of the foams Poisson ratio (252Hz to 288Hz). This can be explained by the decrease in the shear modulus and bulk modulus.
- There's a decrease in the SPL registered in the structural mode for values closer to the upper and lower limit.

6.8. Effect of the density of the foam

To finalize this study, we are going to vary the density of the foam. This is an extremely important property in aeronautical appliances due to the necessity to reduce structural weight. The following plot shows us the result for three different densities: 3925kg/m^3, 7850kg/m^3 and 11775kg/m^3.

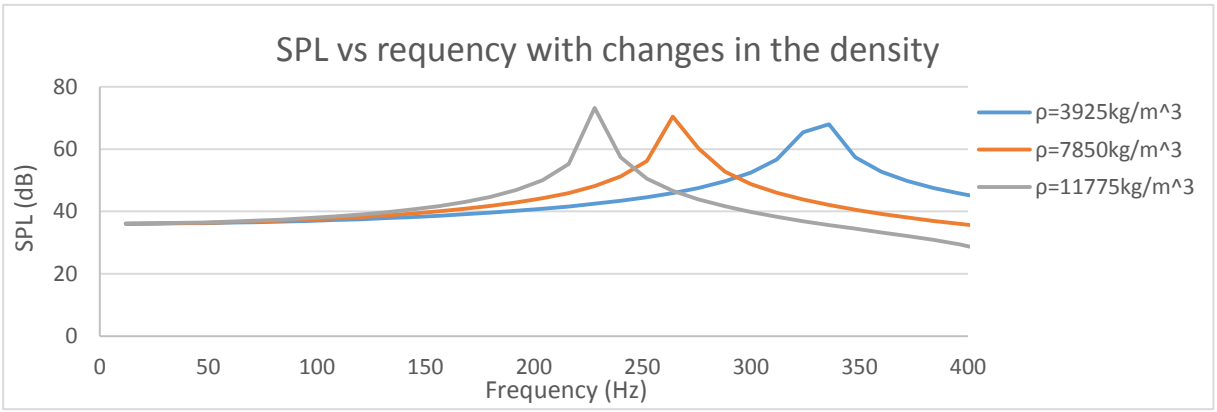

Figure 52 SPL comparison for foams with different density

By analyzing figure 52, two different changes can be perceived for the different mass densities:

- The 1st structural mode moves to higher frequencies with the decrease in density (228Hz to 366Hz)
- There's a decrease in the SPL registered in the structural mode for lower density values

6.9. Damping is Foam dominant

In this subchapter, we show that damping in the foam is dominant. This means that the damping that occurs in the skin can be neglected when a foam is applied. This means that the damping in the skin can be neglected for a sandwich configuration with a foam core.

Considering that the experimental modal damping factors obtained in the experimental thesis, are between 0.01 and 0.1, these damping values are going to be used as limits for our studies. This damping is going to be modelled by the constant damping factor model seen in subchapter 5.9.1. Taking this into account and assuming the worst case scenario in terms of errors, both skin and core are going to have a constant damping factor 0.1 and the foam thickness is 7mm.In order to verify the dominance of the foam, we are going to compare panels: where skin and core have a constant damping coefficient with panels where damping is only applied on the core.

In order to verify the dominance of the foam, we are going to compare panels where skin and core have a constant damping factor with plates where damping is only applied on the core.

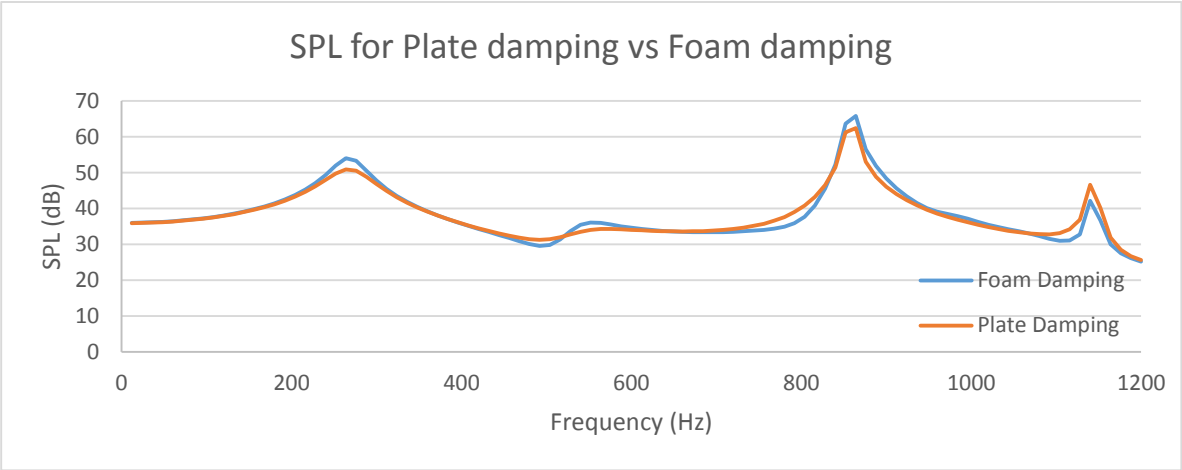

Figure 53 Comparison between fully damped panel and foam only damped panel

Figure 53 is an example of the comparison between two panels (skin: structural steel, foam thickness: 7mm and constant damping factor: 0.1. Also, more panels have been compared where damping coefficients and foam thicknesses vary. In terms of this study the worst possible combination is seen in figure 53: highest damping (0.1) and highest foam thickness being used (7mm). By analyzing the plot, we can conclude that the effect of damping on the skin is negligible compared to the damping in the core.

Chapter 7 Experimental Setups

7.1. Learning Outcomes

The learning outcomes of this chapter are:

- Objectives of Setup 1.
    - Effect of boundary conditions.
    - Effect of microphone height.
    - Effect of loudspeaker height.
    - Effect of loudspeaker radius.
- Objectives of Setup 2
    - Effect of boundary conditions

7.2. Introduction

In this chapter, we start our study of experimental setups. Until now the simulations occurred in ideal conditions, but as this work was also performed in order to assess alternative experimental setups for the experimental thesis, it is important to introduce simulations that can be recreated experimentally.

Setup 1 is a clamped panel surrounded by fluid, where a loudspeaker is placed above the panel [31]. In this experience, we are going to obtain the Transmission Loss across the panel through the use of two microphones: one between the panel and the loudspeaker and the other below the panel.

Setup 2 is a more common acoustic study, where an anechoic chamber and a reverberation chamber are built with the panel separating them. The loudspeaker is placed inside the reverberation chamber and the microphones are placed in similar location to the ones in setup 1.

Also some parametric studies are performed for a structural steel panel discretized with solid elements (solid186 25mm), in order to determine the best: boundary conditions, microphone locations, loudspeaker radius and distance to the panel.

7.3. Setup 1

Figure 54 demonstrates the experimental setup in the computational domain, the panel is seen in blue with clamped boundary conditions and fluid in gray, which encloses the panels and its boundary conditions are defined in order to recreate an infinite fluid domain [24].

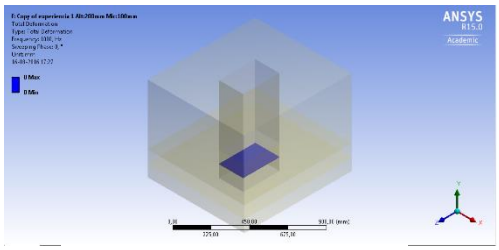

Figure 54 Setup 1 model

The excitation is created by a back enclosed loudspeaker above the center point of the panel top face. After the geometric design and excitation is defined, the experimental setup is concluded by applying two different microphones in order to obtain the pressure before and after the panel: the microphone (P_{int}) is placed below the panel and the other microphone (P_{ext}) is placed between the panel and the loudspeaker. The transmission loss is obtained by the following equation.

$$TL = 20\log_{10}\left(\frac{P_{ext}}{P_{in}}\right) \qquad (23)$$

The reference setup in order to obtain a 1st iteration of results is going to be defined using the following data: the loudspeaker is placed 200mm above the panel with a radius of 100mm and a magnitude of 1Pa, the microphone is placed 200mm below the panel and a microphone 100mm above the panel. Also, in order to obtain "infinite" fluid conditions in the boundary, radiant boundary conditions are going to be applied.

7.4. Procedure

In this setup the geometry is based on the cavity model, where bodies are added to the sides finishing with a cube with dimensions of 1400mm x 1300mm x 1050mm where a panel is placed inside the model as seen in figure 55.

In terms of modeling the panel is made of structural steel, has clamped boundary conditions and is modeled with solid elements (SOLID186 25mm). The fluid bodies involved are defined by acoustic bodies with a coupled unsymmetrical model and two FSI conditions are applied on the two panel faces. The radiant boundary conditions are applied to the outside faces, in order to recreate an infinite fluid domain.

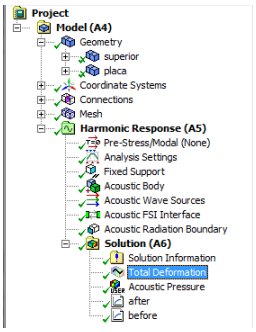

Figure 55 Setup 1 moddeling

For this study only harmonic response simulations are performed due to the "infinite fluid domain". Also in order to obtain the results from the "microphones" two acoustic frequency plots are used.

7.5. Effect of boundary conditions

In Ansys acoustic extension it is possible to recreate “infinite” fluid conditions by three different ways: PML (Perfectly Matched Layers), radiation boundary conditions and infinite fluid elements. These conditions are applied in order to eliminate all acoustic cavity modes. These three different boundary conditions are described and explained below.

Radiation boundary conditions – these boundary conditions can be applied to the outside faces. This condition creates a surface that absorbs mostly normal waves, so some unwanted oblique waves may be reflected into the acoustic domain, not fully eliminating acoustic modes. The advantages of using this type of method is the ease of application and a zero increase in the number of finite elements. [24]

Perfectly matched layers (PML) – This creates a fluid body that encloses our finite fluid domain and provides a “buffer zone”. This zone absorbs all incoming normal and oblique waves that pass to the inner body being the only waves not absorbed the ones that pass tangentially to the surface. The advantage is that this method absorbs all outgoing waves (normal and oblique waves), but also increases the number of elements and computational time because of the addition of the enclosed body [24].

Infinite fluid elements – this is the third type of acoustic wave absorbing elements. These elements are usually applied in pipes to create an infinite fluid on the pipe end. This is performed by creating a hemisphere at the end of the pipe and making the outside surfaces infinite fluid elements, which makes them extremely effective for absorbing radial acoustic waves. These elements are not going to be applied in this study because of the better effectiveness of PML to absorb waves and also because this work mainly uses rectangular geometries [24]

Taking into account the advantages and limitations shown above, the PML region is the best option to create the “infinite” fluid domain wanted. Hence, an additional body needs to be created: a body that encloses all the setup as seen in figure 56 with a uniform dimension of 225mm. Also, the acoustic body is defined with uncoupled acoustic structural conditions, because it has no interaction with the panel.

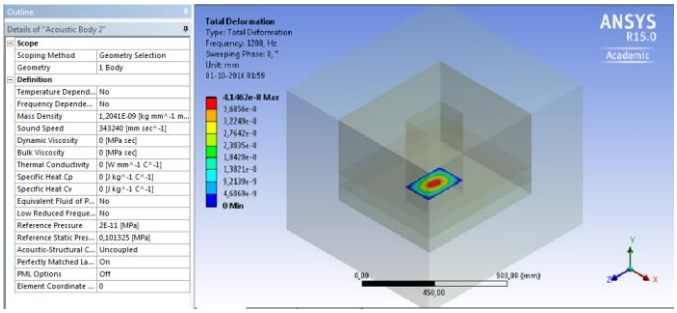

Figure 56 PML model and Parameters

7.6. Convergence of fluid elements

With the addition of new bodies, a new convergence study needs to be performed. In this study there are solid elements and fluid elements. Knowing that solid elements (SOLID186) converge for sizes of 50mm, 25mm are going to be used in this study, as seen in subchapter 3.4.

Taking this into account, only the convergence of fluid elements is going to be studied, starting with fluid elements (FLUID220) of 250mm.

The following plot gives us the relative error in percentage (equation 24) between the SPLs obtained after the panel for several fluid element dimensions.

$$Relative\ error_i(\%) = \frac{|SPL_i - SPL_{75mm}|}{SPL_{75mm}} \times 100 \quad (24)$$

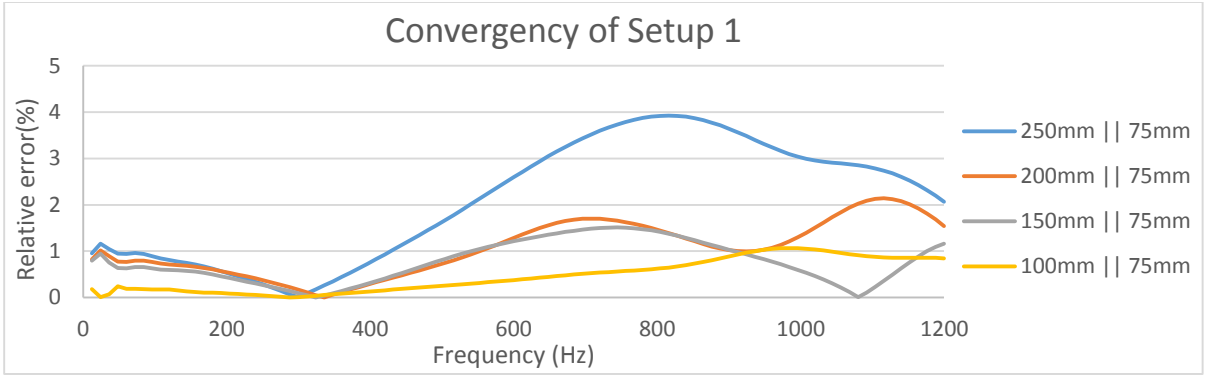

Figure 57 Convergence of finite elements in Setup 1

Analyzing the plot above it can be seen that errors occur inside the 5% range, when comparing different fluid element sizes. With 250mm and 200mm elements it can be seen relatively high relative errors of 3.91% and 2.12% can be seen, respectively, with a high oscillations in errors inside the frequency range. For 150mm the errors obtained are smaller but still some oscillations occurs inside the frequency range (0.011% to 1.44%), which can lead to an erroneous panel behavior. To finalize, elements of size 100mm and 75 mm converge to a good approximation, as the relative error between them is included in the 0% to 1.06% range.

7.7. Effect of microphones height

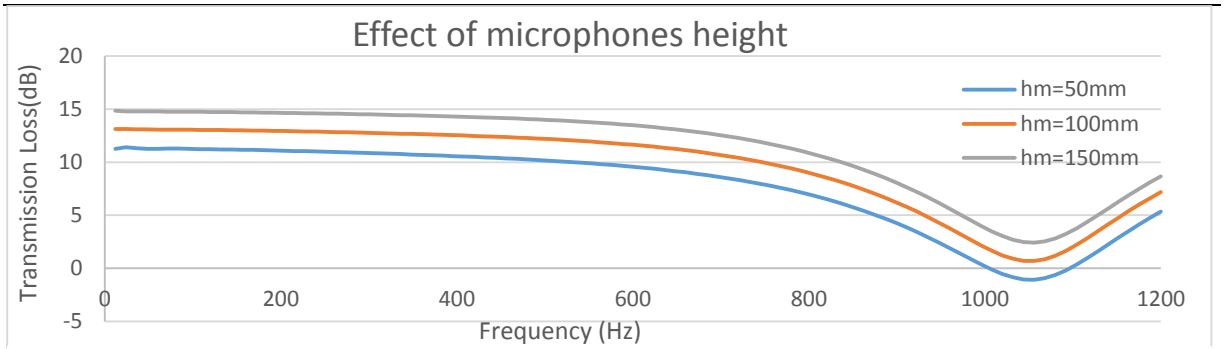

Figure 58 SPL variation with microphones height

To see the effect of the lower microphone location in the SPL frequency plot, three different height studies are shown in figure 58, where the microphones are located 100mm, 200mm and 300mm away from the panel center point. By analyzing these three simulations, it is verified that with the increase in height the transmission loss (TL) also increases but there's no difference in the behavior. This decrease in the transmission loss can be explained by the increase of the fluid between the panel and the microphone. In conclusion, it's better to have the microphone closer to our panel in order to avoid the influence of outside noises.

7.8. Effect of Loudspeaker height

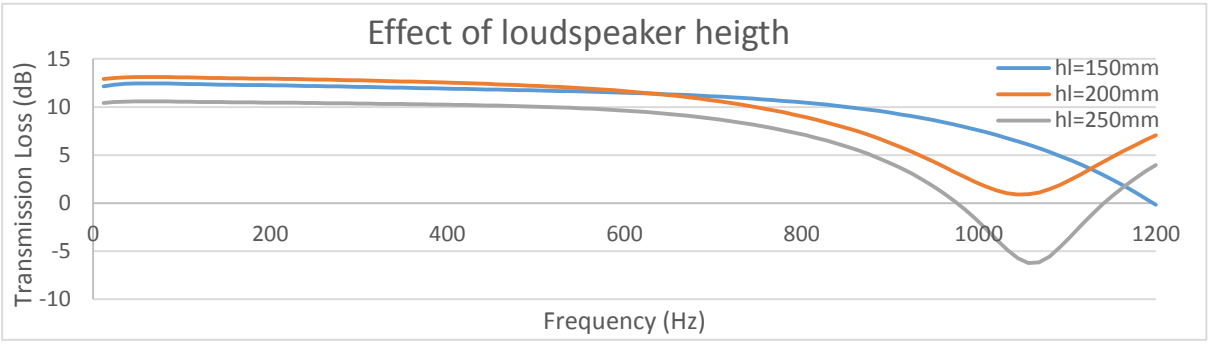

Figure 59 SPL variation with loudspeaker height

Studying the effect of the loudspeaker height shown in figure 59, it can be seen that if the loudspeaker is placed too close to the panel the behavior completely changes, i.e., the valley increases in frequency. This effect can be explained by analyzing the pressure distribution in figure 61. This behavior occurs due to the inability of the waves reflected by the panel to escape without interfering with the incoming waves; this interference creates an increase in pressure on top of the panel and by result a reduction on the transmission loss occurs. To conclude, we want to place the loudspeaker as close to the panel as possible without the reflective waves interfering with the results.

7.9. Effect of Loudspeaker radius

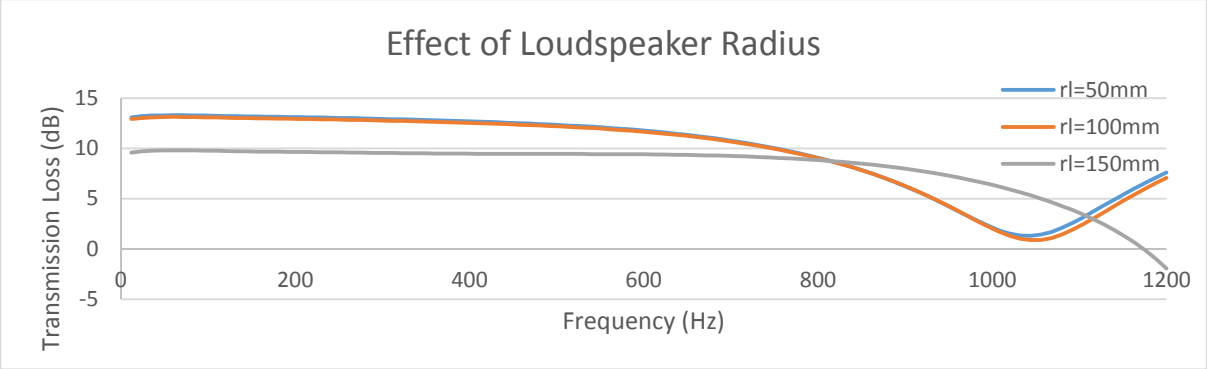

Figure 60 SPL variation with loudspeaker radius

By analyzing the plot above, the variation of the loudspeaker radius creates a similar effect as the loudspeaker height. When the radius increases, the acoustic behavior tends to change and the valley increases in frequency. In figure 61 the pressure distribution produces a similar effect as seen for low loudspeaker height. Also, by comparing the 50mm and 100mm loudspeaker it can be verified that for low radius values the behavior doesn't change, this is important to mention considering the experimental setup and loudspeakers available.

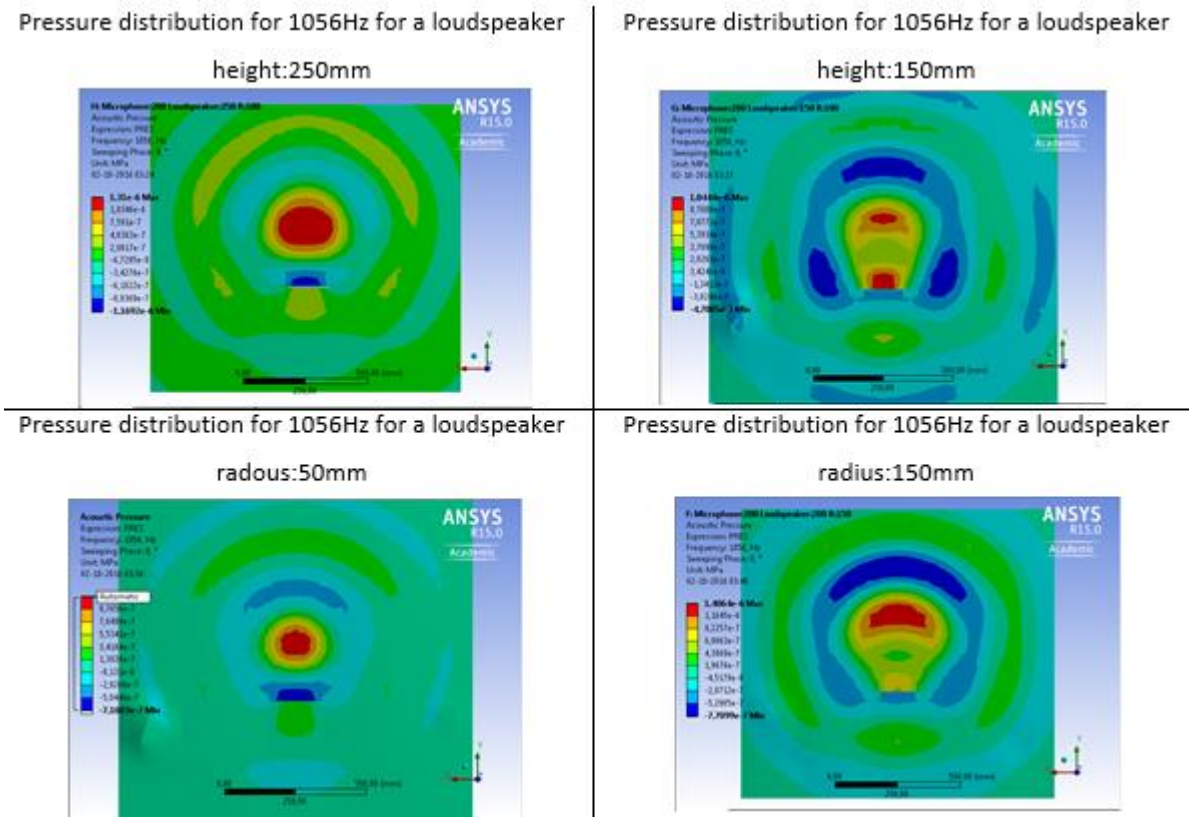

Figure 61 Pressure distribution for varying loudspeaker height and radius

7.10. Setup 2

The setup 2 model is shown in figure 62. This setup is the most common built experimental setup, used for acoustic studies, where an anechoic chamber (top chamber) and a reverberation chamber (bottom chamber) are built.

The reverberation chamber has the following parameters: Rectangular prism (900mm x 800mm x 500mm), constrained with rigid reflective walls, where the bare loudspeaker is applied.

The anechoic chamber has the same dimensions as the reverberation chamber but instead of reflective walls has fully absorbing walls (α=0).

These two chambers are only connected by the faces of the panel. This means that the extra area surrounding the panel between the chambers is modeled as a rigid wall.

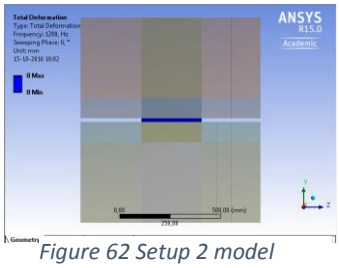

Figure 62 Setup 2 model

In order to obtain a comparison between panels, Transmission Loss is used and it is calculated using a similar procedure from setup 1. Two microphones are going to be used: one above (h_m=100mm) and other below the panel (h_m=100mm). The Transmission loss is obtained from equation 25.

$$TL = 20\log_{10}\left(\frac{P_{rev}}{P_{ane}}\right) \quad (25)$$

Where P_{rev} is the pressure measured by the microphone located in the reverberation chamber and P_{ane} is the pressure measured in the anechoic chamber.

7.11. Procedure

This setup 2 is modeled with three different bodies. The panel, reverberation chamber and anechoic chamber: the panel is modelled with solid elements (SOLID186 25mm) and has clamped conditions, both chambers are defined using fluid elements (FLUID220 75mm) and an unsymmetrical structural coupled method. However the boundary conditions on the outside faces are radiant the anechoic chamber and acoustic absorption surface with an absorption coefficient of α=0 as seen in figure 63.

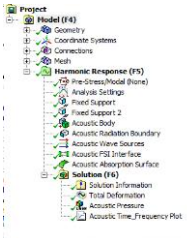

Figure 63 Setup 2 modelling

7.12. Finite elements Convergence

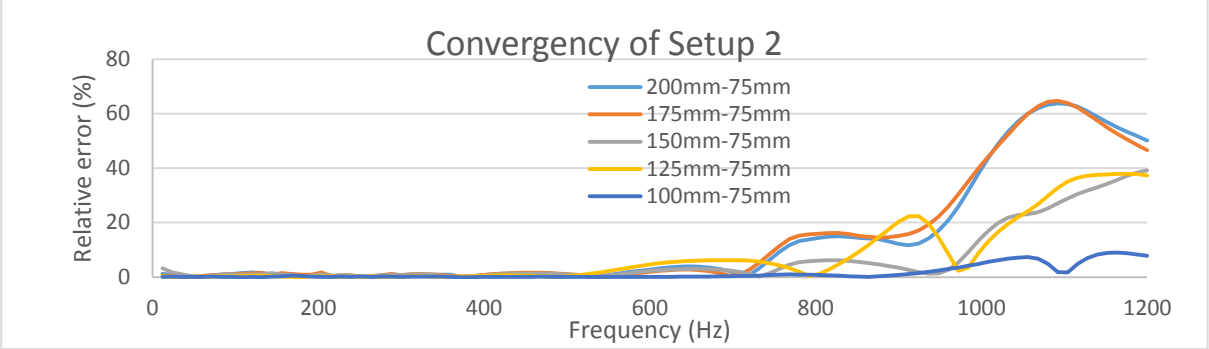

Figure 64 Convergence of finite elements in Setup 2

In figure 64, the relative error defined by equation 26 is shown. These errors are calculated by comparing the SPL results obtained in the microphone after the panel, for different fluid element dimensions, starting with 200mm fluid elements (FLUID220). The panel is discretized by solid elements (SOLID186) of size 25mm and is made of carbon fiber.

$$Relative\ error_i(\%) = \frac{|SPL_i - SPL_{75mm}|}{SPL_{75mm}} \times 100 \quad (26)$$

From the plot of the errors, it can be concluded that for low frequencies, in the 0-500Hz range all fluid element dimension present good results. This was expected, since the fluid element dimensions are proportional to the wave length of the incident wave [24]. However, with the increase in frequency the models start to diverge from the reference element size (75mm). Analyzing the results it can be seen that the models starts to converge in terms of results after the 100mm fluid elements with, a relative error lower than 8.8%. Concluding, fluid elements of 100mm and 75mm can be used in this experimental setup.

7.13. Boundary conditions

After performing some simulations an example is shown in figure 65, with a carbon fiber panel defined by SOLID186 (25mm) elements and the acoustic domain discretized by FLUID220 (75mm). We can perceive that multiple oscillations occur in the frequency interval

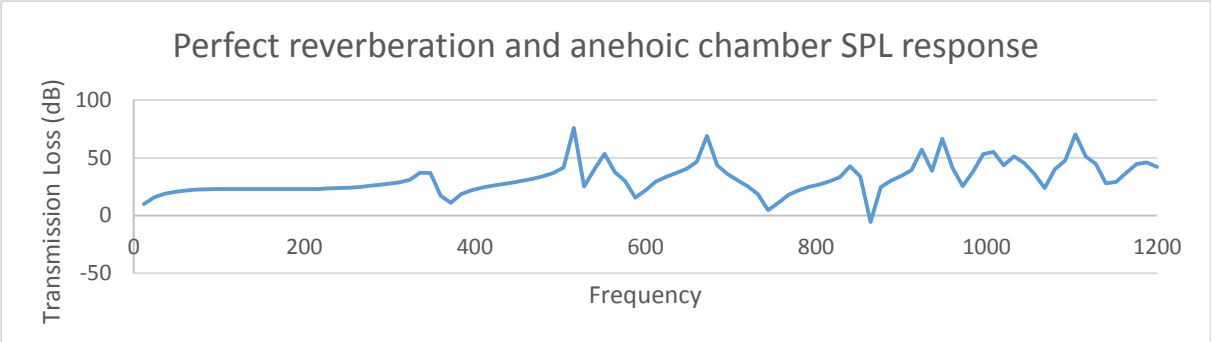

Figure 65 SPL for Setup 2 with perfect reverberation chamber and anechoic chamber

This can be explained by the boundary conditions applied in the reverberation chamber. It was assumed that we had built a perfect reverberation chamber, however this creates dominant acoustic modes and makes the comparison between panels impossible. Taking this into account the absorption coefficient α was altered in order to damp out the acoustic modes.

Figure 66 shows us the setup 2 for a carbon fiber panel behavior when the absorption coefficient α=0.5

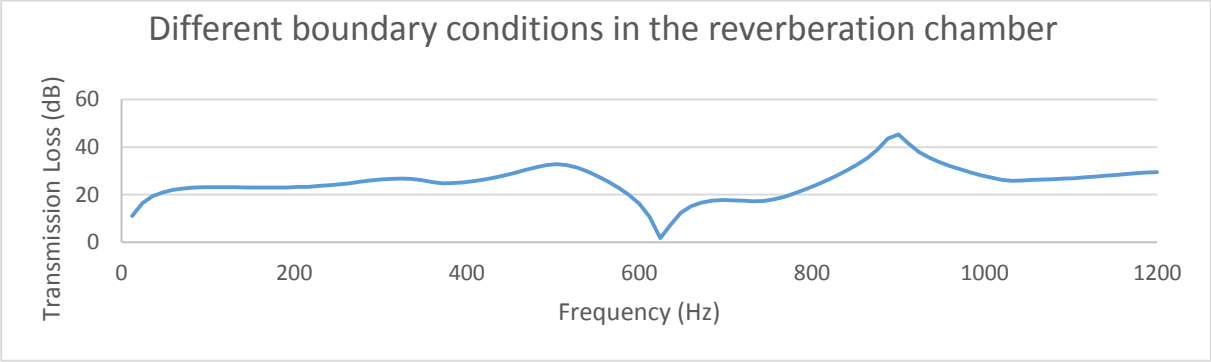

Figure 66 SPL for setup 2 with variation of boundary condition

Comparing both plots we see that the damping in the acoustic modes resulted in more manageable responses, where a critical point can be identified at 624Hz and the pressure distribution can be seen in figure 67, which clearly shows a pressure distribution dependent on the panel deformation

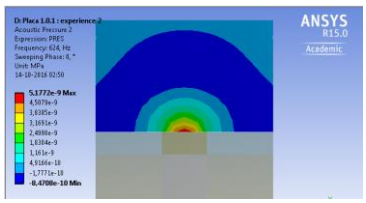

Figure 67 pressure distribution and total panel deformation at 624Hz

7.14. Example of Setup 1 and 2 Results

To finalize this chapter, the results obtained from setup 1 and 2 are going to be analyzed for a sandwich panel with a carbon fiber skin and an Airex C70.75 core. This panel is selected due to the acoustic behavior. In table 14 the parameters of these experimental setups are summarized, taking into consideration the parametric studies performed through this study. However the loudspeaker was chosen from the ones experimentally available.

	Setup 1	Setup 2
Loudspeaker Type	Bare loudspeaker	Bare loudspeaker
Loudspeaker Radius	50mm	50mm
Loudspeaker height	200mm	200mm
Microphones heights	100mm	100mm
PML region	225mm	Not applied
Solid Elements	SOLID186	SOLID186
Solid dimensions	25mm	25mm
Fluid Elements	FLUID220	FLUID220
Fluid dimensions	75mm	75mm

Table 14 Setup 1 and 2 parameters

In table 15 the structural modes frequencies are shown for the carbon fiber panel with clamped conditions. However, by analyzing the deformation on the panel in setup 1 and 2, the panel always shows a deformation similar to the first structural mode as verified in figure 68 for setup 1 on the following frequencies: 300Hz, 600Hz, 900Hz and 1200Hz

Mode	Sandwich Panel
1	685.9Hz
2	962.18Hz
3	1249.1Hz
4	1360.2Hz
5	1431.1Hz
6	1731.1Hz

Table 15 Frequency values of structural modes

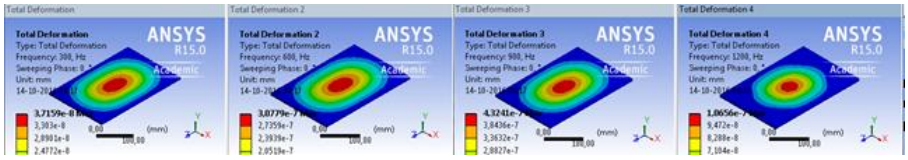

Figure 68 panel deformation in setup 1 for 300Hz,600Hz,900Hz and 1200Hz

In figure 69, the behavior of the panel under study (carbon fiber skin + Airex C70.75 core) is shown in TL versus frequency plots.

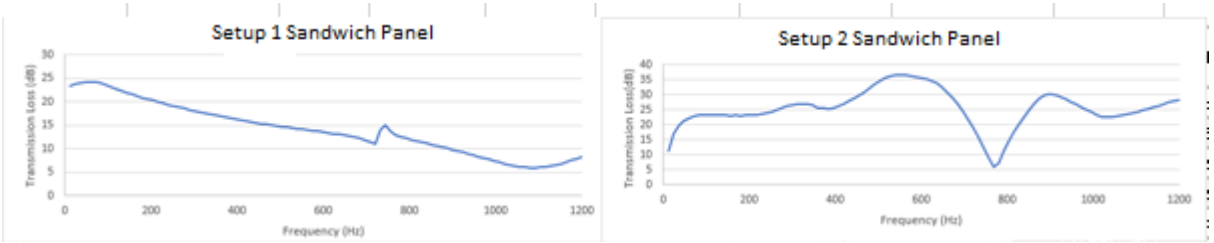

Figure 69 Setups 1 and 2 TL vs frequency plot

From setup 1 two behaviors are going to be investigated: the increase in the TL at 756Hz and the valley that occurs in the 1000Hz to 1200Hz frequency range. The pressure distribution below the panel for an excitation frequency of 756Hz can be seen in figure 69. It can be seen that the pressure depends clearly on the panel

deformation, which is similar to a structural mode. However, for other frequency values the behavior is influenced by the fluid on the upper face of the panel. Regarding the valley that is seen between 1000Hz and 1200Hz, it occurs because of the coincidence frequency (1080Hz). This frequency occurs when both acoustic and flexural vibration wave-lengths coincide [32]. In equation 27 this coincidence frequency is calculated for simply supported panels and infinite panels [33], but since we are working with thin panels this coincidence frequency is going to remain almost constant.

$$f = \frac{c^2}{2\pi}\sqrt{\frac{m_f + 0.5m_c}{D_f}} \quad f = \frac{c^2}{2\pi}\sqrt{\frac{\rho}{D_f}} \qquad (27)$$

With c being the sound velocity, m_f and m_c is skin mass and core mass and D_f and D is the skin stiffness and panel flexural rigidity

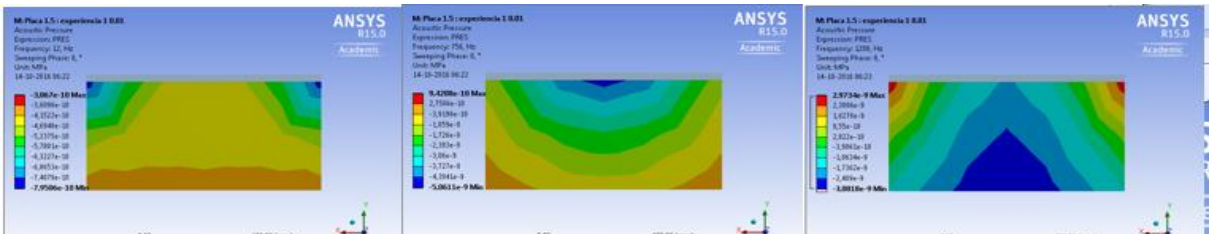

Figure 70 Pressure distribution below the panel in Setup 1 (12Hz, 756Hz and 1200Hz)

From setup 2, only one particular behavior is going to be analyzed, at frequency point 768Hz. The pressure distribution is seen in figure 71, on the acoustic body after the panel. This point is analyzed because it creates the lowest transmission loss in the frequency range. Also comparing both experimental setups, we can see that the pressure distribution is similar for both models and the values are also similar: 756Hz and 768Hz.

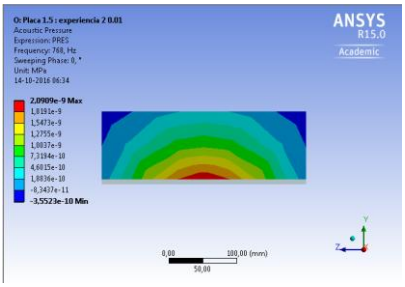

Figure 71 Pressure distribution at 768Hz in Setup 2

Taking these values into account, it can be seen that both these points create a pressure distribution similar to the ones seen from structural modes in chapter 3, although these values do not resemble any of the structural modes obtained from the modal study.

Chapter 8 Panel comparisons

8.1. Learning Outcomes

The learning outcomes of this chapter are:

- Behavior of 8 different panel configuration
- Comparison between panels.
- Best panels for application.

8.2. Introduction

After all the parametric studies performed for geometry, types of excitation, boundary conditions and material properties, this study is going to be concluded with different sandwich panels. These panels are going to be tested in single cavity model, setup 1 and setup 2, for both ξ=0.01 and ξ=0.1 damping coefficients, applied on the foam. The foam being used in all the sandwich panels is Airex C70.75, with the following properties: Young modulus of E=63MPa, density ρ=80kg/m 3 and shear modulus G=30MPa since it is the foam available for experiments.

In order to obtain the best panel to be applied in the UAV structure, several parameters are going to be taken into account: 1st structural mode frequency and Transmission Loss for low frequencies near the operational range of the UAV [300Hz].

To perform these studies eight different panels are considered:

- Single core:
    - Group Panel 1 Carbon fiber/Foam/Carbon fiber (CF / F / CF)
    - Group panel 2 Glass fiber/Foam/Glass fiber (GF / F / GF)
    - Group panel 3 Glass Fiber / Carbon Fiber / Foam / Carbon Fiber / Glass Fiber (GF/CF/F/CF/GF)
    - Group panel 4 Carbon Fiber / Glass Fiber / Foam / Glass Fiber / Carbon Fiber (CF/CG/F/GF/CF)
- Double core:
    - Group panel 5 Carbon Fiber / Foam / Glass Fiber / foam / Carbon Fiber CF/F/GF/F/CF
    - Group panel 6 Carbon Fiber / Foam / Carbon Fiber / Foam / Carbon Fiber (CF/ F / CF / F / CF)
    - Group panel 7 Glass Fiber/ Foam / Carbon Fiber / Foam / Glass Fiber (GF/F/CF/F/GF)
    - Group panels 8 Glass fiber/Foam/Glass fiber/Foam/Glass Fiber (GF/F/GF/F/GF)

The nomenclature used to describe this study is: CF is for carbon fiber, GF is for glass fiber and F describes the foam thickness in millimeters

After all the panels are tested, a comparison between them is performed with the outliers identified in the conclusions.

8.3. Group Panel 1 Carbon fiber/Foam/Carbon fiber (CF / F / CF)

	Panel CF/0/CF	Panel CF/3/CF	Panel CF/5/CF	Panel CF/7/CF
Number of layers	8	9	9	9
Total Thickness	2mm	5mm	7mm	9mm
Weight	0,1884 kg	0,2028 kg	0,2124 kg	0,222 kg
Layup materials	CF/CF/CF/CF CF/CF/CF/CF	CF/CF/CF/CF Airex C70.75 CF/CF/CF/CF	CF/CF/CF/CF Airex C70.75 CF/CF/CF/CF	CF/CF/CF/CF Airex C70.75 CF/CF/CF/CF
Layup orientation	[0/90/90/0] [0/90/90/0]	[0/90/90/0] [Foam] [0/90/90/0]	[[0/90/90/0] [Foam] [0/90/90/0]	[0/90/90/0] [Foam] [0/90/90/0]
Carbon Fiber layer thickness	0.25mm	0.25mm	0.25mm	0.25mm
Foam thickness		3mm	5mm	7mm

Table 16 Panels CF/F/CF Panel layers, thickness and orientation

Natural frequencies (Clamped)

	Frequencies(Hz) Clamped			
Modes	Panel CF/0/CF	Panel CF/3/CF	Panel CF/5/CF	Panel CF/7/CF
1	293,95Hz	571.26Hz	685.9Hz	775.66Hz
2	458,49Hz	811.83Hz	962.18Hz	1081.3Hz
3	723,71Hz	1068.6Hz	1249.1Hz	1395Hz
4	770,61Hz	1170.1Hz	1360.2Hz	1512.8Hz
5	823,84Hz	1225.7Hz	1431.1Hz	1596.7Hz
6	1054,3Hz	1496.2Hz	1731.1Hz	1921.1Hz

Table 17 Panels CF/F/CF natural frequencies

Single cavity model

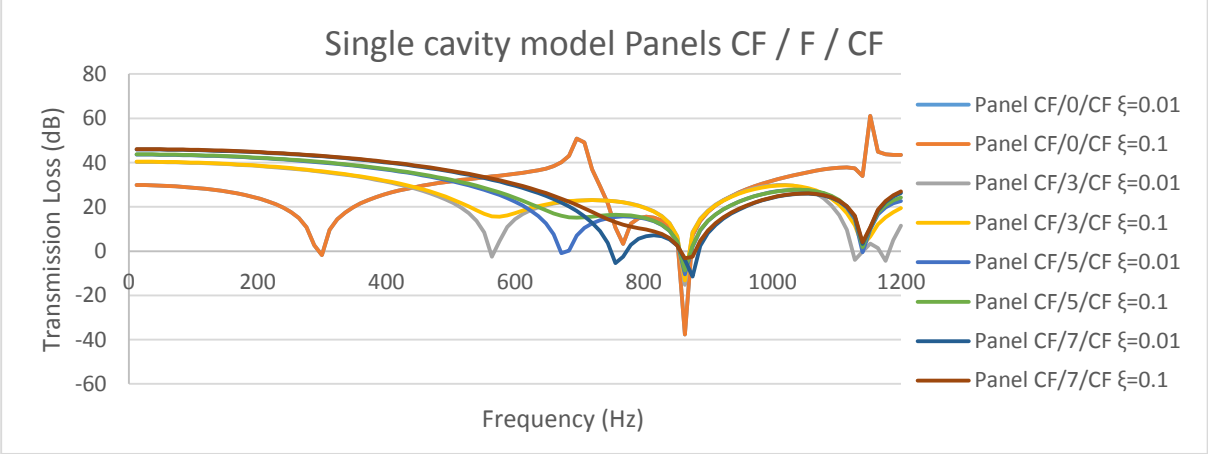

Figure 72 TL single cavity model for panels CF/F/CF

	1st Critical Point CDC : 0.01		TL(Low Frequency)			
	1st CP	TL(CP)	12Hz	150Hz	300Hz	450Hz
Panel CF/0/CF	300Hz	-1.79dB	29,86dB	26.94dB	-1.79dB	29.19dB
Panel CF/3/CF	564Hz	-2.57dB	40,33dB	39.31dB	35.86dB	27.80dB
Panel CF/5/CF	672Hz	-0.97dB	43,61dB	42.77dB	40.06dB	34.58dB
Panel CF/7/CF	756Hz	-5.37dB	45,96dB	45.21dB	42.82dB	38.22dB

Table 18 Critical points frequency and TL for low frequency for single cavity model

Setup 1

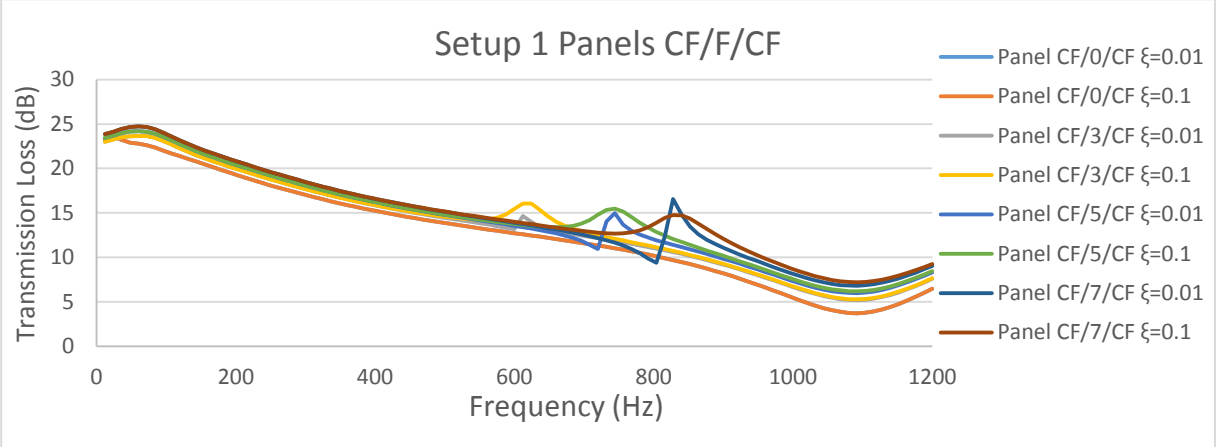

Figure 73 TL for Setup 1 for panels CF/F/CF

1st Critical Point			TL (Low Frequency)			
	CDC: 0.01					
	1st CP	TL (CP)	12Hz	150Hz	300Hz	450Hz
Panel CF/0/CF	ND	ND	23,23dB	20,62dB	17,02dB	14,51dB
Panel CF/3/CF	624Hz	14.00dB	23,02dB	23,15dB	17,68dB	15,11dB
Panel CF/5/CF	756Hz	13.69dB	23,45dB	23,58dB	18,08dB	15,45dB
Panel CF/7/CF	828Hz	14.79dB	23,87dB	24,00dB	18,48dB	15,81dB

Table 19 Critical points frequency and TL for low frequency for Setup 1

Setup 2

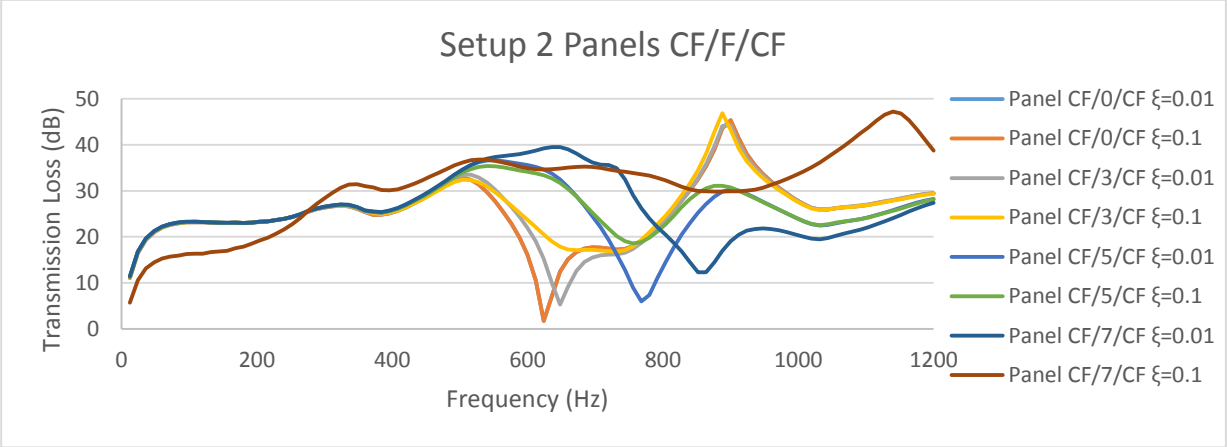

Figure 74 TL for Setup 1 for panels CF/F/CF

	1st Critical Point		TL(Low Frequency)			
	CDC : 0.01					
	1st CP	TL(CP)	12Hz	150Hz	300Hz	450Hz
Panel CF/0/CF	624Hz	1,71dB	11,04dB	23,05dB	26,38dB	28,72dB
Panel CF/3/CF	648Hz	5,30dB	11,20dB	13,92dB	26,42dB	28,84dB
Panel CF/5/CF	768Hz	5,99dB	11,31dB	14,02dB	26,50dB	29,30dB
Panel CF/7/CF	864Hz	12,28dB	11,42dB	14,12dB	26,55dB	33,45dB

Table 20 Critical points frequency and TL for low frequency for Setup 2

8.4. Group panel 2 Glass fiber/Foam/Glass fiber (GF / F / GF)

	Panel GF/0/GF	Panel GF/3/GF	Panel GF/5/GF	Panel GF/7/GF
Number of layers	8	9	9	9
Total Thickness	4mm	7mm	9mm	11mm
Weight	0,6168 kg	0,6312 kg	0,6408 kg	0,6504 kg
Layup materials	GF/GF/GF/GF GF/GF/GF/GF	GF/GF/GF/GF Airex C70.75 GF/GF/GF/GF	GF/GF/GF/GF Airex C70.75 GF/GF/GF/GF	GF/GF/GF/GF Airex C70.75 GF/GF/GF/GF
Layup orientation	[0/90/90/0] [0/90/90/0]	[0/90/90/0] [Foam] [0/90/90/0]	[[0/90/90/0] [Foam] [0/90/90/0]	[0/90/90/0] [Foam] [0/90/90/0]
Glass Fiber layer thickness	0.5mm	0.5mm	0.5mm	0.5mm
Foam thickness		3mm	5mm	7mm

Table 21 Panels GF/F/GF Panel layers, thickness and orientations

Natural frequencies (Clamped)

	Frequencies(Hz) Clamped			
Modo	Panel GF/0/GF	Panel GF/3/GF	Panel GF/5/GF	Panel GF/7/GF
1	388.52Hz	462.27Hz	512.6Hz	558.08Hz
2	607.55Hz	639.89Hz	708.25Hz	770.18Hz
3	946.27Hz	906.92Hz	977.36Hz	1046.4Hz
4	999.26Hz	914.48Hz	999.14Hz	1077.3Hz
5	1111.3Hz	1033.3Hz	1114.8Hz	1193.7Hz
6	1433Hz	1246.9HZ	1339.9Hz	1429.9Hz

Table 22 Panels GF/F/GF natural frequencies

Single cavity model

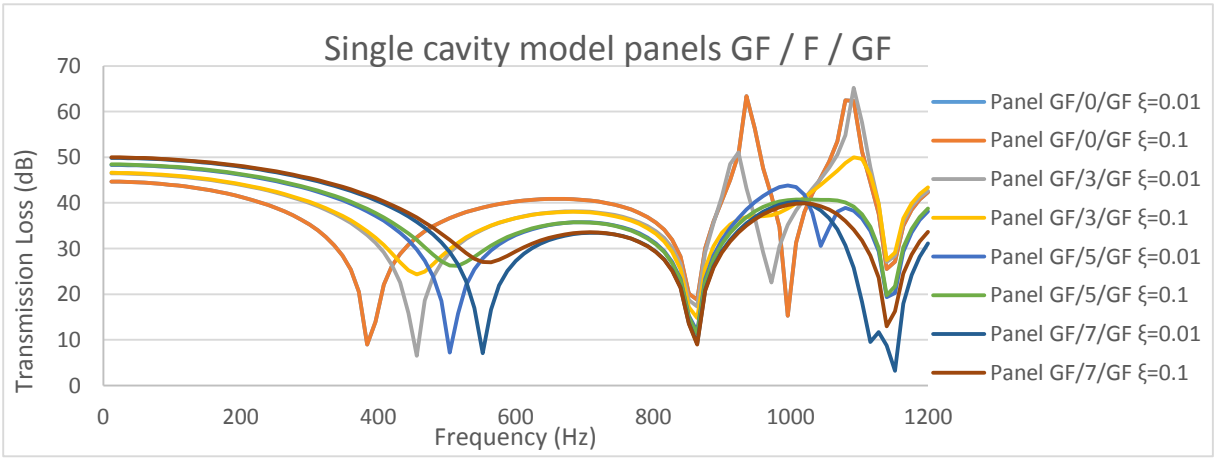

Figure 75 TL for single Cavity model for panels GF/F/GF

	1st Critical Point CDC : 0.01		TL(Low Frequency)			
	1st CP	TL(CP)	12Hz	150Hz	300Hz	450Hz
Panel GF / 0 / GF	384Hz	8,96dB	44,67dB	42,90dB	35,24dB	31,67dB
Panel GF / 3 / GF	456Hz	6,54dB	46,49dB	46,48dB	39,94dB	11,18dB
Panel GF / 5 / GF	504Hz	7,23dB	48,32dB	48,31dB	42,95dB	30,82dB
Panel GF / 7 / GF	552Hz	7,10dB	49,85dB	49,84dB	45,17dB	36,42dB

Table 23 Critical Points frequency and TL for low frequencies for single cavity model

Setup 1

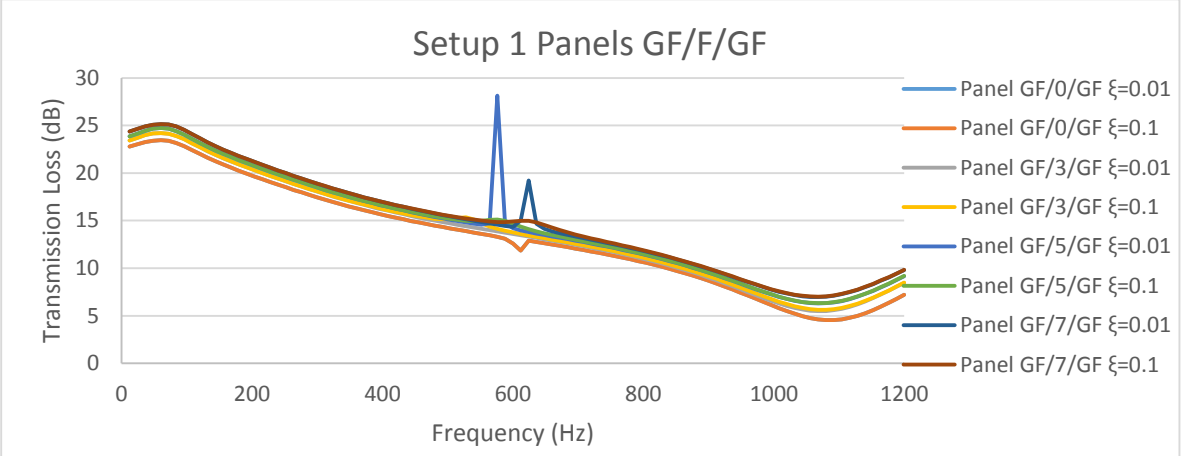

Figure 76 TL for Setup 1 for panels GF/F/GF

	1st Critical Point CDC : 0.01		TL(Low Frequency)			
	1st CP	TL(CP)	12Hz	150Hz	300Hz	450Hz
Panel GF / 0 / GF	ND	ND	22,79dB	21,06dB	17,44dB	14,864dB
Panel GF / 3 / GF	540Hz	15.11dB	23,44dB	23,57dB	18,05dB	15,41dB
Panel GF / 5 / GF	576Hz	28.15dB	23,86dB	23,99dB	18,46dB	15,78dB
Panel GF / 7 / GF	624Hz	19.22dB	24,36dB	24,50dB	18,87dB	16,15dB

Table 24 Critical points frequency and TL for low frequency for Setup 1

Setup 2

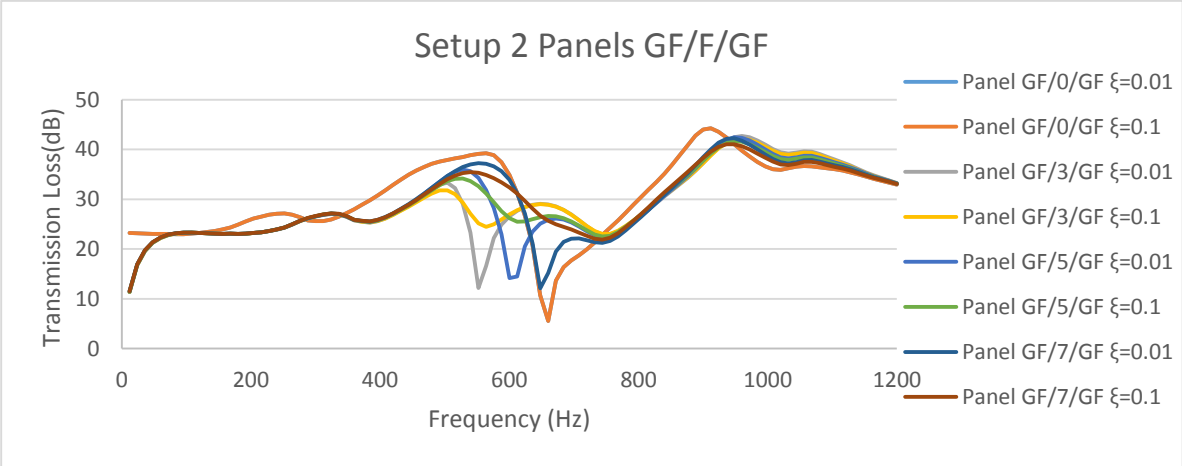

Figure 77 TL for Setup 2 for panels GF/F/GF

	1st Critical Point CDC : 0.01		TL(Low Frequency)			
	1st CP	TL(CP)	12Hz	150Hz	300Hz	450Hz
Panel GF / 0 / GF	660Hz	5,548dB	23,21dB	23,78dB	25,60dB	35,35dB
Panel GF / 3 / GF	552Hz	12,15dB	11,30dB	14,02dB	26,66dB	29,79dB
Panel GF / 5 / GF	600Hz	14.13dB	11,42dB	14,12dB	26,67dB	29,78dB
Panel GF / 7 / GF	648	12,12dB	11,53dB	14,24dB	26,68dB	32,57dB

Table 25 Critical points frequency and TL for low frequency for Setup 2

8.5. Group panel 3 Glass Fiber / Carbon Fiber / Foam / Carbon Fiber / Glass Fiber (GF/CF/F/CF/GF)

	Panel GF/CF/3/CF/GF	Panel GF/CF/5/CF/GF	Panel GF/CF/7/CF/GF
Number of layers	13	13	13
Total Thickness	7mm	9mm	11mm
Weight	0,5112 kg	0,5208 kg	0,5304 kg
Layup materials	GF/GF/CF/CF/CF/CF Airex C70.75 CF/CF/CF/CF/GF/GF	GF/GF/CF/CF/CF/CF Airex C70.75 CF/CF/CF/CF/GF/GF	GF/GF/CF/CF/CF/CF Airex C70.75 CF/CF/CF/CF/GF/GF
Layup orientation	[0/90/0/90/90/0] [Foam] [0/90/90/0/90/0]	[0/90/0/90/90/0] [Foam] [0/90/90/0/90/0]	[0/90/0/90/90/0] [Foam] [0/90/90/0/90/0]
Glass Fiber layer thickness	0.5mm	0.5mm	0.5mm
Carbon Fiber layer thickness	0.25mm	0.25mm	0.25mm
Foam thickness	3mm	5mm	7mm

Table 26 Panels GF/CF/F/CF/GF panel layers, thickness and orientation

Natural frequencies (Clamped)

	Frequencies(Hz) Clamped		
Modo	Panel GF/CF/3/CF/GF	Panel GF/CF/5/CF/GF	Panel GF/CF/7/CF/GF
1	476.18Hz	534.23Hz	585.01Hz
2	709.29Hz	781.59Hz	846.95Hz
3	930.46Hz	1016.5Hz	1095.8Hz
4	1056.9Hz	1139.8Hz	1217.8Hz
5	1095.8Hz	1189.2Hz	1276.5Hz
6	1372.5Hz	1471.1Hz	1566.2Hz

Table 27 Panels GF/CF/F/CF/GF natural frequency

Single cavity model

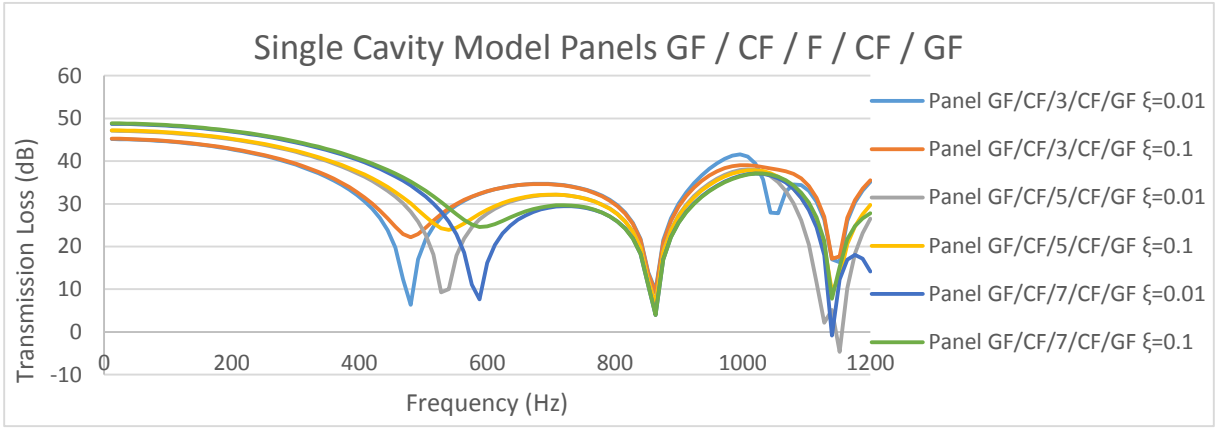

Figure 78 TL for single cavity model for Panels GF/CF/F/CF/GF

	1st Critical Point CDC : 0.01		TL(Low Frequency)			
	1st CP	TL(CP)	12Hz	150Hz	300Hz	450Hz
Panel GF / CF / 3 / CF / GF	480Hz	6.34dB	45,14dB	43,85dB	39,15dB	21,79dB
Panel GF / CF / 5 / CF / GF	540Hz	7.66dB	47,10dB	46,00dB	42,16dB	32,36dB
Panel GF / CF / 7 / CF / GF	588Hz	7.66dB	48,71dB	47,72dB	44,38dB	36,88dB

Table 28 Critical Points frequency and TL for low frequency for single cavity model

Setup 1

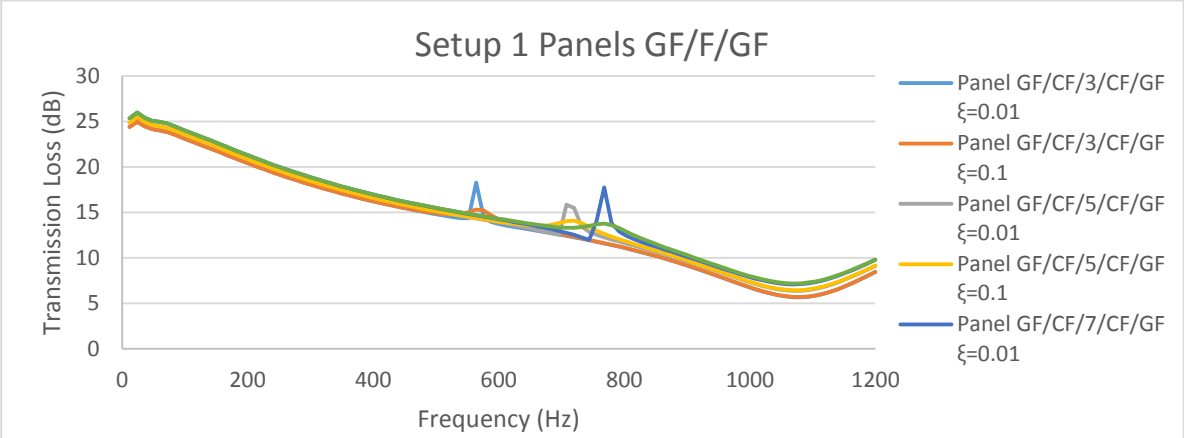

Figure 79 TL for Setup 1 for Panels GF/CF/F/CF/GF

	1st Critical Point		TL(Low Frequency)			
	CDC : 0.01					
	1st CP	TL(CP)	12Hz	150Hz	300Hz	450Hz
Panel GF/CF/3/CF/GF	564Hz	18.28dB	24,40dB	21,76dB	18,06dB	15,47dB
Panel GF/CF/5/CF/GF	708Hz	15.48dB	24,84dB	22.21dB	18,46dB	15,81dB
Panel GF/CF/7/CF/GF	768Hz	17.73dB	25,34dB	22.67dB	18,87dB	16,18dB

Table 29 Critical points frequency and TL for low frequency for Setup 1

Setup 2

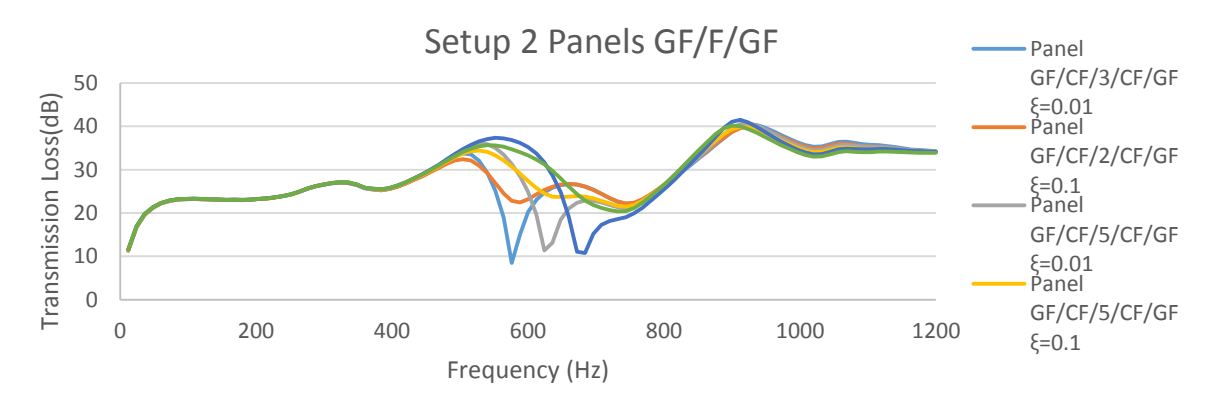

Figure 80 TL for Setup 2 for Panels GF/CF/F/CF/GF

	1st Critical Point		TL(Low Frequency)			
	CDC : 0.01					
	1st CP	TL(CP)	12Hz	150Hz	300Hz	450Hz
Panel GF / CF / 3 / CF / GF	576Hz	8.49dB	11,31dB	23,04dB	26,54dB	29,14dB
Panel GF / CF / 5 / CF / GF	624Hz	11.31dB	11,42dB	23,05dB	26,57dB	29,37dB
Panel GF / CF / 7 / CF / GF	684Hz	10.77dB	11,54dB	23,07dB	26,60dB	29,48dB

Table 30 Critical points frequency and TL for low frequency for Setup 2

8.6. Group panel 4 Carbon Fiber / Glass Fiber / Foam / Glass Fiber / Carbon Fiber (CF/GF/F/GF/CF)

	Panel CF/GF/3/GF/CF	Panel CF/GF/5/GF/CF	Panel CF/GF/7/GF/CF
Number of layers	13	13	13
Total Thickness	7mm	9mm	11mm
Weight	0,5112 kg	0,5208 kg	0,5304 kg
Layup materials	CF/CF/CF/CF/GF/GF Airex C70.75 GF/GF/CF/CF/CF/CF	CF/CF/CF/CF/GF/GF Airex C70.75 GF/GF/CF/CF/CF/CF	CF/CF/CF/CF/GF/GF Airex C70.75 GF/GF/CF/CF/CF/CF
Layup orientation	[0/90/90/0/0/90] [Foam] [90/0/0/90/90/0]	[0/90/90/0/0/90] [Foam] [90/0/0/90/90/0]	[0/90/90/0/0/90] [Foam] [90/0/0/90/90/0]
Glass Fiber layer thickness	0.5mm	0.5mm	0.5mm
Carbon Fiber layer thickness	0.25mm	0.25mm	0.25mm
Foam thickness	3mm	5mm	7mm

Table 31 Panels CF/GF/F/GF/CF panel layers, thickness and orientation

Natural frequencies (Clamped)

	Frequencies(Hz) Clamped		
Modo	**Panel CF/GF/3/GF/CF**	**Panel CF/GF/5/GF/CF**	**Panel CF/GF/7/GF/CF**
1	509.41Hz	561.95Hz	609.59Hz
2	743.89Hz	810.7Hz	872.82Hz
3	992.98Hz	1068.1Hz	1141.5Hz
4	1103.1Hz	1178.9Hz	1252.9Hz
5	1146Hz	1230.6Hz	1313.1Hz
6	1420.2Hz	1511.5Hz	1602.3Hz

Table 32 Panels CF/GF/F/GF/CF

Single cavity model

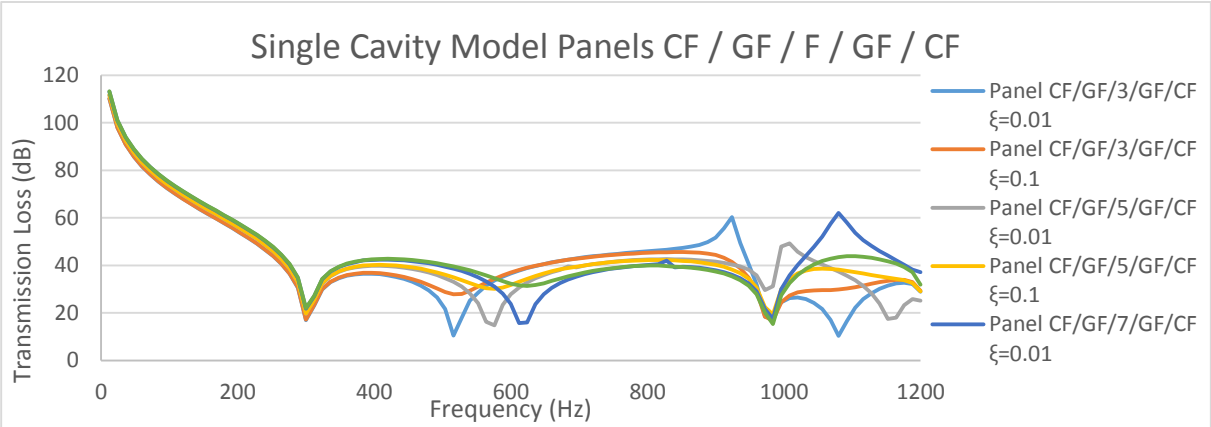

Figure 81 TL for single cavity model for panels CF/GF/F/GF/CF

	1st Critical Point CDC : 0.01		TL(Low Frequency)			
	1st CP	TL(CP)	12Hz	150Hz	300Hz	450Hz
Panel CF / GF / 3 / GF / CF	516Hz	10.49dB	110,14dB	62,70dB	16,97dB	33,66dB
Panel CF / GF / 5 / GF / CF	576Hz	14.74dB	111,60dB	64.43dB	19,59dB	38,77dB
Panel CF / GF / 7 / GF / CF	624Hz	15.95dB	113,13dB	65.92dB	21,79dB	41,91dB

Table 33 Critical point frequency and TL for low frequency for single cavity model

Setup 1

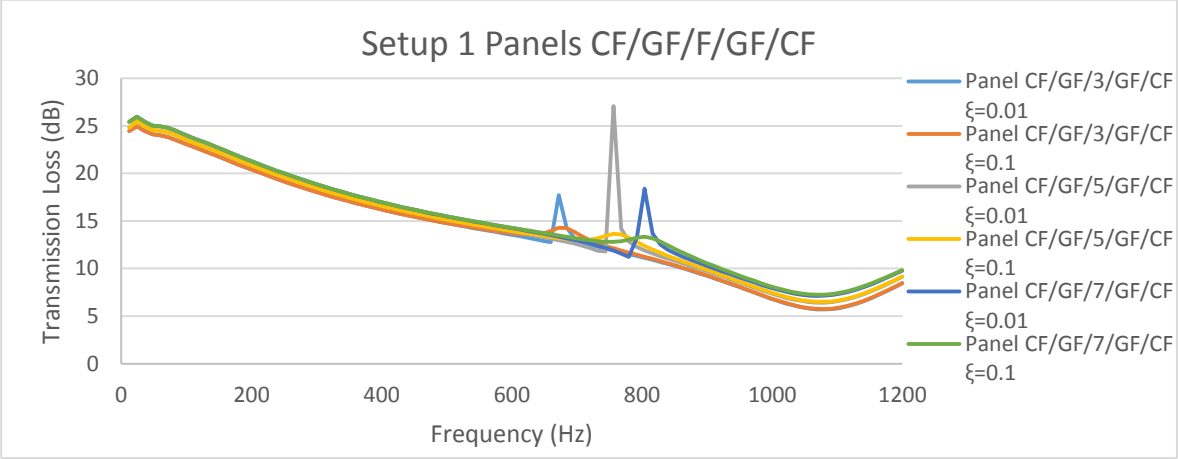

Figure 82 TL for Setup 1 for panels CF/GF/F/GF/CF

	1st Critical Point		TL(Low Frequency)			
	CDC : 0.01					
	1st CP	SPL(CP)	12Hz	150Hz	300Hz	450Hz
Panel CF/GF/3/GF/CF	672Hz	17.71dB	24,46dB	21,76dB	18,05dB	15,44dB
Panel CF/GF/5/GF/CF	756Hz	27.06dB	24,83dB	25,17dB	18,46dB	15,81dB
Panel CF/GF/7/GF/CF	804Hz	18.38dB	25,42dB	25,70dB	18,87dB	16,18dB

Table 34 Critical points frequency and TL for low frequency for Setup 1

Setup 2

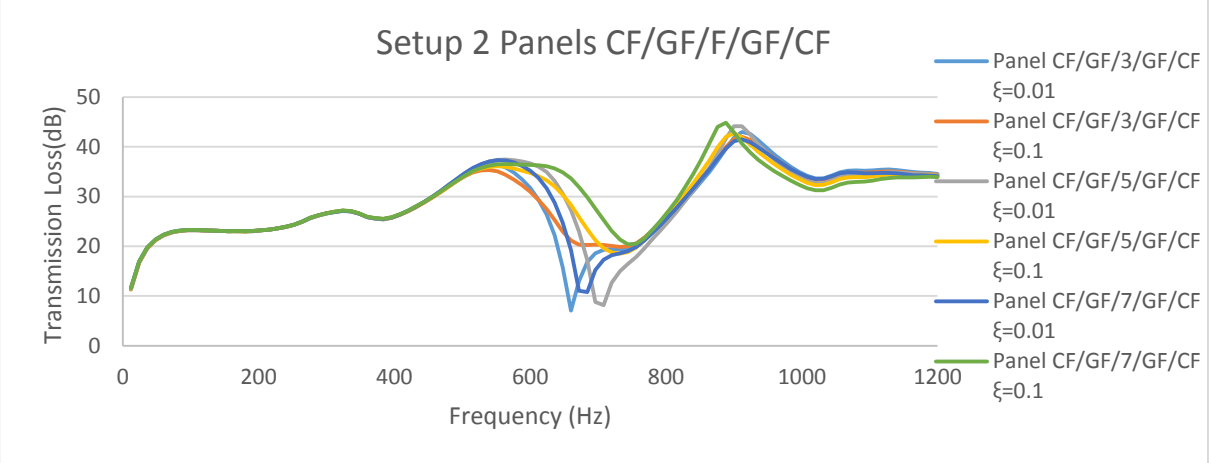

Figure 83 TL for Setup 2 for panels CF/GF/F/GF/CF

	1st Critical Point		TL(Low Frequency)			
	CDC : 0.01					
	1st CP	SPL(CP)	12Hz	150Hz	300Hz	450Hz
Panel CF / GF / 3 / GF / CF	660Hz	7.08dB	11,31dB	23,04dB	26,57dB	29,40dB
Panel CF / GF / 5 / GF / CF	684Hz	10.77dB	11,42dB	23.05dB	26,60dB	29,48dB
Panel CF / GF / 7 / GF / CF	708Hz	8.10dB	11,54dB	23.07dB	26,60dB	29,48dB

Table 35 Critical points frequency and TL for low frequency for Setup 2

8.7. Group panel 5 Carbon Fiber / Foam / Glass Fiber / foam / Carbon Fiber CF/F/GF/F/CF

	Panel CF/1,5/GF/1,5/CF	Panel CF/3/GF/3/CF	Panel CF/4,5/GF/4,5/CF
Number of layers	14	14	14
Total Thickness	7mm	10mm	13mm
Weight	0,5112 kg	0,5256 kg	0,54 kg
Layup materials	CF/CF/CF/CF Airex C70.75 GF/GF/GF/GF Airex C70.75 CF/CF/CF/CF	CF/CF/CF/CF Airex C70.75 GF/GF/GF/GF Airex C70.75 CF/CF/CF/CF	CF/CF/CF/CF Airex C70.75 GF/GF/GF/GF Airex C70.75 CF/CF/CF/CF
Layup orientation	[0/90/90/0] [Foam] [0/90/90/0] [Foam] [0/90/90/0]	[0/90/90/0] [Foam] [0/90/90/0] [Foam] [0/90/90/0]	[0/90/90/0] [Foam] [0/90/90/0] [Foam] [0/90/90/0]
Glass Fiber layer thickness	0.5mm	0.5mm	0.5mm
Carbon Fiber layer thickness	0.25mm	0.25mm	0.25mm
Foam thickness	1.5mm	3mm	4.5mm

Table 36 Panels CF/F/GF/F/CF panel layers, thickness and orientation

Natural frequencies (Clamped)

	Frequencies(Hz) Clamped		
Modo	**Panel CF/1,5/GF/1,5/CF**	**Panel CF/3/GF/3/CF**	**Panel CF/4,5/GF/4,5/CF**
1	488.96Hz	567.6Hz	635.42Hz
2	737.06Hz	838.56Hz	927.26Hz
3	1009.8Hz	1116.7Hz	1218.2Hz
4	1111Hz	1222.1Hz	1326.9Hz
5	1168Hz	1289.2Hz	1403.9Hz
6	1447.5Hz	1576.2Hz	1703Hz

Table 37 Panels CF/F/GF/F/CF natural frequency

Single cavity model

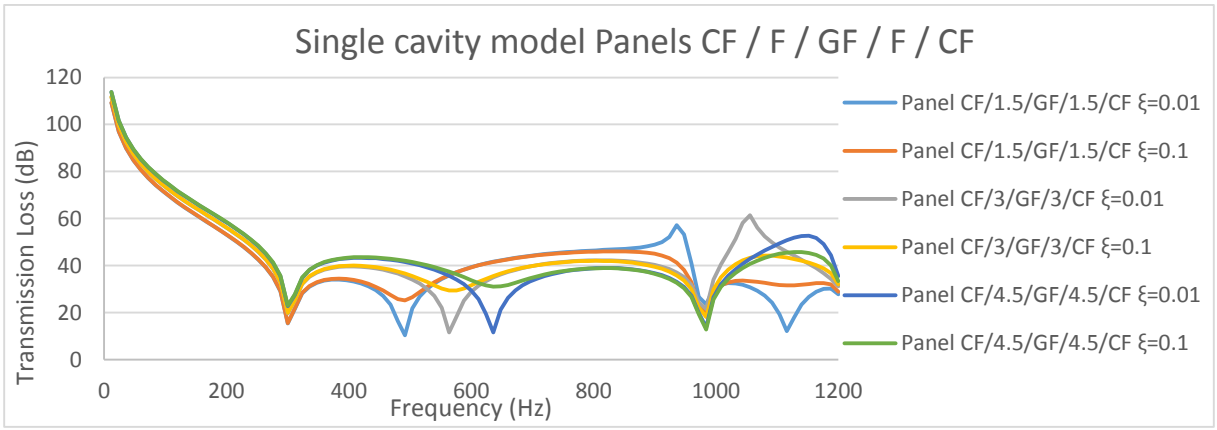

Figure 84 TL for single cavity model for CF/F/GF/F/CF

	1st Critical Point		TL(Low Frequency)			
	CDC : 0.01					
	1st CP	SPL(CP)	12Hz	150Hz	300Hz	450Hz
Panel CF / 1,5 / GF / 1,5 / CF	492Hz	10.34dB	109,14dB	61,62dB	15,36dB	28,35dB
Panel CF / 3 / GF / 3 / CF	564Hz	11.58dB	111,63dB	64.40dB	19,68dB	38,51dB
Panel CF / 4,5 / GF / 4,5 / CF	636Hz	11.66dB	113,74dB	66.54dB	22,83dB	42,97dB

Table 38 Critical points frequency and TL for low frequency for single cavity model

Setup 1

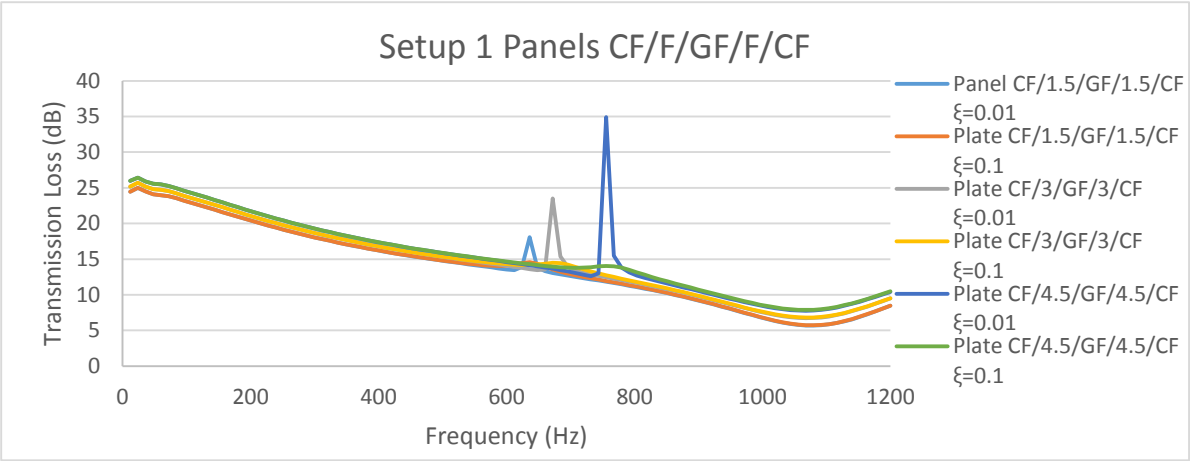

Figure 85 TL for Setup 1 for CF/F/GF/F/CF

	1st Critical Point		TL(Low Frequency)			
	CDC : 0.01					
	1st CP	SPL(CP)	12Hz	150Hz	300Hz	450Hz
Panel CF/1,5/GF/1,5/CF	636Hz	10.06dB	24,46dB	21,76dB	18,06dB	15,45dB
Panel CF/3/GF/3/CF	672Hz	23.49dB	25,17dB	22.44dB	18,67dB	16,00dB
Panel CF/4.5/GF/4,5/CF	756Hz	34.93dB	25,99dB	22.13dB	19,29dB	16,56dB

Table 39 Critical points frequency and TL for low frequency for Setup 1

Setup 2

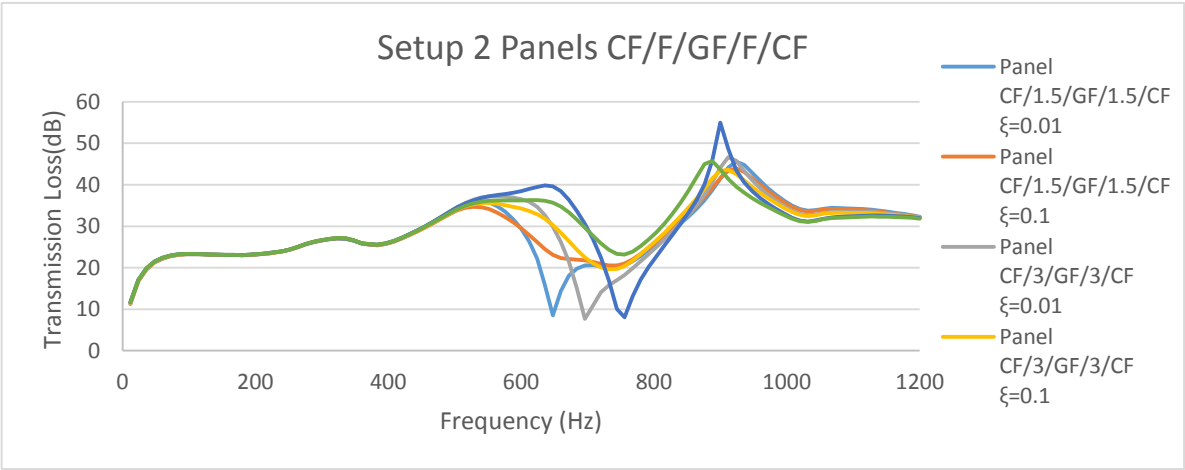

Figure 86 TL for Setup 2 for CF/F/GF/F/CF

	1st Critical Point		TL(Low Frequency)			
	CDC : 0.01					
	1st CP	SPL(CP)	12Hz	150Hz	300Hz	450Hz
Panel CF / 1,5 / GF / 1,5 / CF	624Hz	8.47dB	11,31dB	23,08dB	26,56dB	29,38dB
Panel CF / 3 / GF / 3 / CF	648Hz	7.66dB	11,48dB	23,09dB	26,59dB	29,48dB
Panel CF / 4,5 / GF / 4,5 / CF	768Hz	8.06dB	11,65dB	23,13dB	26,62dB	29,54dB

Table 40 Critical points frequency and TL for low frequency for Setup 2

8.8. Group panel 6 Carbon Fiber / Foam / Carbon Fiber / Foam / Carbon Fiber (CF / F / CF / F / CF)

	Panel CF/1,5/CF/1,5/CF	Panel CF/3/CF/3/CF	Panel CF/4,5/CF/4,5/CF
Number of layers	14	14	14
Total Thickness	6mm	9mm	12mm
Weight	0,297 kg	0,3114 kg	0,3258 kg
Layup materials	CF/CF/CF/CF Airex C70.75 CF/CF/CF/CF Airex C70.75 CF/CF/CF/CF	CF/CF/CF/CF Airex C70.75 CF/CF/CF/CF Airex C70.75 CF/CF/CF/CF	CF/CF/CF/CF Airex C70.75 CF/CF/CF/CF Airex C70.75 CF/CF/CF/CF
Layup orientation	[0/90/90/0] [Foam] [0/90/90/0] [Foam] [0/90/90/0]	[0/90/90/0] [Foam] [0/90/90/0] [Foam] [0/90/90/0]	[0/90/90/0] [Foam] [0/90/90/0] [Foam] [0/90/90/0]
Glass Fiber layer thickness	0.5mm	0.5mm	0.5mm
Carbon Fiber layer thickness	0.25mm	0.25mm	0.25mm
Foam thickness	1.5mm	3mm	4.5mm

Table 41 Panels CF/F/CF/F/CF panel layers, thickness and orientation

Natural frequencies (Clamped)

	Frequencies(Hz) Clamped		
Modo	**Panel CF/1,5/CF/1,5/CF**	**Panel CF/3/CF/3/CF**	**Panel CF/4,5/CF/4,5/CF**
1	590.32Hz	703.5Hz	792.71Hz
2	839.03Hz	985.59Hz	1104.2Hz
3	1102.7Hz	1272.3Hz	1416.6Hz
4	1209.7Hz	1389.4Hz	1539.8Hz
5	1266.1Hz	1459.3Hz	1622.9Hz
6	1547.7Hz	1765.3Hz	1951.6Hz

Table 42 Panel CF/F/CF/F/CF natural frequencies

Single cavity model

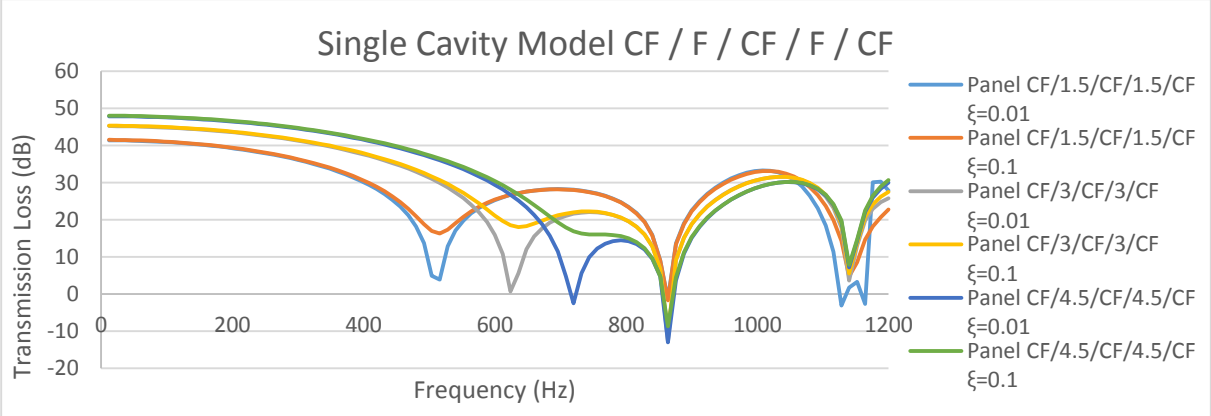

Figure 87 TL for single cavity model for panels CF/F/CF/F/CF

	1st Critical Point CDC : 0.01		TL(Low Frequency)			
	1st CP	SPL(CP)	12Hz	150Hz	300Hz	450Hz
Panel CF / 1,5 / CF / 1,5 / CF	516Hz	3.90dB	41,44dB	40,27dB	36,13dB	24,45dB
Panel CF / 3 / CF / 3 / CF	624Hz	0.72dB	45,24dB	44,32dB	41,31dB	34,95dB
Panel CF / 4,5 / CF / 4,5 / CF	720Hz	-2.50dB	47,90dB	47,11dB	44,55dB	39,52dB

Table 43 Critical points frequency and TL for low frequency for single cavity model

Setup 1

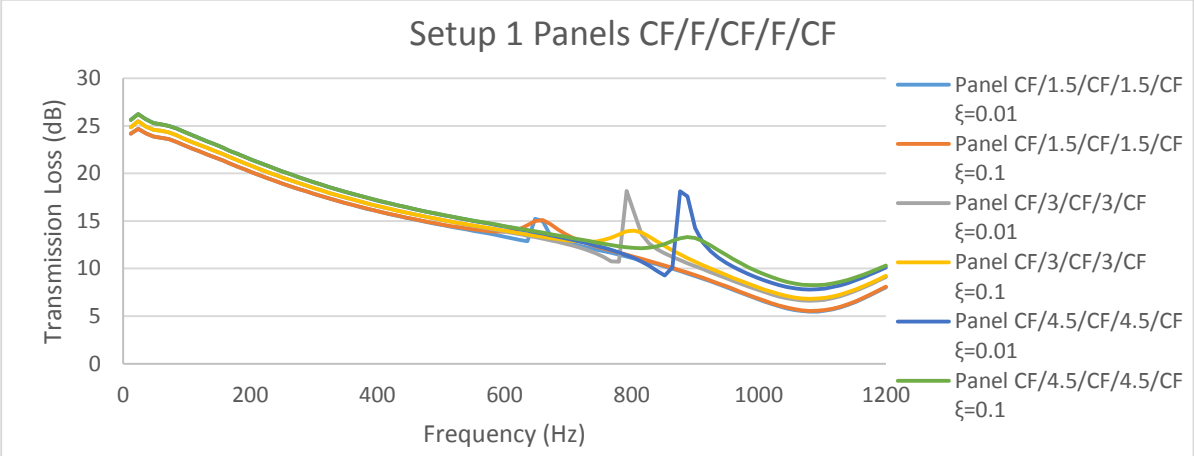

Figure 88 TL for Setup 1 for panels CF/F/CF/F/CF

	1st Critical Point		TL(Low Frequency)			
	CDC : 0.01					
	1st CP	SPL(CP)	12Hz	150Hz	300Hz	450Hz
Panel CF/1.5/CF/1.5/CF	660Hz	13.77dB	24,69dB	21,21dB	17,61dB	15,11dB
Panel CF/3/CF/3/CF	792Hz	18.16dB	25,49dB	25,22dB	18,21dB	15,64dB
Panel CF/4.5/CF/4.5/CF	888Hz	18.14dB	26,23dB	25,97dB	18,83dB	16,20dB

Table 44 Critical points frequency and TL for low frequency for Setup 1

Setup 2

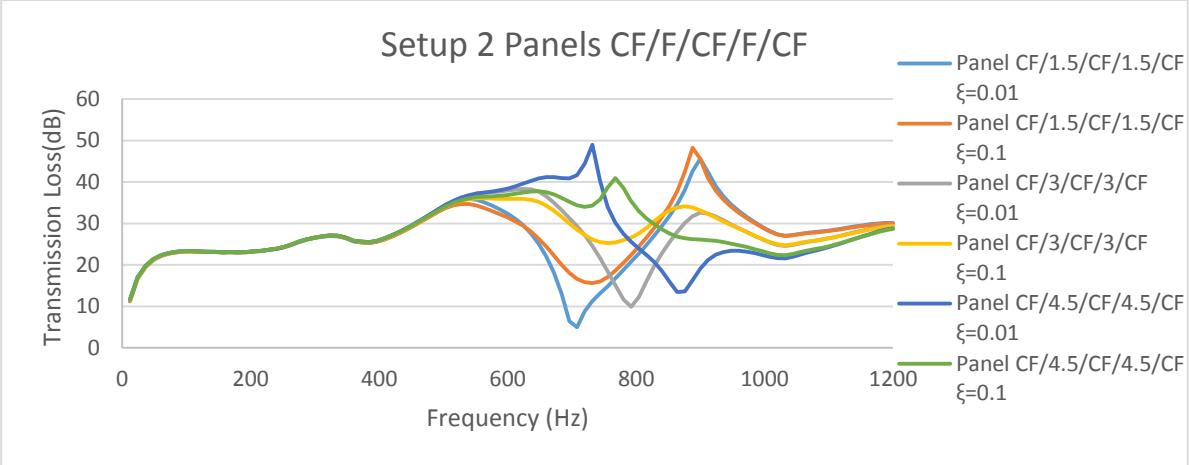

Figure 89 TL for Setup 2 for panels CF/F/CF/F/CF

	1st Critical Point		TL(Low Frequency)			
	CDC : 0.01					
	1st CP	SPL(CP)	12Hz	150Hz	300Hz	450Hz
Panel CF / 1,5 / CF / 1,5 / CF	708Hz	5.01dB	11,25dB	23,08dB	26,52dB	29,26dB
Panel CF / 3 / CF / 3 / CF	792Hz	9.90dB	11,42dB	23,09dB	26,57dB	29,45dB
Panel CF / 4,5 / CF / 4,5 / CF	876Hz	13.62Hz	11,59dB	23,12dB	26,60dB	29,53dB

Table 45 Critical points frequency and TL for low frequency for Setup 2

8.9. Group panel 7 Glass Fiber/ Foam / Carbon Fiber / Foam / Glass Fiber (GF/F/CF/F/GF)

	Panel GF/1,5/CF/1,5/GF	Panel GF/3/CF/3/GF	Panel GF/4,5/CF/4,5/GF
Number of layers	14	14	14
Total Thickness	8mm	11mm	14mm
Weight	0,7254 kg	0,7398 kg	0,7542 kg
Layup materials	GF/GF/GF/GF Airex C70.75 CF/CF/CF/CF Airex C70.75 GF/GF/GF/GF	GF/GF/GF/GF Airex C70.75 CF/CF/CF/CF Airex C70.75 GF/GF/GF/GF	GF/GF/GF/GF Airex C70.75 CF/CF/CF/CF Airex C70.75 GF/GF/GF/GF
Layup orientation	[0/90/90/0] [Foam] [0/90/90/0] [Foam] [0/90/90/0]	[0/90/90/0] [Foam] [0/90/90/0] [Foam] [0/90/90/0]	[0/90/90/0] [Foam] [0/90/90/0] [Foam] [0/90/90/0]
Glass Fiber layer thickness	0.5mm	0.5mm	0.5mm
Carbon Fiber layer thickness	0.25mm	0.25mm	0.25mm
Foam thickness	1.5mm	3mm	4.5mm

Table 46 Panels GF/F/CF/F/GF panel layups, thickness and orientation

Natural frequencies (Clamped)

	Frequencies(Hz) Clamped		
Modo	**Panel GF/1,5/CF/1,5/GF**	**Panel GF/3/CF/3/GF**	**Panel GF/4,5/CF/4,5/GF**
1	499.39Hz	553.98Hz	605.74Hz
2	721.36Hz	789.22Hz	856.83Hz
3	940.55Hz	1015.2Hz	1096.6Hz
4	1050.6Hz	1126.9Hz	1208.9Hz
5	1099.8Hz	1182Hz	1272.1Hz
6	1362.7Hz	1449.2Hz	1548.3Hz

Table 47 Panel GF/F/CF/F/GF natural frequencies

Single cavity model

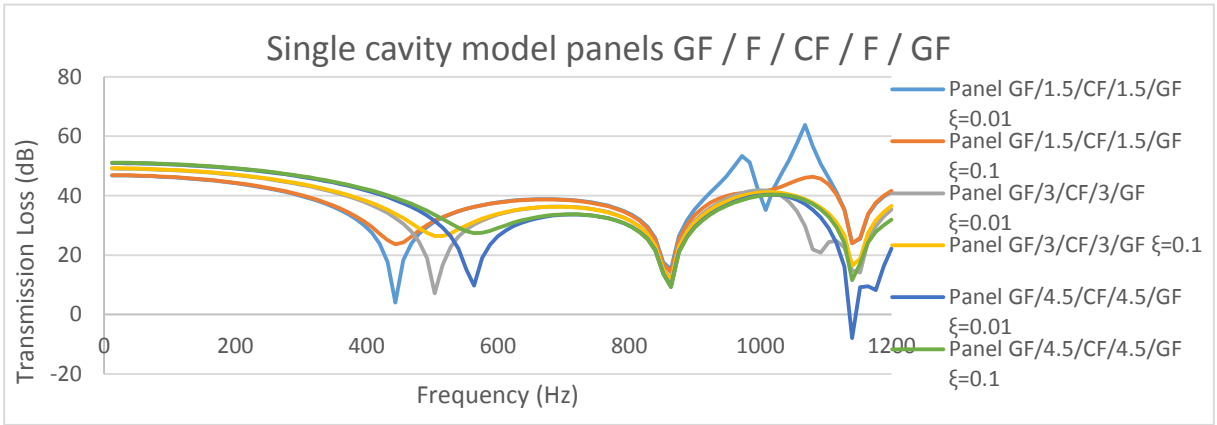

Figure 90 TL for mechanical acoustic cavity for panel GF/F/CF/F/GF

	1st Critical Point		TL(Low Frequency)			
	CDC : 0.01					
	1st CP	SPL(CP)	12Hz	150Hz	300Hz	450Hz
Panel GF / 1,5 / CF / 1,5 / GF	444Hz	4.04dB	46,82dB	45,38dB	39,91dB	11,18dB
Panel GF / 3 / CF / 3 / GF	504Hz	7.10dB	49,10dB	47,91dB	43,70dB	31,48dB
Panel GF / 4,5 / CF / 4,5 / GF	564Hz	9.74dB	50,96dB	49,92dB	46,38dB	37,99dB

Table 48 Critical points frequency and TL for low frequency for single cavity model

Setup 1

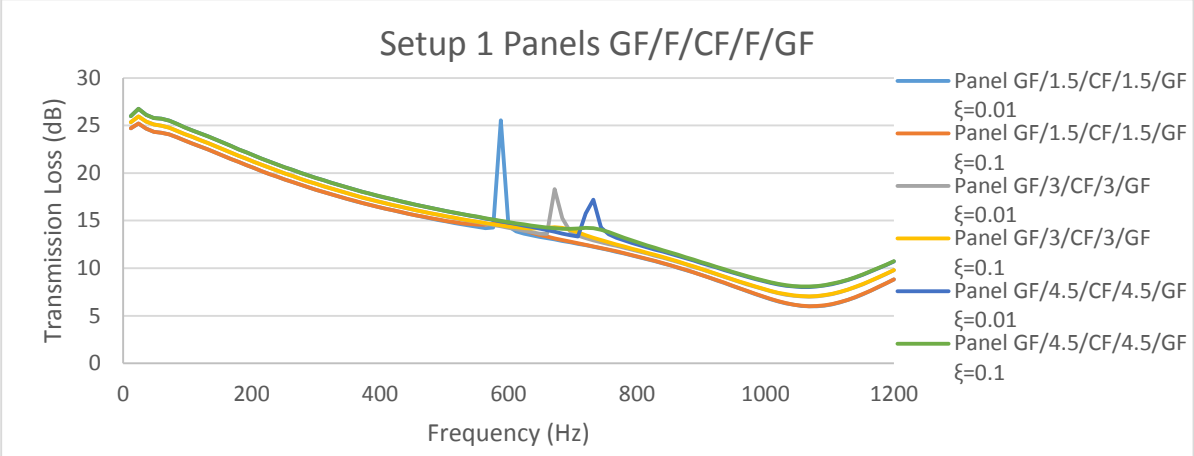

Figure 91 TL for Setup 1 for panel GF/F/CF/F/GF

	1st Critical Point		TL(Low Frequency)			
	CDC : 0.01					
	1st CP	SPL(CP)	12Hz	150Hz	300Hz	450Hz
Panel GF/1,5/CF/1,5/GF	588Hz	25.53dB	24,72dB	21,99dB	18,26dB	15,63dB
Panel GF/3/CF/3/GF	672Hz	18.32dB	25,36dB	25,66dB	18,87dB	16,18dB
Panel GF/4,5/CF/4,5/GF	732Hz	17.19dB	25,98dB	26,38dB	19,50dB	16,75dB

Table 49 Critical points frequency and TL for low frequency for Setup 1

Setup 2

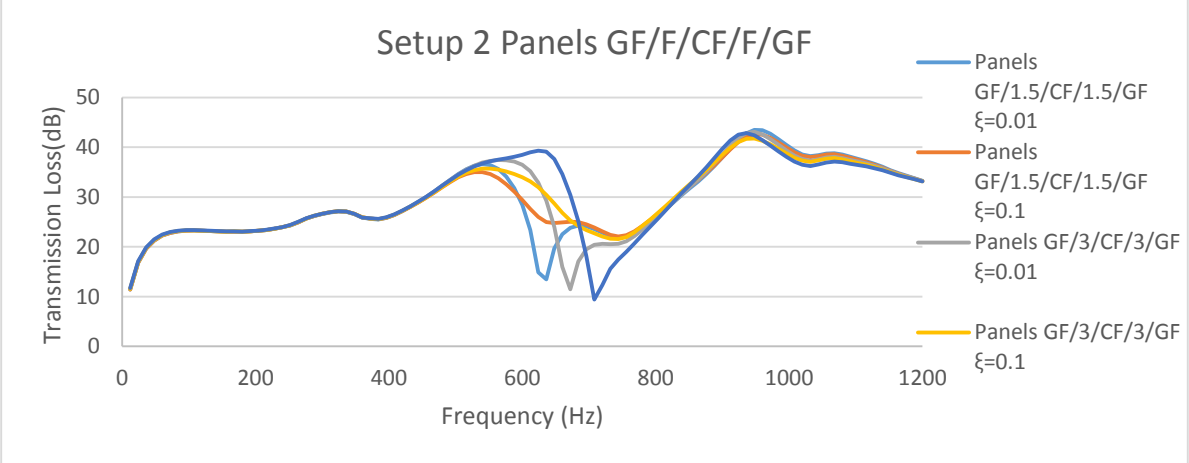

Figure 92 TL for Setup 2 for panel GF/F/CF/F/GF

	1st Critical Point		TL (Low Frequency)			
	CDC : 0.01					
	1st CP	SPL(CP)	12Hz	150Hz	300Hz	450Hz
Panel GF / 1,5 / CF / 1,5 / GF	636Hz	14.36dB	11,36dB	23,08dB	26,59dB	29,49dB
Panel GF / 3 / CF / 3 / GF	672Hz	14.19dB	11,54dB	23,10dB	26,62dB	29,54dB
Panel GF / 4,5 / CF / 4,5 / GF	708Hz	9.41dB	11,71dB	23,13dB	26,64dB	29,58dB

Table 50 Critical points frequency and TL for low frequency for Setup 2

8.10. Group panels 8 Glass fiber/Foam/Glass fiber/Foam/Glass Fiber (GF/F/GF/F/GF)

	Panel GF/1,5/GF/1,5/GF	**Panel GF/3/GF/3/GF**	**Panel GF/4,5/GF/4,5/GF**
Number of layers	14	14	14
Total Thickness	9mm	12mm	15mm
Weight	0,9396 kg	0,954 kg	0,9684 kg
Layup materials	GF/GF/GF/GF Airex C70.75 GF/GF/GF/GF Airex C70.75 GF/GF/GF/GF	GF/GF/GF/GF Airex C70.75 GF/GF/GF/GF Airex C70.75 GF/GF/GF/GF	GF/GF/GF/GF Airex C70.75 GF/GF/GF/GF Airex C70.75 GF/GF/GF/GF
Layup orientation	[0/90/90/0] [Foam] [0/90/90/0] [Foam] [0/90/90/0]	[0/90/90/0] [Foam] [0/90/90/0] [Foam] [0/90/90/0]	[0/90/90/0] [Foam] [0/90/90/0] [Foam] [0/90/90/0]
Glass Fiber layer thickness	0.5mm	0.5mm	0.5mm
Carbon Fiber layer thickness	0.25mm	0.25mm	0.25mm
Foam thickness	1.5mm	3mm	4.5mm

Table 51 Panel GF/F/GF/F/GF panel layers, thickness and orientation

Natural frequencies (Clamped)

	Frequencies(Hz) Clamped		
Modo	Panel GF/1,5/GF/1,5/GF	Panel GF/3/GF/3/GF	Panel GF/4,5/GF/4,5/GF
1	512.41Hz	545.92Hz	584.59Hz
2	739.78Hz	779.36Hz	829.35Hz
3	966.03Hz	1003.9Hz	1062.8Hz
4	1076.8Hz	1116Hz	1175Hz
5	1129.5Hz	1170.3Hz	1235.2Hz
6	1399	1438.2HZ	1508.5Hz

Table 52 Panel GF/F/GF/F/GF natural frequencies

Single Cavity Model

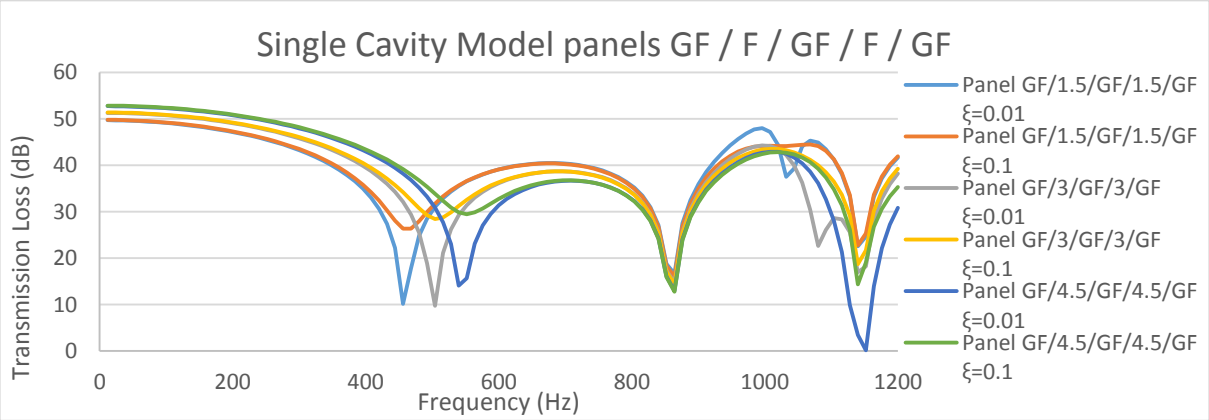

Figure 93 TL for single cavity model for panels GF/F/GF/F/GF

	1st Critical Point		**TL(Low Frequency)**			
	CDC : 0.01					
	1st CP	SPL(CP)	12Hz	150Hz	300Hz	450Hz
Panel GF / 1,5 / GF / 1,5 / GF	456Hz	10.17dB	49,73dB	48,36dB	43,28dB	16,21dB
Panel GF / 3 / GF / 3 / GF	504Hz	9.77dB	51,30dB	50,10dB	45,84dB	33,23dB
Panel GF / 4,5 / GF / 4,5 / GF	540Hz	14.10dB	52,76dB	51,69dB	47,98dB	38,85dB

Table 53 Critical points frequency and TL for low frequency for single cavity model

Setup 1

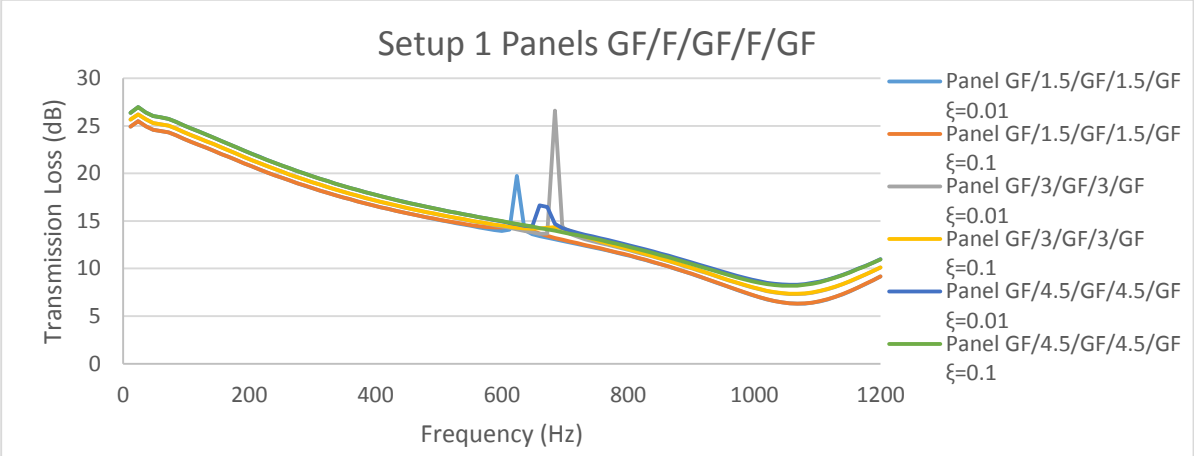

Figure 94 TL for Experience 1 for panels GF/F/GF/F/GF

	1st Critical Point		TL(Low Frequency)			
	CDC : 0.01					
	1st CP	SPL(CP)	12Hz	150Hz	300Hz	450Hz
Panel GF / 1,5 / GF / 1,5 / GF	624Hz	19.74dB	24,92dB	22,22dB	18,46dB	15,81dB
Panel GF / 3 / GF / 3 / GF	672Hz	16.48dB	25,68dB	22,89dB	19,08dB	16,37dB
Panel GF / 4,5 / GF / 4,5 / GF	684Hz	26.62dB	26,39dB	23,59dB	19,71dB	16,95dB

Table 54 Critical points frequency and TL for low frequency for Setup 1

Setup 2

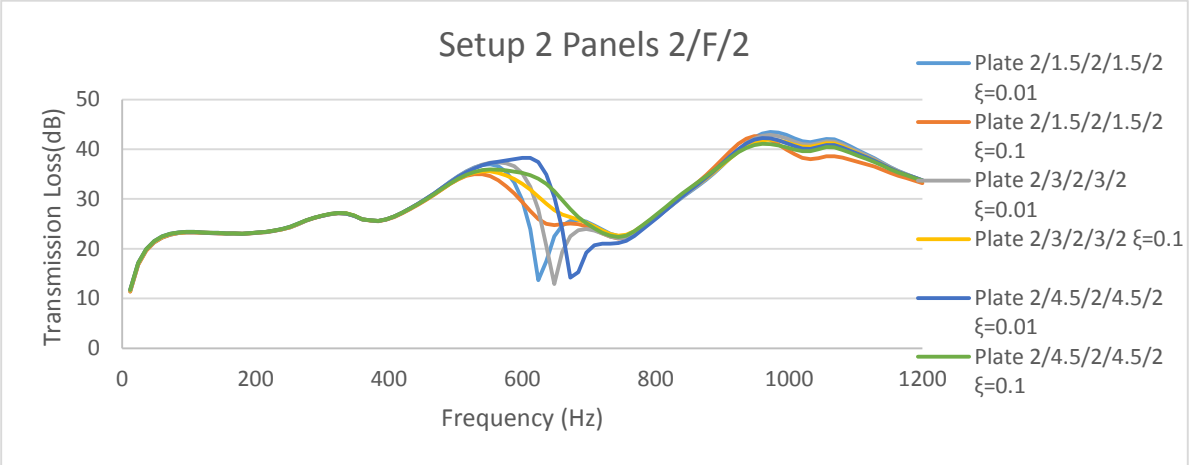

Figure 95 SPL for Experience 2 for panels GF/F/GF/F/GF

	1st Critical Point		TL(Low Frequency)			
	CDC : 0.01					
	1st CP	SPL(CP)	12Hz	150Hz	300Hz	450Hz
Panel GF / 1,5 / GF / 1,5 / GF	624Hz	13.67dB	11,42dB	23,08dB	26,61dB	29,55dB
Panel GF / 3 / GF / 3 / GF	648Hz	12.90dB	11,59dB	23,11dB	26,63dB	29,57dB
Panel GF / 4,5 / GF / 4,5 / GF	672Hz	14.19dB	11,77dB	23,14dB	26,65dB	29,59dB

Table 55 Critical points frequency and TL for low frequency for Setup 2

8.11. Panel comparison

In the previous subchapters, the different panel behaviors are identified in transmission loss versus frequency plots. Multiple panels have been compared, one example can be seen in figure 96.

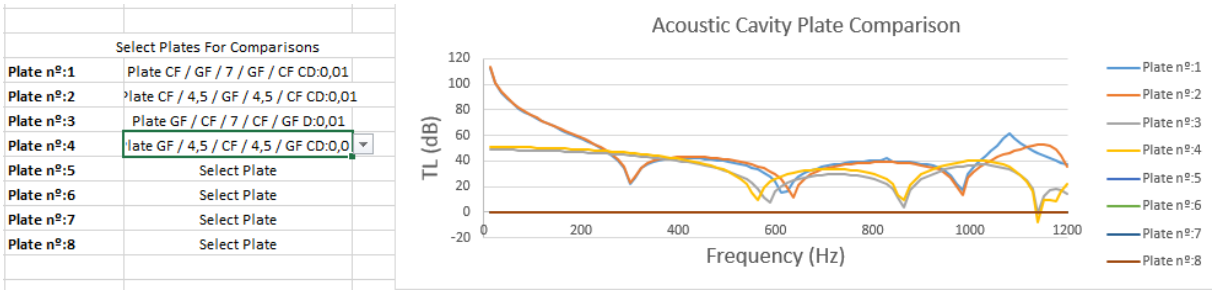

Figure 96 Comparison between best panels in transmission loss vs frequency

In Figure 96, four panels are being compare and two of them have an extremely good behavior for low frequencies: panel CF/GF/7/GF/CF and CF/4.5/GF/4.5/CF. Comparing both panels it can be seen that panels with carbon fiber on the outside and glass fiber on the inside create a good absorption for low frequency values. However panels GF/CF/7/CF/GF and GF/4.5/CF/4.5/CF don't share the same behavior, although they have the same layers and materials. The only difference is the order of the layups of the carbon fiber and glass fiber. To conclude the good behavior occurs when carbon fiber layup is applied with glass fiber inside.

8.12. Conclusion

From the previous chapter, we concluded that panels with a combination of carbon fiber, applied on outside layers, and glass fiber, applied in inside layers generate lower noise levels for low frequencies, as seen in table 56 for groups 4 and 5.

Also from table 56, we can also compare panel CF/GF/3/GF/CF(Group 4) and panel CF/1.5/GF/1.5/CF (group 5) 1st structural mode because both have the same amount of carbon, glass fiber and foam, with the only difference being a one foam and a two foam design, respectively. Panel CF/GF/3/GF/CF 1st structural mode is located at 516Hz (10.49dB) and panel CF/1.5/GF/1.5/CF 1st structural mode is located at 492Hz (10.34dB). The higher structural mode is desired for our application because it occurs further away from the frequency operational range of the UAV.

With this in mind, we can conclude that group 4 panels have the best acoustic behavior, per unit of foam thickness, to be applied in the UAV structure, due to the high transmission loss for low frequency values and a relatively high structural mode frequency.

		1st Critical Point		**TL(Low Frequency)**			
		CDC : 0.01					
		1st CP	TL(CP)	12Hz	150Hz	300Hz	450Hz
Group 1	**Panel CF/0/CF**	300Hz	-1.79dB	29,86dB	26.94dB	-1.79dB	29.19dB
	Panel CF/3/CF	564Hz	-2.57dB	40,33dB	39.31dB	35.86dB	27.80dB
	Panel CF/5/CF	672Hz	-0.97dB	43,61dB	42.77dB	40.06dB	34.58dB
	Panel CF/7/CF	756Hz	-5.37dB	45,96dB	45.21dB	42.82dB	38.22dB
Group 2	**Panel GF / 0 / GF**	384Hz	8,96dB	44,67dB	42,90dB	35,24dB	31,67dB
	Panel GF / 3 / GF	456Hz	6,54dB	46,49dB	46,48dB	39,94dB	11,18dB
	Panel GF / 5 / GF	504Hz	7,23dB	48,32dB	48,31dB	42,95dB	30,82dB
	Panel GF / 7 / GF	552Hz	7,10dB	49,85dB	49,84dB	45,17dB	36,42dB
Group 3	**Panel GF / CF / 3 / CF / GF**	480Hz	6.34dB	45,14dB	43,85dB	39,15dB	21,79dB
	Panel GF / CF / 5 / CF / GF	540Hz	7.66dB	47,10dB	46,00dB	42,16dB	32,36dB
	Panel GF / CF / 7 / CF / GF	588Hz	7.66dB	48,71dB	47,72dB	44,38dB	36,88dB
Group 4	**Panel CF / GF / 3 / GF / CF**	516Hz	10.49dB	110,14dB	62,70dB	16,97dB	33,66dB
	Panel CF / GF / 5 / GF / CF	576Hz	14.74dB	111,60dB	64.43dB	19,59dB	38,77dB
	Panel CF / GF / 7 / GF / CF	624Hz	15.95dB	113,13dB	65.92dB	21,79dB	41,91dB
Group 5	**Panel CF / 1,5 / GF / 1,5 / CF**	492Hz	10.34dB	109,14dB	61,62dB	15,36dB	28,35dB
	Panel CF / 3 / GF / 3 / CF	564Hz	11.58dB	111,63dB	64.40dB	19,68dB	38,51dB
	Panel CF / 4,5 / GF / 4,5 / CF	636Hz	11.66dB	113,74dB	66.54dB	22,83dB	42,97dB
Group 6	**Panel CF / 1,5 / CF / 1,5 / CF**	516Hz	3.90dB	41,44dB	40,27dB	36,13dB	24,45dB
	Panel CF / 3 / CF / 3 / CF	624Hz	0.72dB	45,24dB	44,32dB	41,31dB	34,95dB
	Panel CF / 4,5 / CF / 4,5 / CF	720Hz	-2.50dB	47,90dB	47,11dB	44,55dB	39,52dB
Group 7	**Panel GF / 1,5 / CF / 1,5 / GF**	444Hz	4.04dB	46,82dB	45,38dB	39,91dB	11,18dB
	Panel GF / 3 / CF / 3 / GF	504Hz	7.10dB	49,10dB	47,91dB	43,70dB	31,48dB
	Panel GF / 4,5 / CF / 4,5 / GF	564Hz	9.74dB	50,96dB	49,92dB	46,38dB	37,99dB
Group 8	**Panel GF / 1,5 / GF / 1,5 / GF**	456Hz	10.17dB	49,73dB	48,36dB	43,28dB	16,21dB
	Panel GF / 3 / GF / 3 / GF	504Hz	9.77dB	51,30dB	50,10dB	45,84dB	33,23dB
	Panel GF / 4,5 / GF / 4,5 / GF	540Hz	14.10dB	52,76dB	51,69dB	47,98dB	38,85dB

Table 56 all panels single cavity model 1st critical point and TL for low frequencies

8.13. Future work

From the conclusions and the transmission loss plots show in figure 97, it can be seen that panels with inside layers of glass fiber and carbon fiber layers on the outside (group 4 and 5) have a different acoustic behavior for low frequency values which creates an increase of transmission loss of around 50dB.

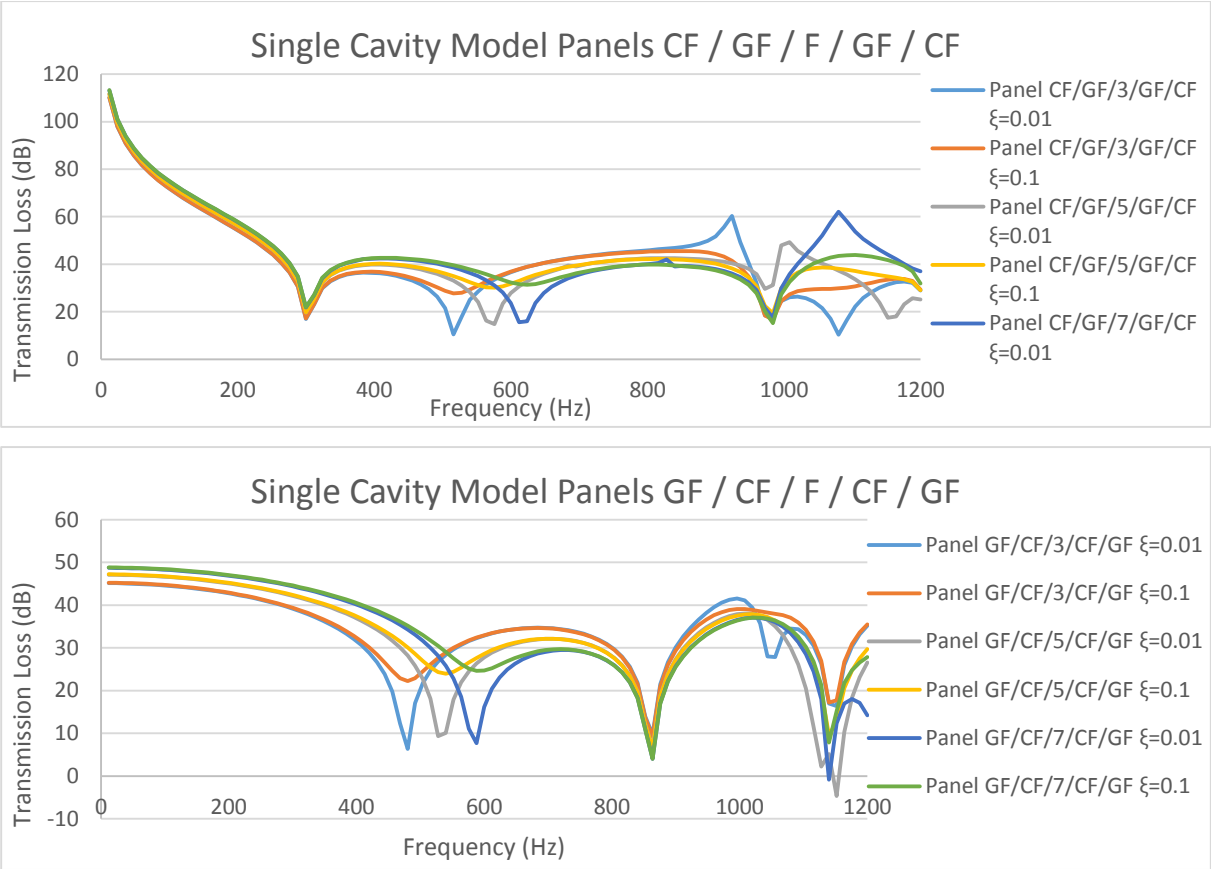

Figure 97 Transmission loss vs frequency plots for group 3 and 4 in the single cavity model

Comparing both plots in figure 97, one question arises: why does this behavior at low frequency occur when carbon fiber is on the outside and glass fiber is on the inside layers?

Analyzing the composition of both panels in group 4 (Table 31) and 5 (Table 36), it can be seen that both groups have: the same number of layers (14) and same percentage of materials (8 layers carbon and 4 layers glass) but differ in orientations, thicknesses and where flexural rigidity is located.

With this into considerations two different studies were performed:

First, layer thicknesses and orientations were all changed: to uniform layers of 0.25mm and 50mm, orientations changed to 0º and 90º with the results being shown in figure 98, these simulations have panel GF/CF/7/CF/GF as a reference.

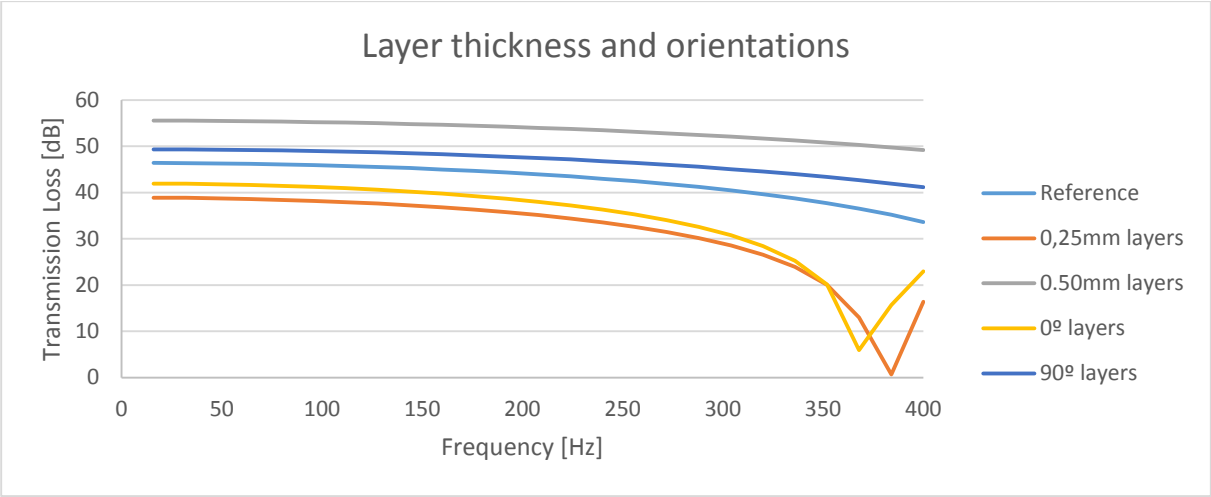

Figure 98 Layer thickness and orientations study

From the plot above it can be seen that, we are only obtaining small deviations (around 10dB) in the transmission loss when we change to uniform thicknesses (0.25mm and 0.50mm) or uniform orientations (0º and 90º) across the panel, this deviations derive from the rigidity changes of the panels tested.

Secondly the decrease that occurs in the transmission loss around 300Hz for the panels CF/GF/F/GF/CF as exemplified in figure 99.

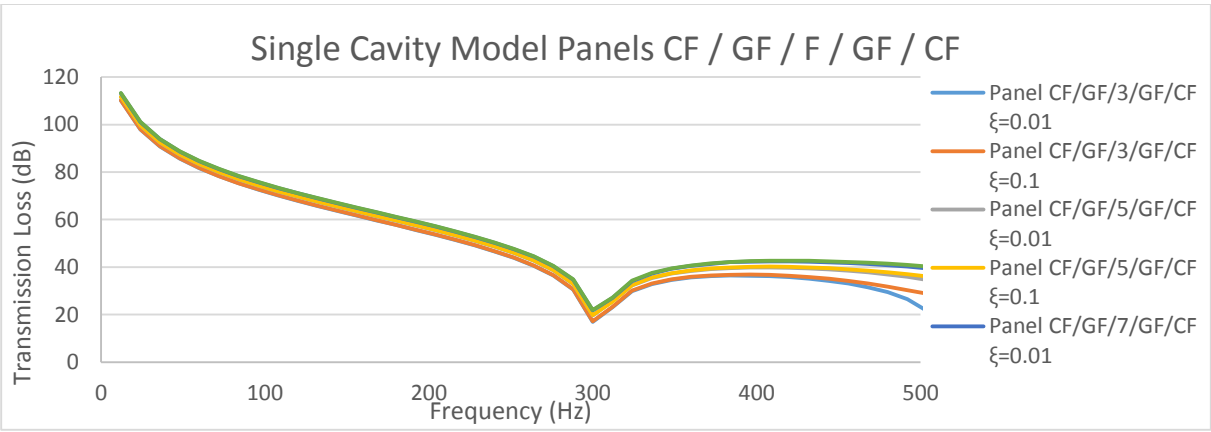

Figure 99 Single cavity model panels CF/GF/F/GF/CF

Taking into account that this behavior is similar to the ones seen in acoustic and structural modes a modal study of the panel + cavity was performed. In table 57 the modes for the system can be seen and it was expected that either an acoustic or a structural mode would appear around 300Hz but the first mode detected in the modal study is 571.47Hz. With this results in mind a harmonic study was performed and the displacement in the direction perpendicular to thickness was obtained for intermediate layers of the panel in study.

Modes	Panel CF/GF/7/GF/CF
1st	571,47Hz
2nd	649,69Hz
3rd	857,54Hz
4th	860,91Hz
5th	897,89Hz
6th	1030,8Hz

Table 57 Panel + Cavity system modes

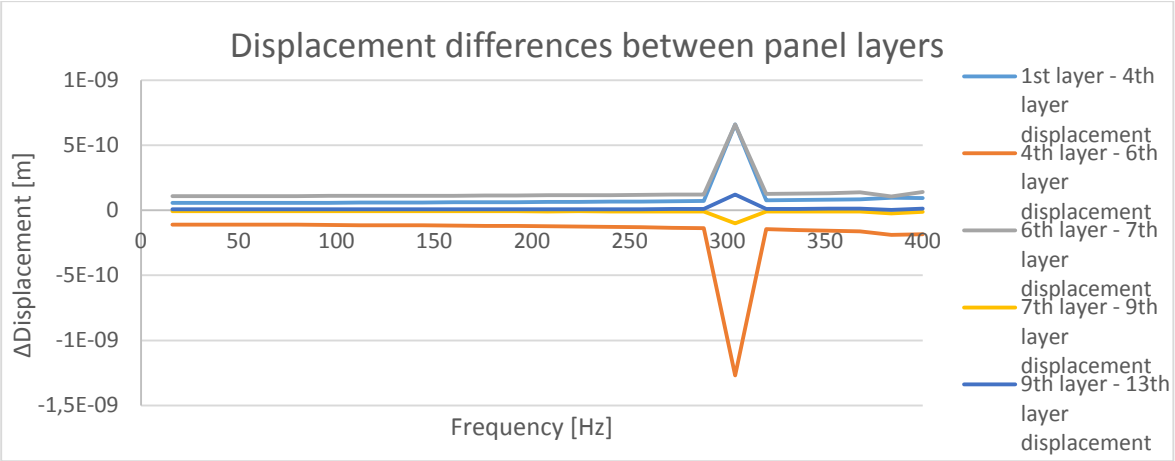

Figure 100 Displacement differences between layers

In figure 100, the difference in displacement between layers is analyzed and by the plot it can be concluded that the panel global thickness is varying around the 300Hz range. This behavior occurs due to a compression/expansion effects inside the panel which is derived from a structural mode.

Considering both studies, we cannot conclude the specific reason for why there is such a good acoustic behavior for low frequency, when carbon fiber layers are on the outside and glass fiber on the inside layers.

This work is finalized with two major questions pending to be solved in future works:

- Does the 300Hz panel behavior influence transmission loss for low frequencies?
- Does the transmission loss increase occurs due to a coupling of material properties, thickness and/or orientation distribution?

References

[1] http://sydney.edu.au/engineering/aeromech/structures/acs1-p1.html. October 2013

[2] Mustapha Assarar, Abderrahim El Mahi, Jean-Marie Berthelot (June 2013). Analysis of the Damping of Sandwich Materials and Effect of the Characteristics of the Constituents. International journal of Material Science volume, 3 issue 2

[3] http://www.anft.net/f-14/f14-detail-horizstab.htm. October 2013

[4] http://scribol.com/technology/aviation/airbus-a350-composites-on-trial-part-i/. October 2013

[5] http://www.boeing.com/commercial/aeromagazine/articles/qtr_4_06/article_04_2.html. October 2013

[6] Vincenzo D'Alessandro and Giuseppe Petrone (2013). A review of the vibroacustics of sandwich panels: Models and experiments. Journal of sandwich structures and materials volume 15(5) pages 541-582

[7] http://www.compositesworld.com/articles/the-outlook-for-unmanned-aircraft. October 2013

[8] Vincenzo D'Alessandro and Giuseppe Petrone (2013). A review of the vibroacustics of sandwich panels: Models and experiments. Journal of sandwich structures and materials volume 15 pages 541-582

[9] Ford R.D., Lord P. and Walker A. (1967). Sound Transmission through sandwich constructions. Journal Sound Vibrations volume 5 pages 9-21

[10] Smolenski C. and Krokosky E. (1973). Dilatational-mode sound transmission in sandwich panels. Journal acoustics and sound volume 54 pages 1449-1457

[11] Sharp B. and Beauchamp J. (1969). The transmission loss of multilayer structures. Journal Sound vibrations volume 9 pages 383-392

[12] Narayanan S. and Shangbhag T. (1982). Sound Transmission thorough a damped sandwich panel. Journal of sound and vibrations volume 80 pages 315-327

[13] Zienkiewicz O. and Taylor R. (2000). The finite element method 5th edition. Oxford; Boston; Butterworth-Heinenmann

[14] Kirkup S. (1998). The boundary element method in acoustics: a development in FORTRAN. Integral equation methods in engineering series. Hebden Bridge: Integrated Sound Software

[15] Assf S. and Guerich M. (2008). Numerical prediction of noise transmission loss through viscoelastically damped sandwich plates. Journal of sandwich Struct Mater volume 10 pages 359-384

[16] Lee C. and Kondo K. (1999). Noise transmission loss of sandwich plates with viscoelastic core. In proceedings of AIAA 1999: 40th structures, structural dynamics and materials conference and exhibit. The American Institute of Aeronautics and Astronautics (AIAA) St. Louis 1999 page 2137-2147

[17] Zhou R. and Crocker (2010). Boundary element analyses for sound transmission loss of panels. Journal of Acoustic volume 127 page 829-840

[18] Moore J. and Lyon (1991). Sound Transmission Loss characteristics of sandwich panel constructions. Journal Acoustics volume 88 page 777-791

[19] Kim Y-J and Han J-H (2013). Identification of Acoustic characteristics of honeycomb sandwich composite panels using hybrid analytical/finite element method. Journal Vibrations an Acoustics volume 135 page 11

[20] Lyon R. (1975). Statistical energy analyses of dynamical systems theory and applications. Cambridge, MA: MIT Press.

[21] Guyader J. and Lesueur C. (1980). Transmission of reverberant sound through orthotropic viscoelastic multilayered plates, part II: The transmission Loss. Journal of Sound and Vibration volume 70 pages 319-332

[22] Zhou R. and Crocker M. (2010). Sound transmission loss of foam-filled honeycomb sandwich panels using statistical energy analyses and theoretical and measured dynamic properties. Journal of Sound and vibrations volume 329 page 673-686

[23]Wang T., Li S., Rajaram S., et al (2004). Predicting the sound transmission loss of sandwich panels by statistical energy analyses approach. Journal of Vibrations and Acoustics volume 132 pages 011004-1-011004-7

[24] Carl Q. Howard and Benjamin S. Cazzolato (2015). Acoustic Analyses Using Matlab and ANSYS. CRC press Taylor and Francis group.

[25] https://www.sharcnet.ca/Software/Ansys/17.0/en-us/help/ans_thry/thyacous_afsi.html#thyacous_cafsss. October 2016

[26] Xiaolin Chen and Yijun Liu (2014). Finite Element Modelling and Simulation with Ansys Workbench pages 254-258. CRC press Taylor and Francis group.

[27] http://composites.owenscorning.com/processes/Hand_Lay_Up.aspx. October 2016

[28] Carl Q.Howard and Benjamin S. Cazzolato (2015). Acoustic Analyses Using Matlab and ANSYS. CRC press Taylor and Francis group.

[29] Carl Q.Howard and Benjamin S. Cazzolato(2015). Acoustic Analyses Using Matlab and ANSYS, CRC press Taylor and Francis group, 2015

[30] http://www.airexbaltekbanova.com/en/market-solutions/aerospace.html. October 2016

[31] http://www.airexbaltekbanova.com/en/airex-c70-pvc-foam .html. October 2016

[32] K. Renji and P.S. Nair (1997). Critical Coincidence frequencies of flat panels. Indian Institute of technology.

[33]M. Abid and M. S. Abbes (2012). Acoustic Response of a Multilayer Panel with viscoelastic material. University of Sfax, Enis, Tunisia.